

## ABSTRACT

RIEGL, SIERRA DAWN. A Novel Role for the Imprinted Gene *Zac1* and the Imprinted Gene Network in Developmental Toxicant-Induced Non-Alcoholic Fatty Liver Disease. (Under the direction of Dr. Michael Cowley).

Cadmium (Cd) is a toxic heavy metal that is classified as a top ten chemical of public health concern by the World Health Organization. It is used in or is a byproduct of various industrial practices, and once in the atmosphere, Cd can travel long distances and deposit into agricultural land and water sources. Human exposure occurs mainly through the inhalation of tobacco smoke, but for non-smokers, the primary route of exposure is through ingestion of contaminated food or water. Exposure to Cd leads to various negative health outcomes, justifying its classification as a public health concern.

In humans, non-alcoholic fatty liver disease (NAFLD) is one health outcome of Cd exposure during adulthood. NAFLD describes a spectrum of pathologies that include steatosis, inflammation, and fibrosis. The disease currently affects 30 % of US adults and is predicted to be the leading cause of liver disease in children in the upcoming decade. Increasingly more diagnoses are being made in young individuals, with up to 20 % of adolescents and young adults currently affected. This increasing prevalence of NAFLD among young people suggests that susceptibility to this disease may be programmed by the environment during early life.

After the Developmental Origins of Health and Disease (DOHaD) hypothesis was proposed in the 1980s, a rapidly growing body of evidence has shown that maternal exposure to a broad range of environmental stressors including toxic heavy metals, diet, and endocrine disruptors affect offspring health in later life. Through epidemiological studies, associations have repeatedly been found between adverse uterine environments and negative health outcomes. These associations have been supported by *in vivo* models. However, the contribution of different

environmental stressors to the programming of diseases, including NAFLD, and the underlying molecular mechanisms remain poorly understood.

Epigenetic mechanisms have been proposed as mediators through which maternal exposure to stressors such as Cd may act to program adverse offspring health outcomes including NAFLD. Our lab and others have proposed that perturbation of imprinted gene expression is one candidate mechanism for disease programming because of the unique properties and modes of epigenetic regulation of imprinted genes during development. DNA methylation at Imprinting Control Regions (ICRs) is particularly sensitive to environmental perturbation in early development. Once established, ICR epigenetic states are maintained throughout life, providing an epigenetic memory that may link the early life environment and later life health outcomes in offspring. Many imprinted genes are coordinately expressed as part of an Imprinted Gene Network (IGN) controlled by the transcription factor encoded by the imprinted gene *Zac1*, and they have been shown to play roles in liver development and homeostasis.

Our central hypothesis is that developmental Cd exposure is sufficient to program NAFLD, and further, that this process is mediated by *Zac1* and the IGN. In **Chapter 2**, we demonstrate through histological, biochemical, and molecular analyses that juvenile NAFLD can be programmed in F<sub>1</sub> female and male mouse offspring in response to maternal ingestion of CdCl<sub>2</sub>. In **Chapter 3**, exploiting our novel mouse model, we show that the IGN plays a central role in mediating between Cd exposure in development and juvenile NAFLD and identify the imprinted gene *Zac1* as a novel regulator of prosteatotic pathways in the liver. In **Chapter 4**, analysis of publicly available RNA-sequencing and microarray data reveal that the IGN acts as a conserved pathway that is dysregulated in response to several different environmental exposures that program NAFLD.

The research in this dissertation demonstrates that maternal CdCl<sub>2</sub> exposure is sufficient to program NAFLD in offspring in later life and identifies the IGN as a pathway that may be responsible for programming these phenotypes in response to CdCl<sub>2</sub> and other environmental stressors. Ultimately, these studies provide further insights into roles for imprinted genes in linking early-life adverse exposures to disease susceptibility. Future research can capitalize on these findings to identify potential therapeutic targets for mediating NAFLD susceptibility and adverse liver health outcomes in adolescence.

© Copyright 2022 by Sierra Riegl

All Rights Reserved

A Novel Role for the Imprinted Gene *Zac1* and the Imprinted Gene Network in Developmental  
Toxicant-Induced Non-Alcoholic Fatty Liver Disease

by  
Sierra Dawn Riegl

A dissertation submitted to the Graduate Faculty of  
North Carolina State University  
in partial fulfillment of the  
requirements for the degree of  
Doctor of Philosophy

Toxicology

Raleigh, North Carolina  
2022

APPROVED BY:

---

Dr. Michael Cowley  
Committee Chair

---

Dr. Arion Kennedy

---

Dr. David Aylor

---

Dr. David Buchwalter

---

Dr. Scott Belcher

## **DEDICATION**

To my granny, Helen Moorefield, PhD, and my mom, Patricia Moorefield-Lilly. Since I was a young girl, you both inspired me to pursue the highest levels of education and showed me what it means to be an intelligent, strong woman. I hope I have made you proud.

## BIOGRAPHY

Sierra Dawn Riegl (née Moorefield) was born in Rock Hill, SC. She grew up in the small town of Newport, NC. The beach and NC Aquarium at Pine Knoll Shores fueled her passion for science, and after graduating from West Carteret High School in 2014, she was awarded the Legacy Scholarship to attend Meredith College. During her undergraduate education, she interned at Burleson Research Technologies, Inc., gaining experience with *in vivo* models in toxicology. She was also an intern at the Environmental Protection Agency, where she gained experience using *in vitro* models in toxicology. From that opportunity, she was able to present her research for the first time at the NC Society of Toxicology's annual meeting and was a co-author on a publication. She earned degrees in biology and chemistry from Meredith College in 2018. Deciding to continue to pursue her passion, she entered the graduate program in toxicology at NCSU in 2018 and began her doctoral project under the direction of Dr. Michael Cowley in 2019, where she has brought together her past research experiences using cell culture and animal models.

## ACKNOWLEDGMENTS

There are many people I would like to thank for making this dissertation possible. First, I would like to thank my husband, Raymund Riegl, for his unconditional love and support during the course of my research project. Thank you for never failing to believe in me and encouraging me to be better every day. To my mom, Patricia Moorefield-Lilly: thank you for always being there for me, listening to me drone on about work, and teaching me the importance of an education. Without you, I would not be here today. To my best friend and sister in all the ways that matter, Meredith Lewis: thank you for always having my back and being one of my biggest cheerleaders. To all my undergraduate mentors, especially Dr. Jason Andrus: thank you for instilling passion in me for research, preparing me for a graduate education, and guiding me throughout my career. I would especially like to thank Dr. Michael Cowley for helping me grow into the scientist I am today, for listening to my crazy hypotheses with patience, and for never failing to fight for my goals like they were his own. To my committee members: thank you for your guidance and collaboration on this project. Lastly, thank you to the Toxicology program faculty members and graduate students- especially members of my cohort- for supporting me in too many ways to list here. I am so incredibly grateful to you all.

## TABLE OF CONTENTS

LIST OF TABLES .....	vii
LIST OF FIGURES .....	viii
<b>CHAPTER 1: Introduction</b> .....	1
<b>Cadmium</b> .....	1
<b>Mechanisms of Cd Toxicity</b> .....	2
<b>Epigenetics</b> .....	4
<b>Genomic Imprinting</b> .....	9
<b>Developmental Origins of Health and Disease</b> .....	11
<b>The Liver</b> .....	13
<b>Non-Alcoholic Fatty Liver Disease</b> .....	17
<b>From Mouse to Human</b> .....	20
<b>CHAPTER 2: Developmental Cadmium Exposure Programs Non-Alcoholic Fatty Liver Disease</b> .....	23
<b>Abstract</b> .....	24
<b>Introduction</b> .....	24
<b>Materials and Methods</b> .....	26
<b>Results</b> .....	30
<b>Discussion</b> .....	38
<b>Acknowledgements</b> .....	42
<b>CHAPTER 3: Developmental Cadmium-Induced Non-Alcoholic Fatty Liver Disease is Programmed via Up-Regulation of <i>Zac1</i> and the Imprinted Gene Network</b> .....	44
<b>Abstract</b> .....	45
<b>Introduction</b> .....	46
<b>Materials and Methods</b> .....	48
<b>Results</b> .....	56
<b>Discussion</b> .....	64
<b>Acknowledgements</b> .....	67
<b>CHAPTER 4: Imprinted Gene Network Dysregulation is a Conserved Hepatic Response to Different Environmental Stressors</b> .....	68
<b>Abstract</b> .....	69
<b>Introduction</b> .....	69
<b>Materials and Methods</b> .....	72
<b>Results</b> .....	77
<b>Discussion</b> .....	86
<b>Acknowledgements</b> .....	89
<b>CHAPTER 5: Conclusions &amp; Future Directions</b> .....	90
<b>REFERENCES</b> .....	99

<b>APPENDICES</b> .....	133
<b>Appendix A: Chapter 2 Supplemental Data</b> .....	134
<b>Appendix B: Chapter 3 Supplemental Data</b> .....	135
<b>Appendix C: Chapter 4 Supplemental Data</b> .....	136

## LIST OF TABLES

<b>Supplementary Table 2.1.</b> Primer sequences used for qRT-PCR. ....	134
<b>Supplementary Table 2.2.</b> F <sub>1</sub> proportional organ data at PND0, 21, and 90.....	134
<b>Table 3.1.</b> Inputs for hypergeometric calculations of enrichment.....	55
<b>Supplementary Table 3.1.</b> Primer sequences used for qRT-PCR. ....	135
<b>Supplementary Table 3.2.</b> Primer sequences used for pyrosequencing. ....	135
<b>Supplementary Table 3.3.</b> RNA-sequencing DEG information and enrichment data for PND0 and 21.....	135
<b>Supplementary Table 3.4.</b> Determination of allele-specific expression of imprinted genes among DEGs for females and males at PND21.....	135
<b>Table 4.1.</b> Direction of IGN gene dysregulation in response to different environmental exposures.....	81
<b>Supplementary Table 4.1.</b> Details for the studies used in the analysis. ....	136
<b>Supplementary Table 4.2.</b> Ensembl gene IDs for RNA-sequencing and microarray datasets.....	136
<b>Supplementary Table 4.3.</b> Primer sequences used for qRT-PCR. ....	136
<b>Supplementary Table 4.4.</b> RNA-sequencing and microarray analysis from various adult environmental exposures. ....	136
<b>Supplementary Table 4.5.</b> Exposure model comparisons for shared IGN genes.....	136

## LIST OF FIGURES

<b>Figure 1.1.</b> Generalized nucleosome structure.....	7
<b>Figure 1.2.</b> Dynamics of DNA methylation during development.....	9
<b>Figure 1.3.</b> Centrilobular model.....	17
<b>Figure 1.4.</b> Stages of NAFLD progression. ....	20
<b>Figure 2.1.</b> Mating strategy and CdCl <sub>2</sub> exposure model used to produce maternally-exposed F <sub>1</sub> hybrid offspring.....	30
<b>Figure 2.2.</b> Female F <sub>0</sub> summary data. ....	31
<b>Figure 2.3.</b> F <sub>1</sub> litter summary data.....	31
<b>Figure 2.4.</b> Effects of CdCl <sub>2</sub> exposure on F <sub>1</sub> female and male body and liver mass. ....	32
<b>Figure 2.5.</b> Effect of developmental CdCl <sub>2</sub> exposure on NAFLD at PND0, 21, and 90. ....	34
<b>Figure 2.6.</b> Effect of developmental CdCl <sub>2</sub> exposure on NAFLD programming at PND21. ....	35
<b>Figure 2.7.</b> Effect of developmental CdCl <sub>2</sub> exposure on F <sub>1</sub> response to glucose challenge at PND76. ....	35
<b>Figure 2.8.</b> Effects of CdCl <sub>2</sub> exposure on F <sub>1</sub> hepatic gene expression at PND0.....	36
<b>Figure 2.9.</b> Effects of CdCl <sub>2</sub> exposure on F <sub>1</sub> hepatic gene expression at PND21.....	37
<b>Figure 2.10.</b> Effects of CdCl <sub>2</sub> exposure on F <sub>1</sub> hepatic gene expression at PND90.....	38
<b>Figure 3.1.</b> Effects of CdCl <sub>2</sub> exposure on F <sub>1</sub> hepatic gene expression at PND0, 21, and 90. ....	57
<b>Figure 3.2.</b> RNA-sequencing analysis on F <sub>1</sub> livers at PND0. ....	59
<b>Figure 3.3.</b> RNA-sequencing analysis on F <sub>1</sub> livers at PND21. ....	60
<b>Figure 3.4.</b> Determination of F <sub>1</sub> hepatic <i>Zac1</i> ICR methylation.....	61
<b>Figure 3.5.</b> <i>Zac1</i> allele-specific expression in female and male 0 and 50 ppm CdCl <sub>2</sub> -exposed mice.....	61
<b>Figure 3.6.</b> Association between <i>Zac1</i> and <i>Pparγ</i> expression. ....	63
<b>Figure 3.7.</b> Role of <i>Zac1</i> in lipid accumulation. ....	64

<b>Figure 4.1.</b> IGN gene enrichment among different developmental environmental exposure models.....	79
<b>Figure 4.2.</b> Imprinted gene enrichment among different developmental environmental exposure models. ....	80
<b>Figure 4.3.</b> Hepatic transcriptome changes measured by RNA-sequencing and microarray analysis on different environmental exposure models.....	82
<b>Figure 4.4.</b> Viability of AML12 cells after CdCl <sub>2</sub> exposure.....	83
<b>Figure 4.5.</b> Effects of CdCl <sub>2</sub> exposure on <i>MT-1</i> gene expression in AML12 cells.....	84
<b>Figure 4.6.</b> Viability of HepG2 cells after CdCl <sub>2</sub> exposure. ....	85
<b>Figure 4.7.</b> Effects of CdCl <sub>2</sub> exposure on HepG2 gene expression. ....	85

# CHAPTER 1

## Introduction

### Cadmium

Cadmium (Cd) is a heavy metal, defined as having a density over 5 g/cm<sup>3</sup>, and is one of the 53 that are naturally occurring in the Earth's crust<sup>1</sup>. Cd is usually present in the soil at about 0.1-0.5 ppm<sup>2,3</sup>. Some heavy metals are considered micronutrients and are essential for life-sustaining metabolic activities<sup>4</sup>. However, Cd is a toxic heavy metal with no known biological function and is classified as one of the top ten chemicals of major public health concern by the World Health Organization<sup>5</sup>.

Anthropogenic activities deposit Cd into the environment at about 8,300 tons/year, compared to about 1,400 tons/year that can be expected from natural sources like forest fires, volcanic eruptions, airborne soil particles, and oceanic spray<sup>6</sup>. Municipal waste incineration and fossil fuel combustion release Cd into the atmosphere while metal mining, battery manufacturing, electronic appliance disposal, and phosphate fertilizer and sewage sludge application contaminate soil with Cd<sup>2,3,7,8</sup>. These activities have led to areas with especially high Cd levels<sup>9,10</sup>.

The release of Cd into the environment is a public health concern because it can travel long distances in the atmosphere before depositing in drinking water sources and agricultural land<sup>2,7</sup>. It should be noted that organisms such as some species of archaea, bacteria, algae, and fungi are resistant to environmental Cd exposure and can potentially be used in remediation practices<sup>11,12</sup>. Some yeast species may also be useful in remediating Cd from the environment because they create biosurfactants, which have been used to remove heavy metals from soil<sup>13</sup>. Many plant and animal species can accumulate Cd in their tissues, allowing it to transfer through the food chain<sup>2-4,14</sup>. For humans, the main source of Cd exposure is via inhalation of cigarette smoke; however, for non-

smokers, the major exposure route is through ingestion<sup>3,7,8</sup>. For humans, the Minimal Risk Level from oral exposures lasting from 15 to 365 days is 0.5 µg Cd/kg/day and is 0.1 µg Cd/kg/day for exposures lasting longer than one year<sup>2</sup>. The United States Environmental Protection Agency has determined the maximum contaminant level for Cd in drinking water is 0.005 ppm<sup>15</sup>.

Exposure to Cd during adulthood leads to renal and hepatotoxicity and is associated with Itai-Itai disease (characterized by softening of the bones), cancer, cardiovascular disease, and metabolic disorders including prediabetes and non-alcoholic fatty liver disease (NAFLD)<sup>16-19</sup>. Because exposure to environmental pollutants can occur during gestation, developmental exposure is of special concern. Prenatal exposure to Cd is associated with harmful effects on fetal development including altered birth weight and cognition<sup>20,21</sup>.

### **Mechanisms of Cd Toxicity**

Inhaled Cd is absorbed much more effectively than ingested Cd with up to 50 % and 10 % absorbed, respectively<sup>2,3</sup>. Cd is poorly excreted and thus accumulates in the body over time<sup>3,22</sup>. Cd has an estimated half-life of between 6-38 years in humans<sup>3,23</sup>. The half-life of Cd does vary by sex and age. Females absorb more Cd, especially during pregnancy, and show a longer half-life than males<sup>24,25</sup>.

Absorbed Cd from the lungs or gastrointestinal tract enters the blood and binds to blood cells, highlighting the importance of analyzing whole blood Cd levels<sup>3</sup>. Metallothionein (MT) binds to Cd, which sequesters it into an inert form intracellularly in the liver<sup>26</sup>. However, an overabundance of Cd can lead to a deficiency of MT in the liver, leading to oxidative damage, and Cd bound to MT can be released from liver cells and travel to the kidneys, making them both key target organs of Cd toxicity and accumulation<sup>16,22,26,27</sup>.

There are multiple mechanisms of Cd toxicity. Cd as a divalent cation shares similar chemical and physical properties with other essential elements including zinc, iron, copper, selenium, and manganese<sup>28,29</sup>. These trace metals are absorbed from the diet or the environment by various transporters and proteins, including solute carriers, divalent metal transporter 1, and MT<sup>30-32</sup>. Cd competes with their uptake, especially zinc, leading to toxicity<sup>33</sup>. Preexisting deficiencies in these essential trace metals can exacerbate Cd toxicity, and in contrast, supplementing the diet with them can mitigate toxicity because MT production is dependent on the availability of zinc and selenium<sup>33,34</sup>. MT is important to trace metal homeostasis, heavy metal detoxification, and protection against oxidative stress and DNA damage<sup>34</sup>. The disruption of the roles of MT by Cd is one of the primary mechanisms of Cd toxicity.

As reviewed elsewhere, Cd can perturb calcium, cAMP, and nitric oxide signaling<sup>3,35</sup>. Briefly, it is proposed that Cd induces the release of calcium in the endoplasmic reticulum, leading to cell death; however, results from different studies are conflicting. Cd inhibits the cAMP signaling pathway by inhibiting protein kinase A activity, leading to alterations in the phosphorylation of target proteins and gene expression. Nitric oxide production is indirectly decreased by Cd via the release of zinc from MT, which inhibits nitric oxide synthase 2, leading to changes in cell physiology.

Cd can act as a metallohormone, mimicking the effects of the hormones estrogen and androgen<sup>36,37</sup>. It has been shown to bind to estrogen receptor  $\alpha$  and androgen receptor ligand binding domains<sup>38</sup>. However, more work needs to be completed to fully elucidate the mechanism by which Cd activates these receptors and leads to negative health outcomes *in vivo*.

Mitochondrial permeability transition can be initiated by Cd from the creation of a pore in the mitochondrial membrane, thereby leading to osmotic swelling and inhibition of the electron

transport chain, inducing apoptosis<sup>3</sup>. Disrupting the electron transport chain as well as inhibiting antioxidative enzymes leads to increased levels of reactive oxygen species within cells, leading to oxidative stress. Oxidative stress can induce endoplasmic reticulum stress signaling, Mitogen Activated Protein Kinases, and Nuclear Factor Kappa B<sup>3,39</sup>. These processes are known to mediate cell apoptosis, or programmed cell death.

Cd exerts genotoxic effects through the induction of oxidative stress, which was described above, and interactions with the DNA damage response systems. Hydroxyl radicals induced by Cd can cause double bonds between DNA bases giving rise to altered function or DNA damage<sup>40</sup>. Cd is a weak mutagen that does not directly bind to DNA but rather alters gene expression patterns, ultimately affecting key cell processes<sup>3</sup>. Repair mechanisms, such as mismatch repair, nucleotide excision repair, and base excision repair for DNA damage can be blocked by Cd interference with zinc finger proteins used in these processes<sup>3,41</sup>. As discussed in more detail below, epigenetic changes can be caused by Cd exposure such as alterations in histone modifications, DNA methylation patterns, and microRNA expression<sup>3,42</sup>.

## **Epigenetics**

Epigenetics was first described as a group of developmental processes connecting the genotype and phenotype<sup>43</sup>. The term joined the widely accepted ideas in the field of genetics of preformation and epigenesis, which represent the unchanging nature of the gene and the dynamic nature of gene expression, respectively<sup>44</sup>. Today, the term epigenetics describes the heritable alteration of gene function without changes to the DNA code, which has been the prevailing definition of the term since the beginning of the modern era of epigenetics research which began in 1996<sup>45,46</sup>. Current molecular mechanisms that are studied within epigenetics include non-coding RNA, post-translational histone modifications and chromatin states, and DNA methylation<sup>45,47</sup>.

These various epigenetic mechanisms do not act in isolation and often impact each other through complex cross-talking.

### Non-coding RNA

Putting a kink in the central dogma of biology, which states that one gene forms one RNA molecule that produces one protein, non-coding RNAs (ncRNAs) are various RNA molecules that are transcribed from genomic DNA but not translated into proteins<sup>48,49</sup>. About 70 % of the human genome is thought to be transcribed into ncRNA<sup>50</sup>. These numerous RNA molecules were once thought to be junk DNA or noise; however, they are now known to have many regulatory and housekeeping functions within cells<sup>48,51</sup>. Regulatory ncRNAs are classified based on their size and include small non-coding RNAs (sncRNAs) and long non-coding RNAs (lncRNAs)<sup>50,52</sup>.

Of the sncRNAs, short interfering RNA (siRNA), microRNA (miRNA), piwi-interacting RNA (piRNA), and tRNA-derived small RNAs (tsRNAs) have been shown to have roles in epigenetic regulation<sup>52,53</sup>. DNA methylation alterations by siRNAs have led to gene silencing<sup>54</sup>. Both siRNA and miRNA bind to messenger RNA (mRNA) that is at least partially complementary to their sequences and, with their protein partners, cleave the mRNA<sup>48,51</sup>. Chromatin state can be altered by miRNAs through their action on remodeling enzymes<sup>55</sup>. DNA methylation has also been shown to be regulated by miRNAs<sup>56-58</sup>. The miRNAs miR-590-5p, miR21, miR-221, and miR-222 have been implicated in fibrogenesis<sup>59-61</sup>. Studies have shown that piRNA regulates histone modifications, chromatin state, and DNA methylation<sup>62-64</sup>. As a relatively newly identified sncRNA involved in epigenetic regulation, there is still much to learn about tsRNAs. So far, they have been shown to associate with piRNAs and regulate chromatin states as well as act as heritable factors of disease<sup>53,65</sup>. Though these sncRNAs have been shown to have roles regulating

developmental processes in plants<sup>66</sup>, further work needs to be done to understand the roles they play in mammalian development.

There are a few roles for lncRNAs. It has been shown that lncRNAs can bind to and stabilize mRNAs, promoting their expression<sup>67</sup>. The maternally expressed imprinted gene *H19* encodes a lncRNA. Among its many roles, H19 can modulate post-translational histone modifications by associating with the histone modifying complex methyl-CpG-binding domain protein 1 to control embryo growth factor expression<sup>68</sup>. The lncRNA *Hotair* regulates DNA methylation at target genes, and, in mice, the loss of *Hotair* leads to bone developmental abnormalities<sup>69</sup>. Another lncRNA, *Xist*, is fundamental to X chromosome inactivation, and improper functioning can lead to abnormalities in female development and cell death<sup>70,71</sup>. Other lncRNAs act as miRNA precursors or decoys for transcription factors and repressors, altering gene expression patterns<sup>52,72</sup>. Recent research has indicated that some lncRNAs can act as biomarkers of environmental exposures, including to toxic heavy metals such as Cd<sup>73</sup>.

### *Histone modifications and chromatin states*

While the most basic units of the DNA molecule are the nucleotides adenine, guanine, cytosine, and thymine, the chromatin subunit model proposed that the basic unit of chromatin structure is the nucleosome<sup>74</sup>. The nucleosome (Figure 1.1) is composed of approximately 150 base pairs of DNA wound around a histone octamer, forming a core particle<sup>75</sup>. The histone types are H2A, H2B, H3, and H4, which form the histone core, and H1 or H5, which links DNA between histone cores<sup>76,77</sup>. Histones associate with the DNA molecule through hydrostatic interactions and hydrogen bonding with DNA phosphates and nonpolar interactions with deoxyribose groups<sup>75</sup>.

Nucleosomes allow DNA within a cell to condense into chromatin, whose structure can be modulated through ATP-dependent chromatin remodeling complexes and histone tail

modifications. Heterochromatin is transcriptionally silenced DNA that is created through the interaction of nucleosome histone tails with silencing proteins<sup>75</sup>. Euchromatin is transcriptionally active DNA. Chromatin remodeling complexes such as SWI/SNF and ISWI use ATP to change the nucleosome structure and allow for DNA transcription<sup>75</sup>. Over 200 histone post-translational modifications have been described including acetylation, methylation, phosphorylation, ubiquitination, sumoylation, ADP-ribosylation, proline isomerization, citrullination, butyrylation, propionylation, and glycosylation<sup>52,78,79</sup>. The most studied of these include histone modifications by small chemical groups such as acetylation, phosphorylation, and methylation. Histone acetyltransferase and histone deacetylase enzymes work to activate and repress genes, respectively<sup>80,81</sup>. Similarly, protein kinases and phosphatases activate and repress genes, respectively<sup>45</sup>. Histone lysine methyltransferase and histone lysine demethylase act to methylate and demethylate histones, respectively<sup>82,83</sup>. Unlike with histone acetylation and phosphorylation, histone methylation acts to either activate or repress genes in a context-dependent manner<sup>45</sup>. The histone tail modifications act as a histone code that regulates chromatin in various biological settings, the perturbation of which has recently been implicated in developmental reprogramming of the epigenome after exposure to environmental contaminants such as Cd<sup>84,85</sup>.

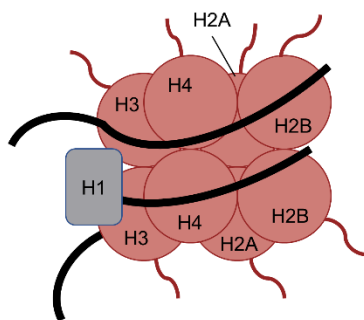


**Figure 1.1.** Generalized nucleosome structure. About 150 DNA base pairs are wound around a histone octamer core composed of H2A, H2B, H3, and H4. H1 or H5 links DNA between histones and helps control nucleosome positioning. Variable modifications on the histone tails alter chromatin state.

## DNA methylation

Like histones, DNA can also be methylated. Generally, DNA hypermethylation at gene promoters is associated with gene repression, and conversely, DNA hypomethylation is associated with gene expression<sup>86-88</sup>. When DNA undergoes methylation, a methyl group is added to the cytosine preceding a guanine in the 5' to 3' DNA sequence (CpG), forming 5-methylcytosine (5mC)<sup>79</sup>. About 70 % of CpGs in cells are methylated<sup>89</sup>. One area in the genome that is the main exception to this global CpG methylation is called a CpG island (CGI), which is an unmethylated 200-2,000 base pair region with more than 50 % being CpGs<sup>89,90</sup>. About 60 % of human genes have CGIs in their 5' promoter regions, and the methylation state of many CGIs has been correlated with transcription initiation and RNA polymerase II binding<sup>89,91</sup>.

Enzymes that add methyl groups to DNA are termed DNA methyltransferases (DNMTs). DNMT1 plays a role in methylation maintenance whereby the enzyme uses one methylated DNA strand as a template to add methyl groups to the other<sup>92</sup>. DNMT3a/b are involved in *de novo* methylation<sup>93</sup>. DNA methylation can be removed passively through the inhibition of DNMT1 during cell division or through an active mechanism by Tet dehydrogenase proteins<sup>89,94</sup>. For active demethylation, Tet proteins oxidize 5mC to 5-hydroxymethylcytosine and further oxidize it to 5-formylcytosine and 5-carboxylcytosine<sup>95-97</sup>. The 5fC and 5caC are excised by DNA glycosylase and converted to cytosine through the base excision DNA repair mechanism<sup>96,98</sup>.

DNA methylation patterns (Figure 1.2) are not static and can change throughout life<sup>89</sup>. When fertilization occurs, a zygote is formed, and demethylation occurs across the parental genomes that it inherited<sup>89,99,100</sup>. After implantation, *de novo* DNA methylation occurs within the offspring cells, which are maintained during replication as the embryo continues to grow<sup>99</sup>. It should be noted that there are areas of the paternal genomes that are resistant to post-fertilization

demethylation. These areas include imprinting control regions (ICRs), intracisternal A particles, and variably erased CpG islands, and could provide possible mechanisms for epigenetic memory between generations<sup>101,102</sup>.

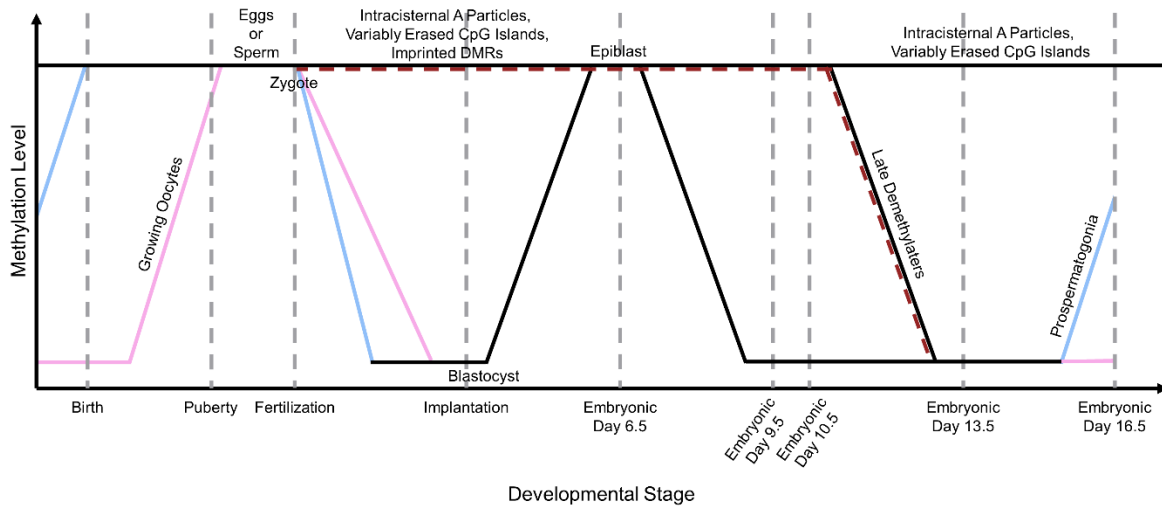


**Figure 1.2.** Dynamics of DNA methylation during development. In the developing zygote, the paternal genome (light blue line) is actively demethylated and the maternal genome (light pink line) is passively demethylated. Imprinted gene differentially methylated regions (DMRs) (dashed red line) do not undergo demethylation and intracisternal A particles and variably erased CpG islands are resistant to demethylation. After implantation, *de novo* methylation occurs (black line). After embryonic day 6.5, the figure is showing methylation dynamics of primordial germ cells in the developing embryo. Sperm and eggs are fully methylated at different stages of development.

## Genomic Imprinting

In eukaryotes, most genes are biallelically expressed; however, some are only expressed from one allele. Random monoallelic expression occurs for X chromosome inactivated genes and some autosomal genes<sup>103</sup>. Depending on the cell, the gene will be expressed from both alleles or from either the maternal allele or the paternal allele, leading to a mosaic expression pattern within the organism. When a gene is expressed from one allele in a parent-of-origin dependent manner because of differential DNA methylation patterns on maternal and paternal alleles established during gametogenesis, this phenomenon is termed genomic imprinting and the genes are

considered imprinted genes<sup>104,105</sup>. Flowering plants, insects, and placental mammals have been shown to have imprinted genes<sup>104</sup>. It is possible to determine parent-of-origin inheritance based on this differential DNA methylation<sup>100</sup>. The protein DNMT3L, which does not possess enzymatic activity, has been shown to be an essential co-factor for the *de novo* methyltransferases DNMT3a/b in establishing germ cell methylation<sup>100,106</sup>.

There are about 130 imprinted genes in humans and about 150 in mice<sup>105,107</sup>. They have been shown to have roles in important developmental processes, including cell division and proliferation, fetal and placental growth, metabolism, and neurodevelopment<sup>105</sup>. Many imprinted genes are controlled by CpG-rich cis-acting regions known as ICRs that overlap with differentially methylated regions within the genome<sup>104,108</sup>. To date, 23 germline ICRs have been identified in mice, and additional somatic ICRs that are established post-fertilization<sup>109</sup>. ICRs control imprinted gene clusters, thereby regulating the expression of multiple imprinted genes<sup>108,110</sup>. ICR function is based on its methylation state<sup>108</sup>. For example, unmethylated ICRs at promoter regions of imprinted genes are associated with gene expression, and methylation is associated with gene silencing. The transcription factor CTCF binds to the H19/Igf2 ICR and acts as an insulator by regulating the interaction between the genes and their enhancers<sup>104,108</sup>. The ICRs at the Kcnq1, Snrpn, and Gnas clusters regulate the expression of lncRNAs, which act in *cis* to control the expression or repression of imprinted genes<sup>108</sup>.

Using *in silico* methods, many imprinted genes have been revealed to be coordinately expressed as part of an Imprinted Gene Network (IGN) composed of 409 mono- and biallelically expressed genes<sup>111</sup>. The IGN has been shown to be controlled by the transcription factor Zac1 (also known as Plagl1), which is encoded by an imprinted gene<sup>112</sup>. IGN co-regulation was confirmed *in vivo* and has been shown to regulate extracellular matrix composition, muscle regeneration, and

adipocyte differentiation<sup>111,113</sup>. Though *Zac1* and other IGN members have human orthologs, to date, functional conservation of the IGN has not been shown. However, alterations of proper imprinting patterns can negatively affect human health as exhibited by disorders such as Prader-Willi, Angelman, Beckwith-Wiedemann, and Silver-Russell syndromes<sup>114,115</sup>.

Though DNA methylation patterns at ICRs are sensitive to environmental perturbation during development, once set up, the patterns are maintained throughout the life of the organism, and thus, are potential epigenetic candidates that could provide an epigenetic memory of early life environmental exposures<sup>110</sup>. In support of this, exposure to bisphenol A leads to imprinting perturbations during fetal and placental development, which corresponds with the window of epigenetic reprogramming, but not during postnatal development<sup>116</sup>. Maternal Cd exposure in humans has been associated with altered DNA methylation patterns in the offspring, and among differentially methylated regions, ICRs are more sensitive to maternal Cd exposure than similar sequences within the genome<sup>117,118</sup>.

### **Developmental Origins of Health and Disease**

The Developmental Origins of Health and Disease (DOHaD) hypothesis, which expands on the fetal origins of disease hypothesis from epidemiological studies in the 20<sup>th</sup> century, states that exposure to environmental stressors during development can negatively impact later life health<sup>119</sup>. It is now considered a theory and continues to be supported by both human epidemiological studies and animal models of exposure<sup>120,121</sup>. Maternal exposure to endocrine disrupting chemicals, over- or undernutrition, and heavy metals have all been shown to negatively affect offspring health in later life<sup>122–127</sup>.

### Endocrine disrupting chemicals

Endocrine disrupting chemicals (EDCs) include man-made chemicals such as pharmaceuticals, plasticizers, some pesticides, and naturally-occurring phytoestrogens that mimic sex hormones like estrogen and androgen, ultimately affecting their production and regulation<sup>128</sup>. Humans are exposed to EDCs through everyday products like bottles, cans, detergents, foods, toys, cosmetics, and flame retardants. Exposure to EDCs in early life has been shown to be associated with reproductive issues, cancer, metabolic disease, cognitive defects, and NAFLD<sup>127,129–131</sup>. However, there are currently no longitudinal studies evaluating the effects of developmental exposure to EDCs on liver health in humans, but evidence from rodent models suggest they can program NAFLD in adulthood<sup>132</sup>.

### Maternal diet

Proper nutrition is essential to human health outcomes, and there are daily requirements for macro- and micronutrients according to various factors and life stages like age, sex, physical activity level, and pregnancy<sup>133</sup>. Macronutrients are biomolecules such as fat, protein, and carbohydrates. Micronutrients are chemicals including vitamins and minerals<sup>134</sup>.

Maternal undernutrition is more common in underdeveloped countries while maternal overnutrition is a more common concern in developed countries<sup>134</sup>. Maternal under- and overnutrition can both lead to negative health effects. During pregnancy, proper nutrition is essential to offspring health outcomes. Deficiencies in only one micronutrient have been linked to fetal defects including cretinism, neural tube defects, night blindness, and stunted growth<sup>134</sup>. Improper amounts of multiple macro- and micronutrients have been associated with increased risk of obesity, cardiovascular disease, osteoporosis, type 2 diabetes, and asthma<sup>120</sup>. A study in humans showed an association between maternal nutrition and NAFLD outcomes in adulthood for their

children, and work from our lab and others have shown that exposure to maternal metabolic syndrome during development programs NAFLD phenotypes of steatosis and fibrosis in mice<sup>135-139</sup>.

### Heavy metals

Cd, lead (Pb), arsenic (As), and mercury (Hg) are all top ten chemicals of health concern listed by the World Health Organization. Humans can be exposed to individual or mixtures of metals through occupational means or through contaminated food and water consumption. Prenatal As exposure has been linked to increased risk of stillbirth and child mortality<sup>140</sup>. Exposure to Pb during pregnancy has been associated with preterm delivery, reduced birth weight, and altered neurodevelopment in children<sup>141,142</sup>. Developmental exposure to Hg has been shown to lead to neurological abnormalities and also impaired cardiovascular and immune function<sup>143</sup>. Developmental Cd exposure is associated with harmful effects on fetal development including altered birth weight and cognition<sup>20,21</sup>. A recent study found a positive association between mercury exposure and NAFLD in human US adolescents<sup>144</sup>. However, longitudinal studies need to be performed to confirm these findings.

### **The Liver**

As the name suggests, the main organ affected by NAFLD is the liver. Like other organs in the body such as the brain and heart, the liver is conserved in all vertebrates<sup>145</sup>. The liver is a complex organ, which arises from cells of the endoderm during development<sup>145,146</sup>. Progenitor cells called hepatoblasts within the hepatic bud of the posterior region in the endoderm give rise to hepatocytes, the main cell type of the liver, and cholangiocytes<sup>145,146</sup>. The liver requires signaling from fibroblast growth factor, bone morphogenic proteins, Wnt, Notch, and transforming growth factor beta (TGF $\beta$ ) for cell differentiation and proper functional development<sup>145,146</sup>.

Specifically, the TGF $\beta$  gradient is crucial for hepatocyte and cholangiocyte differentiation; therefore, disruption of proper signaling can have negative health outcomes for the developing organism. In the portal vein, cholangiocytes are formed through higher TGF $\beta$  signals while cells farther away from the portal vein become hepatocytes by receiving less TGF $\beta$ <sup>145</sup>. Differentiation of hepatocytes is finalized by signaling from oncostatin M, glucocorticoids, hepatocyte growth factor, yes-associated protein signaling, and Wnt/ $\beta$ -catenin signaling<sup>145,146</sup>.

In humans, the liver is the largest organ and makes up about 2 % to 3 % of average bodyweight<sup>147</sup>. It is a vascular organ that receives up to 25 % of total cardiac output while resting, and anything that enters the bloodstream including xenobiotics or toxins will eventually filter through the liver<sup>147</sup>. The liver is a heterogenous organ composed of multiple cell types. The primary epithelial liver cell making up about 80 % of the cell population is the hepatocyte, which is the primary metabolic and biosynthetic cell<sup>145,148</sup>. Cholangiocytes are epithelial cells that line the bile ducts, serving as an interface between the blood and the hepatocytes in the liver<sup>145,148</sup>. They are the second most abundant cell in the liver<sup>145</sup>. Hepatic stellate cells represent about 10 % of liver cells and exist in either quiescent or activated states, which determines their function. In the quiescent state, they mainly store vitamin A and lipids<sup>145,148,149</sup>. In the activated state, which usually occurs during liver injury, they are responsible for depositing collagens<sup>145</sup>. Because the entire blood volume of the organism circulates through the liver, many pathogens can be introduced and need to be cleared. Kupfer cells act as macrophages to recognize these stimuli and help induce pro- or anti-inflammatory responses to combat them<sup>145,148</sup>.

Various models have been used to describe the microarchitecture of the liver; however, the centrilobular concept (Figure 1.3) is the most widely-accepted<sup>150</sup>. In this model, hepatocytes surround the central hepatic vein in a hexagonal shape and the portal vein, hepatic artery, and bile

ducts demarcate the periphery of the lobule<sup>145,150</sup>. Each lobule is supplied with blood by portal vein and hepatic artery and drained by the hepatic vein<sup>148</sup>. As mentioned above, the lobule is divided into metabolic zones. Although these are described as discrete areas, they truly function on a gradient within the liver. The hepatocytes in Zone 1 are closest to the portal areas and receive the richest oxygen and nutrient supply<sup>148</sup>. The intermediate zone is Zone 2, which lies between Zones 1 and 3. The hepatocytes in Zone 3 are closest to the central veins. There is not much oxygen available in this zone, but the cytochrome P450 (CYP) enzymes responsible for metabolizing many xenobiotics are present here<sup>148</sup>.

As the organism develops, the liver takes on various roles during its lifetime. Prior to bone marrow development, the immature liver bud is the site of fetal hematopoiesis<sup>145</sup>. During early and middle gestation in both humans and mice, the liver is involved in glucose consumption with high expression of glycolytic enzymes; however, in the final term of gestation (week 34–37 in humans and day 18–21 in rodents), the liver switches to glucose storage and production by increasing the expression of gluconeogenic and glycogenic enzymes including cyclic adenosine monophosphate (cAMP) and glucocorticoids<sup>145</sup>. Increased glucagon levels promote glycogenolysis, gluconeogenesis, fat oxidation and metabolism of other macronutrients by hepatocytes<sup>145</sup>. The neonatal liver has less than 20 % of the hepatocytes that are present in the adult liver, so even after birth, the liver continues to grow and develop<sup>148</sup>. During the perinatal period, the liver further matures in its ability to store, synthesize, metabolize, and release glucose, which is crucial for postnatal organismal development and metabolism<sup>145</sup>. Once fully matured, the liver's role in the organism is maintained throughout its life. The main role of the liver is as a metabolic organ. It is the site of bile production, glucose, plasma protein, and blood volume regulation, and lipid and cholesterol homeostasis<sup>145,148</sup>. When lipid handling in the liver is disrupted, vitamin deficiencies

can occur in the organism<sup>145</sup>. The liver is also responsible for the metabolism of drugs and xenobiotics by Phase I and Phase II biotransformation reactions and Phase III elimination<sup>145,148,151</sup>.

The liver is the primary site of xenobiotic metabolism because it is the organ with the highest expression of biotransformation enzymes<sup>151</sup>. Xenobiotic metabolism can be divided into three phases. In Phase I, hydrolysis, reduction, or oxidation occurs, which exposes a functional group on the molecule or introduces one to it, making it more hydrophilic<sup>151</sup>. Those functional groups are then used in Phase II conjugation reactions, which further increases its hydrophilicity<sup>151</sup>. Phase I and II reactions make it possible for the xenobiotic to be excreted in urine or bile, and the enzymes involved in these processes depend on the chemical nature of the xenobiotic<sup>151</sup>. Phase III xenobiotic metabolism involves the elimination of the compounds through ATP-binding cassette transporter family, subfamily C efflux proteins and the multidrug resistance proteins in the apical and sinusoidal membranes of hepatocytes<sup>151</sup>. In the fetal liver but not the adult liver, CYP3A7 metabolizes xenobiotics in Phase I metabolism, making it of special interest in developmental toxicology studies<sup>148</sup>. The neonatal liver has a decreased capacity for glucuronide conjugation, which is a Phase II reaction. N-acetyltransferase 2, which is a Phase II enzyme, is not fully expressed in humans until 3 years of age, making infants and young toddlers slow acetylators<sup>148</sup>. The neonatal organism also has an immature ability to produce and excrete bile, which is essential for the excretion of waste products from endogenous processes and xenobiotic metabolism, putting the neonatal organism at an increased risk of toxic liver injury<sup>148</sup>.

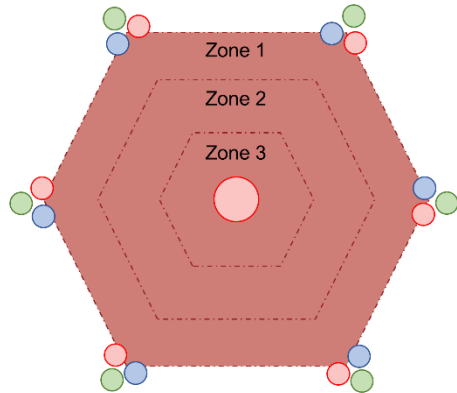


**Figure 1.3.** Centrilobular model. Hepatocytes surround the central vein in a roughly hexagonal pattern, forming three metabolic zones that are not discrete but exist on a gradient. At the vertices are the portal triads composed of the hepatic artery (blue), portal vein (red), and bile duct (green).

### Non-Alcoholic Fatty Liver Disease

NAFLD was first described in adults, but the first case of pediatric NAFLD was reported in 1983, making juvenile NAFLD a relatively new field of study<sup>152</sup>. For children, adolescents, and adults, NAFLD describes a spectrum of pathologies (Figure 1.4): steatosis is caused by the accumulation of fat in more than 5 % of hepatocytes, steatohepatitis is identified by inflammation and swelling in the liver caused by fat buildup, fibrosis is scarring of the liver caused by collagen deposition, and cirrhosis is identified by nodules that cause liver hardening<sup>153–155</sup>. Many individuals with cirrhosis advance to end stage liver disease and evidence suggests that NAFLD will be the number one reason for liver transplantation in juveniles and adults in the near future<sup>153,155</sup>.

NAFLD is currently a public health concern. The direct costs of NAFLD in the US in 2016 was estimated to be \$103 billion/year<sup>156</sup>. A recent study found that up to 20 % of adolescents and young adults are currently affected by NAFLD, and another study showed that about 30 % of obese juveniles have NAFLD<sup>157,158</sup>. NAFLD is estimated to affect about 30 % of adults in Western countries and affects about 85 % of those with obesity<sup>159</sup>. One model estimated that about 64

million people have NAFLD in the US, but another study estimates that number to be about 80 million individuals<sup>156,160</sup>. In total, about 52 million individuals are estimated to have NAFLD in Germany, France, Italy, and the United Kingdom<sup>156</sup>. Current evidence suggests that in both children and adults, mortality occurs within 10 years of cirrhosis developing<sup>155</sup>.

Children and adolescents are at higher risk of developing NAFLD if they are overweight or obese, have insulin resistance, type 2 diabetes, or dyslipidemia, follow a poor diet, do little to no exercise, or carry genetic polymorphisms<sup>153</sup>. It has been shown that the average age of diagnosis in children is 11 to 13 years old, but it is thought to develop even earlier and remain asymptomatic<sup>155</sup>. In adults, NAFLD is highly associated with insulin resistance, dyslipidemia, cardiovascular disease and, obesity<sup>155,159</sup>. NAFLD can be diagnosed through urine and blood tests, oral glucose tolerance tests, fibroscans, ultrasounds, and liver biopsies<sup>153</sup>.

The pathogenesis of NAFLD includes the activation of pathways that disrupt lipid metabolism, promote inflammation, and drive fibrogenic transformation in the various liver cell types. Hepatocytes are the main cell type affected by steatosis, or fat accumulation in the liver<sup>161</sup>. Peroxisome proliferator-activated receptor (Ppar) $\gamma$  expression is highly up-regulated in steatotic livers<sup>162,163</sup>. Ppar $\gamma$  heterodimerizes with retinoid X receptor and is involved in lipid storage, metabolism, regulation of glucose homeostasis, adipogenesis, and inflammation<sup>162,164</sup>. There are two sources of fatty acids that are delivered to the liver. One source is from the lipolysis of triglycerides in adipose tissue, which is delivered to the liver via the blood<sup>165</sup>. Insulin resistance in adipose tissue can lead to an excess of fatty acids that are delivered to the liver<sup>166</sup>. The second source is from fatty acid synthesis by *de novo* lipogenesis in the liver where they are metabolized by mitochondrial  $\beta$ -oxidation or esterification, forming triglycerides, which are exported to the blood as very low-density lipoprotein<sup>165</sup>. Accumulation of lipids occurs when *de novo* lipogenesis

is increased or when mitochondrial  $\beta$ -oxidation or secretion of very low-density lipoprotein is decreased<sup>167</sup>. An overabundance of lipids within hepatocytes can lead to their ballooning and lipotoxicity, which ultimately injures the hepatocyte<sup>168</sup>. Lipotoxicity can lead to the release of danger associated molecular patterns and reactive oxygen species, which are known to stimulate hepatic stellate cells (HSCs)<sup>168-170</sup>. Up-regulated Notch signaling in hepatocytes in response to injury can lead to the production of osteopontin, a known activator of HSCs<sup>171</sup>. Macrophages and injured hepatocytes release inflammatory cytokines, which also activate HSCs<sup>161,169</sup>. HSCs are considered the major driver of fibrogenesis by responding to liver injury after differentiating into active myofibroblast-like cells<sup>155,169</sup>. TGF $\beta$ -1 is considered to be the most potent fibrogenic agonist and exerts its effects by binding to the TGF $\beta$ -1 receptor, inducing SMAD3 phosphorylation, thereby leading to the production of fibril-forming type I and III collagens<sup>161,165,169,172</sup>.

There are various treatments for NAFLD, including diet modification, increasing exercise, and liver transplantation<sup>153</sup>. There are also many drugs for NAFLD that are in clinical trials. Obeticholic acid is a synthetic agonist for farnesoid X receptor, which increases glycogen synthesis and fatty acid oxidation in the liver<sup>173,174</sup>. Elafibranor is a PPAR agonist that ameliorates insulin insensitivity and reduces hepatic steatosis, inflammation, and fibrosis<sup>175,176</sup>. Cenicriviroc inhibits both CCR2 and CCR5 and has been shown to have beneficial effects on fibrosis<sup>177</sup>. Thiazolidinedione (TZD) is a *PPAR $\gamma$*  agonist in adipocytes currently used to treat individuals with type 2 diabetes by increasing insulin sensitivity and increasing adipose tissue fat storage<sup>174,178</sup>. However, a study has shown in mice with up-regulated hepatic *Ppar $\gamma$*  expression that prolonged TZD treatment results in severe hepatic steatosis, suggesting its administration to individuals with altered *PPAR $\gamma$*  signaling may result in detrimental effects in hepatic lipid metabolism and energy balance<sup>179</sup>.

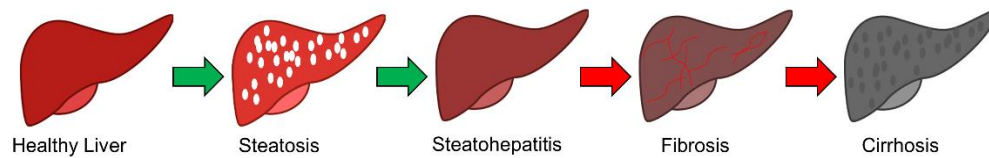


**Figure 1.4.** Stages of NAFLD progression. Excess lipid accumulation in the liver leads to steatosis, which can damage hepatocytes and cause inflammation. Unresolved inflammation causes steatohepatitis and ultimately fibrosis, or collagen deposition in the liver. The red arrow indicates the stage at which NAFLD can no longer be reversed.

### From Mouse to Human

Humans have utilized animal models in scientific inquiry for thousands of years, many species are considered model organisms to study biological processes fundamental to development. A few of these models include the soil roundworm *Caenorhabditis elegans*, the fruit fly *Drosophila melanogaster*, the frog *Xenopus laevis*, the zebrafish *Danio rerio*, the chick *Gallus gallus domesticus*, the laboratory rat *Rattus norvegicus*, and the laboratory mouse *Mus musculus*<sup>180</sup>.

Mice are used in research because they are easy to maintain and breed and many strains are commercially available<sup>181</sup>. Like rats, they are a useful model of development because they are placental mammals; however, there are more resources and tools available for studies using mice than rats, making them the preferred model organism for developmental studies. Mice are also a useful model for human biology and disease because about 80 % of their genes have a human ortholog, 90 % of their genome has synteny with the human genome, and mice have similar physiological processes to humans<sup>181,182</sup>. Unlike rodents, humans have a non-lobated liver; however, it has been shown that liver size and rate of perfusion increases proportionally to body size, making rates of exposure to certain xenobiotics comparable between the species<sup>183</sup>.

The average length of gestation in humans is about nine months, while for mice, gestation takes about 18-20 days depending on the strain, making the mouse a more feasible and convenient

placental model for studying the effects of maternal environmental exposures on offspring health<sup>184</sup>. While mice and humans share many physiological and molecular processes, their placenta differ in anatomy and molecular biology<sup>185,186</sup>. However, despite these differences, some toxicants such as Cd do not efficiently cross the placental barrier in either species, indicating that mice are useful models in understanding the effects of maternal exposures on offspring health<sup>187,188</sup>.

As stated above, Cd has an estimated half-life of between 6-38 years in humans, and its half-life in mice is about 42-350 days<sup>3,23,189</sup>. The absorption rate for Cd in humans is between 1 and 10 % while in rodents it is between 1 and 2 %, and both species inefficiently excrete Cd<sup>2</sup>. Though the half-life for Cd varies between the species, for both humans and mice, it does similarly vary by sex and age. Females also absorb more Cd and show a longer half-life than males and younger individuals accumulate more Cd than older individuals<sup>24,189</sup>. This indicates that mice are a useful model of Cd exposure; however, care should be taken when translating toxicological outcomes observed in mice to humans without proper epidemiological evidence. Mouse models with humanized livers have been shown to more accurately mimic human metabolism and toxicity, but their use is limited to adult studies because they are generated by repopulating the damaged livers with human cells<sup>190</sup>. Future studies are needed to generate humanized mice with heritable humanized genetics, which would then allow for their use in early life developmental studies.

This dissertation project utilizes a hybrid mouse model that combines two genetically divergent inbred strains of mice (C57Bl/6J and CAST/EiJ, shorthand: BxC) with fully sequenced reference genomes. Crossing these two strains results in over 20 million single nucleotide polymorphisms that allow for the analysis of allele-specific changes in DNA methylation and gene expression at target genes caused by maternal CdCl<sub>2</sub> exposure. This work shows that maternal

CdCl<sub>2</sub> exposure can program NAFLD in juvenile offspring and identifies the Imprinted Gene Network (IGN) as a molecular pathway in the liver that is perturbed in response to maternal CdCl<sub>2</sub> exposure.

## **CHAPTER 2**

### **Developmental Cadmium Exposure Programs Non-Alcoholic Fatty Liver Disease**

The following chapter has been submitted to a peer-reviewed journal as part of a larger publication.

## **Abstract**

Cadmium (Cd) is a naturally occurring, toxic heavy metal present in the Earth's crust. However, human industrial activities such as mining, manufacturing, and combustion of waste and fossil fuels have led to an accumulation of Cd in the environment, leading to the contamination of water sources and crop land. Exposure to Cd in adulthood is associated with various negative health effects, including cancer, heart disease, and non-alcoholic fatty liver disease (NAFLD), which is characterized by steatosis, inflammation, and fibrosis. The prevalence of NAFLD in children is increasing, suggesting that the developmental environment can program susceptibility. However, the role of developmental Cd exposure in programming NAFLD remains unclear. Here, we test the hypothesis that developmental Cd exposure can lead to NAFLD in later life. Using a mouse model, we show that developmental CdCl<sub>2</sub> exposure leads to histological, biochemical, and molecular signatures of steatosis and fibrosis in juvenile offspring. Our findings demonstrate that developmental CdCl<sub>2</sub> exposure is sufficient to program juvenile NAFLD in mice. Future studies can capitalize on this model to test potential therapeutic interventions for NAFLD, including small molecule inhibitors and pharmaceuticals.

## **Introduction**

Anthropogenic activities deposit cadmium (Cd) into the environment at about 8,000 tons/year, which is five times more than can be expected from natural sources<sup>6</sup>. As a result, Cd accumulates in drinking water sources and agricultural land<sup>2</sup>. It is classified as one of the top ten chemicals of major public health concern by the World Health Organization. The main route of human exposure is via inhalation of cigarette smoke; however, for the non-smoking portion of the population, the major route is through ingestion. Grains and leafy vegetables that are recommended

to pregnant women as part of a healthy diet often lead to Cd exposure because they absorb it from the soil<sup>8</sup>.

Chronic Cd exposure during adulthood causes renal and hepatotoxicity, and is associated with softening of the bones, cancer, cardiovascular disease, and metabolic disorders including non-alcoholic fatty liver disease (NAFLD)<sup>16-18</sup>. NAFLD describes a spectrum of liver defects ranging from steatosis and non-alcoholic steatohepatitis to fibrosis and cirrhosis<sup>154</sup>. In mice, exposure to Cd causes hepatic steatosis, the first major histological hallmark of NAFLD, although a role for Cd in promoting progression of the disease beyond steatosis has not been shown<sup>191</sup>.

NAFLD is the leading type of chronic liver disease, resulting in \$103 billion per year in medical costs and affecting 30 % of the adult US population<sup>156,159</sup>. Diagnosis of NAFLD is occurring at increasingly younger ages, with up to 20 % of adolescents and young adults currently affected, suggesting that susceptibility to NAFLD may be programmed by the environment during early life<sup>157</sup>. Consistent with this hypothesis, we previously showed that mice nursed by dams with metabolic syndrome develop NAFLD as juveniles, presenting with steatosis and fibrosis<sup>136</sup>.

In mice, developmental Cd exposure has been shown to program metabolic dysfunction and cardiovascular impairment<sup>188,192</sup>. Epidemiological studies in humans have shown that Cd exposure during gestation and early life is associated with neurobehavioral, cognitive, and renal impairments<sup>193,194</sup>. However, its contribution to the programming of NAFLD in later life is unclear.

To address this knowledge gap, we tested the hypothesis that developmental CdCl<sub>2</sub> exposure in mice is sufficient to program NAFLD in later life. We comprehensively evaluated female and male mice exposed to CdCl<sub>2</sub> during development using histological, biochemical, and molecular approaches.

## Materials and Methods

### Animal model and CdCl<sub>2</sub> exposure

Animal work was approved by the North Carolina State University Institutional Animal Care and Use Committee, under protocols 15-013-B and 19-049-B. Experiments were conducted in accordance with the Guiding Principles in the Use of Animals in Toxicology.

Female C57Bl/6J and male CAST/EiJ mice were obtained from Jackson Laboratory at three and four weeks old, respectively, and were allowed an acclimation period of one week before experimental manipulations. Mice were maintained on a 14-hour/10-hour light/dark cycle at 30-70 % humidity, 22°C ± 4°C and housed in Green Line IVC Sealsafe cage housing systems (Tecniplast) and fed AIN-93G rodent diet (Research Diets, D10012G) ad libitum for the duration of the study. At 4 weeks of age, female mice were provided unrestricted access to filtered drinking water (Millipore RiOs Essential RO water purification system) containing 0, 1, or 50 ppm cadmium chloride (CdCl<sub>2</sub>) (Sigma-Aldrich, 202908). At 9 weeks of age, female mice were mated with unexposed CAST/EiJ males. CdCl<sub>2</sub> exposure ended when offspring reached postnatal day (PND) 10, the developmental equivalent of human birth<sup>195</sup>.

The United States Environmental Protection Agency has determined the maximum contaminant level for Cd in drinking water is 0.005 ppm, which is much less than the water concentrations used in this study<sup>15</sup>. For humans, the Minimal Risk Level (MRL) from oral exposures lasting from 15 to 365 days is 0.5 µg Cd/kg/day<sup>2</sup>. Our mice in the 1 ppm and 50 ppm groups were exposed to 28 µg Cd/kg/day and 1501 µg Cd/kg/day, respectively. Though there is a large discrepancy between our doses and the MRL, there are regions of high Cd contamination where humans are exposed to 180 to 600 µg Cd/day<sup>196</sup>. Our female mice were exposed to about 0.5 to 26 µg Cd/day, indicating that our model is still relevant to human exposures even though it

exceeds the established MRL and EPA recommendation. Indeed, we have previously shown that both the 1 ppm and 50 ppm CdCl<sub>2</sub> exposures lead to maternal blood Cd levels comparable to the circulating blood Cd levels of humans in polluted areas<sup>9,188,197</sup>.

F<sub>1</sub> offspring were euthanized at PND0 to standardize the litters to 6 pups with a male:female ratio of 3:3 whenever possible and tissues were collected and flash frozen. At PND21, a subset of F<sub>1</sub> mice were euthanized after a 6-hour fasting period and tissues were flash frozen and stored at -80°C until processing or prepared for histology as described below. The remaining F<sub>1</sub> mice were weaned at PND21 and given ad libitum access to AIN-93G diet until euthanasia at PND90 after a 6-hour fasting period, at which point tissues were collected and processed as described for PND21. The study was blinded until animals were selected for histological, biochemical, and molecular analyses. For both sexes in all three treatment groups at each timepoint, the 5-8 animals with liver masses closest to the mean for that group, avoiding animals from the same litter, were selected for further analyses.

#### Glucose tolerance test

Mice at PND76 were fasted for 16 hours in preparation for the procedure. Blood from the tail vein was applied to a glucose strip (Fisher Scientific, 23-111-276) in a handheld glucometer (Fisher Scientific, 23-111-275) to measure fasting blood glucose (T<sub>0</sub>). An intraperitoneal injection was used to administer glucose at 1.5 mg glucose/g body weight in 1X Dulbecco's Phosphate Buffered Saline (Fisher Scientific, 17-515Q). Blood glucose concentrations were measured at 15, 30, 45, 60, 90, and 120 minutes after injection.

#### Histology

A portion of F<sub>1</sub> median liver lobes was fixed in 4 % formaldehyde overnight at 4°C. Lobes were transferred to 70 % ethanol and dehydrated, paraffin embedded, and sectioned. Sections were

stained with hematoxylin and eosin (H&E) or Sirius red (SR) using protocols described previously<sup>136</sup>. A portion of the left lobe for each animal was flash frozen and cryosectioned to 10  $\mu\text{m}$  thick and stored at  $-80^{\circ}\text{C}$ . Cryosections were stained with Oil Red O (ORO) (Sigma, O-0625) using protocols previously described<sup>136</sup>. All images were taken at 40X magnification using brightfield microscopy, and a central vein was centered in each image.

#### Biochemical assays

An assay of hepatic hydroxyproline (BioVision, K226) was performed according to the manufacturers' instructions on a portion of the left liver lobe.

An assay of hepatic triacylglycerides (ThermoFisher, TR22421) was performed on a portion of the median liver lobe. To prepare the lobes for the triacylglyceride assay, they were weighed then placed in an equal volume of a solution to their mass, which was composed of 50  $\mu\text{L}$  sterile water, 650  $\mu\text{L}$  100% molecular grade ethanol (ThermoFisher, BP2818), and 300  $\mu\text{L}$  3M KOH (Emsure, 1310-58-3). The samples were then heated at  $70^{\circ}\text{C}$  for 1 hour and vortexed every 20 minutes. Samples sat at room temperature overnight. The next day, the total volume of each sample was brought to 250  $\mu\text{L}$  with 2M Tris-base (ThermoFisher, BP152) pH 7.5. Each sample was diluted 1:500 in the same Tris-base. Control and glycerol standards were prepared. All samples were loaded in duplicate into a 96-well plate using 100  $\mu\text{L}$  of material. Then 150  $\mu\text{L}$  of the triglyceride reagent was added. The plate was incubated at  $37^{\circ}\text{C}$  for 10 minutes. Samples were analyzed according to the manufacturer's instructions on a plate reader (FluoStar Omega, BMG Labtech).

#### Nucleic acid isolation

A portion of the left liver lobe for females and males at PND0, 21, and 90 was homogenized using a microtube homogenizer (Biospec 3110Bx Cell Disrupter 4800, BZ10124883) in Trizol

reagent (Invitrogen, 15596026) according to the manufacturer's instructions. Nucleic acids were quantified on a Nanodrop 2000 and RNA integrity was confirmed using a 1.3 % agarose gel.

### qRT-PCR

500 ng of total RNA from livers was used to synthesize first strand cDNA according to the manufacturer's protocol (M-MLV RT enzyme, Promega). cDNA was diluted 1/5 or 1/10 for qRT-PCR, which was performed in triplicate on 96-well plates with a QuantStudio 3 system (ThermoFisher) using SsoAdvanced Universal SYBR Green Supermix (Bio-Rad, 1725271) with standards in sequential dilution 1/5, 1/10, 1/20, 1/40, and 1/80 and water as a no template control (NTC). The cycling conditions were as follows: 95°C for 30 seconds; 40 cycles of 95°C for 15 seconds, 60°C for 30 seconds. The primer sequences are provided in Supp. Table 2.1. The dissociation curves showed that there were no products in the NTC and that primers amplified a single PCR product. Amplification efficiencies were calculated. Beta actin was used as a reference gene and was not significantly differentially expressed between treatment groups (data not shown). Gene expression was quantified using the  $\Delta\Delta C_t$  method<sup>198</sup>.

### Statistical analyses

Unless otherwise stated, statistical analyses were performed using a one-way analysis of variance (ANOVA) with Dunnett's post hoc test comparing 0 ppm to 1 ppm and 50 ppm CdCl<sub>2</sub> exposure groups using GraphPad Prism Version 8, or a Student's t-test, two-tailed, comparing 0 ppm and 50 ppm CdCl<sub>2</sub> exposure groups using Excel. Data are presented as the mean  $\pm$  standard error of the mean. \*p<0.05, \*\*p<0.01, \*\*\*p<0.001, \*\*\*\*p<0.0001.

## Results

### Mouse model of developmental CdCl<sub>2</sub> exposure

We established a mouse model of developmental CdCl<sub>2</sub> exposure by exposing female C57Bl/6J mice to 0 (control), 1, or 50 ppm CdCl<sub>2</sub> through drinking water for 5 weeks prior to mating. Females were bred to unexposed CAST/EiJ male mice to generate F<sub>1</sub> hybrid animals that enabled analyses of allele-specific gene expression and DNA methylation (Figure 2.1a), as we have described previously<sup>199</sup>. Exposure continued through gestation until offspring reached PND10 (Figure 2.1b). The presence of CdCl<sub>2</sub> did not significantly alter F<sub>0</sub> female water consumption (Figure 2.2a) or body mass (Figure 2.2b) from those of controls. Exposure to CdCl<sub>2</sub> did not affect offspring sex ratio (Figure 2.3a) or litter size at PND0 (Figure 2.3b), but exposure to 50 ppm CdCl<sub>2</sub> did reduce offspring survival (Figure 2.3c) compared to the control group.

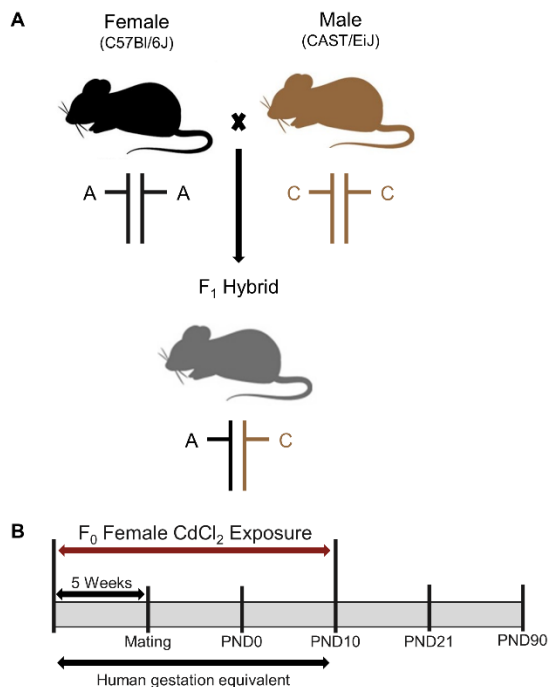


**Figure 2.1.** Mating strategy and CdCl<sub>2</sub> exposure model used to produce maternally-exposed F<sub>1</sub> hybrid offspring. (A) Mating strategy in which parental alleles can be discriminated by single nucleotide polymorphisms (SNPs). (B) Human gestational-equivalent exposure model.

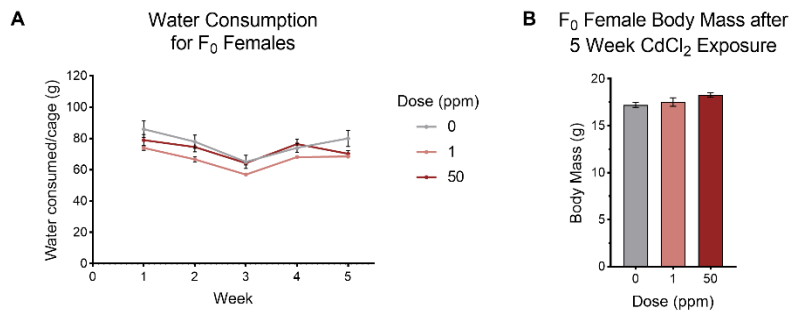


**Figure 2.2.** Female F<sub>0</sub> summary data. (A) Water consumption over the five weeks prior to mating. Repeated measures ANOVA with Dunnett’s post-hoc test comparing 1 ppm and 50 ppm CdCl<sub>2</sub>-exposed mice to 0 ppm controls. (B) Body mass after five weeks of CdCl<sub>2</sub> exposure prior to mating. One-way ANOVA with Dunnett’s post-hoc test comparing 1 ppm and 50 ppm CdCl<sub>2</sub>-exposed mice to 0 ppm controls. All data are presented as means ± S.E.



**Figure 2.3.** F<sub>1</sub> litter summary data. (A) Sex ratios. Chi-squared test with expected values to be equal. (B) Litter size. One-way ANOVA with Dunnett’s post-hoc test comparing 1 ppm and 50 ppm CdCl<sub>2</sub>-exposed mice to 0 ppm controls. For (A-B): Data are presented as means ± S.E. (C) Survival curve.

Developmental CdCl<sub>2</sub> exposure alters body and liver masses

*In utero* Cd exposure in humans is associated with fetal growth restriction and smaller body mass at birth<sup>200,201</sup>. Consistent with this, F<sub>1</sub> females and males exposed to 50 ppm CdCl<sub>2</sub> weighed significantly less than those in the 0 ppm group at PND0 (Figure 2.4a). This phenotype persisted at PND21 (Figure 2.4b), when mice presented with a significantly reduced proportional mass of leg muscle and increased proportional masses of retroperitoneal white adipose tissue, brain (females only), heart, and kidney (Supp. Table 2.2). The proportional mass of brown adipose tissue

was also reduced for both sexes, albeit not significantly (Supp. Table 2.2). At PND90, both sexes showed similar body weights between groups (Figure 2.4c).

At PND0, there were no differences in liver mass as a proportion of body mass between groups for either sex (Figure 2.4d). However, at PND21, both males and females in the 50 ppm group showed significantly increased proportional liver mass compared to control mice (Figure 2.4e). At PND90, only the males in the 50 ppm group showed significantly increased proportional liver mass (Figure 2.4f).

Overall, these data indicate that developmental CdCl<sub>2</sub> exposure induces growth defects, including of the liver, that persist beyond the period of exposure.

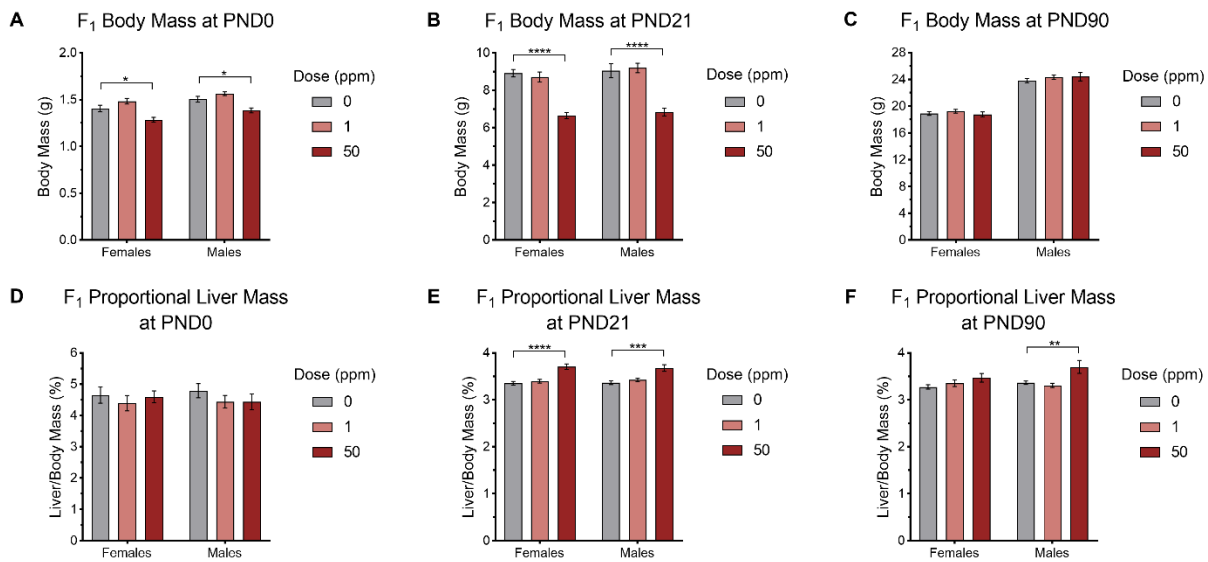


**Figure 2.4.** Effects of CdCl<sub>2</sub> exposure on F<sub>1</sub> female and male body and liver mass. (A-C) Body mass at PND0, PND21, and PND90. (D-F) Liver mass as a proportion of body mass at PND0, PND21, and PND90. All data are presented as means ± S.E. One-way ANOVA with Dunnett's post-hoc test comparing 1 ppm and 50 ppm CdCl<sub>2</sub>-exposed mice to 0 ppm controls. \*p < 0.05, \*\*p < 0.01, \*\*\*p < 0.001, \*\*\*\*p < 0.0001.

### Developmental CdCl<sub>2</sub> exposure is sufficient to program NAFLD

We next determined if developmental CdCl<sub>2</sub> exposure leads to evidence of metabolic syndrome, and histological and biochemical signatures of NAFLD. At PND0, there was no

evidence of differences in hepatic lipid accumulation between groups for either females or males (Figure 2.5a-b). At PND21, both female and male F<sub>1</sub> mice exposed to 50 ppm CdCl<sub>2</sub> during development presented with steatosis, indicated by increased neutral lipid accumulation in hepatocytes. Mice exposed to 50 ppm CdCl<sub>2</sub> also presented with fibrosis, indicated by increased collagen deposition (Figure 2.5c-d). The fibrosis phenotype was more pronounced in females than males. No differences in the accumulation of lipids and collagens between the 1 ppm CdCl<sub>2</sub> group and controls were observed at this timepoint. At PND90, males and females from all treatment groups showed hepatic lipid accumulation and no differences between the groups were observed (Figure 2.5e-f).

Histological evidence for NAFLD at PND21 was supported by biochemical assays on liver tissue. Both females and males in the 50 ppm group showed significantly increased accumulation of hepatic triacylglycerides (Figure 2.6a), a measure of steatosis, compared to controls. Females but not males showed a significant increase in hepatic hydroxyproline (Figure 2.6b), a readout for fibrosis, compared to controls. This is consistent with the sex difference observed at the histological level. The 1 ppm CdCl<sub>2</sub> group did not show significant increases in either measure when compared to the 0 ppm group.

Glucose tolerance testing at PND76 revealed no impaired response in either sex (Figure 2.7a, c). Area under the curve (AUC) analysis for both sexes also indicated no effect of gestational CdCl<sub>2</sub> exposure on the response to glucose challenge (Figure 2.7b, d).

Together, these data show that developmental CdCl<sub>2</sub> exposure is sufficient to program advanced stages of NAFLD in juvenile mice, without long-term effects on glucose homeostasis.

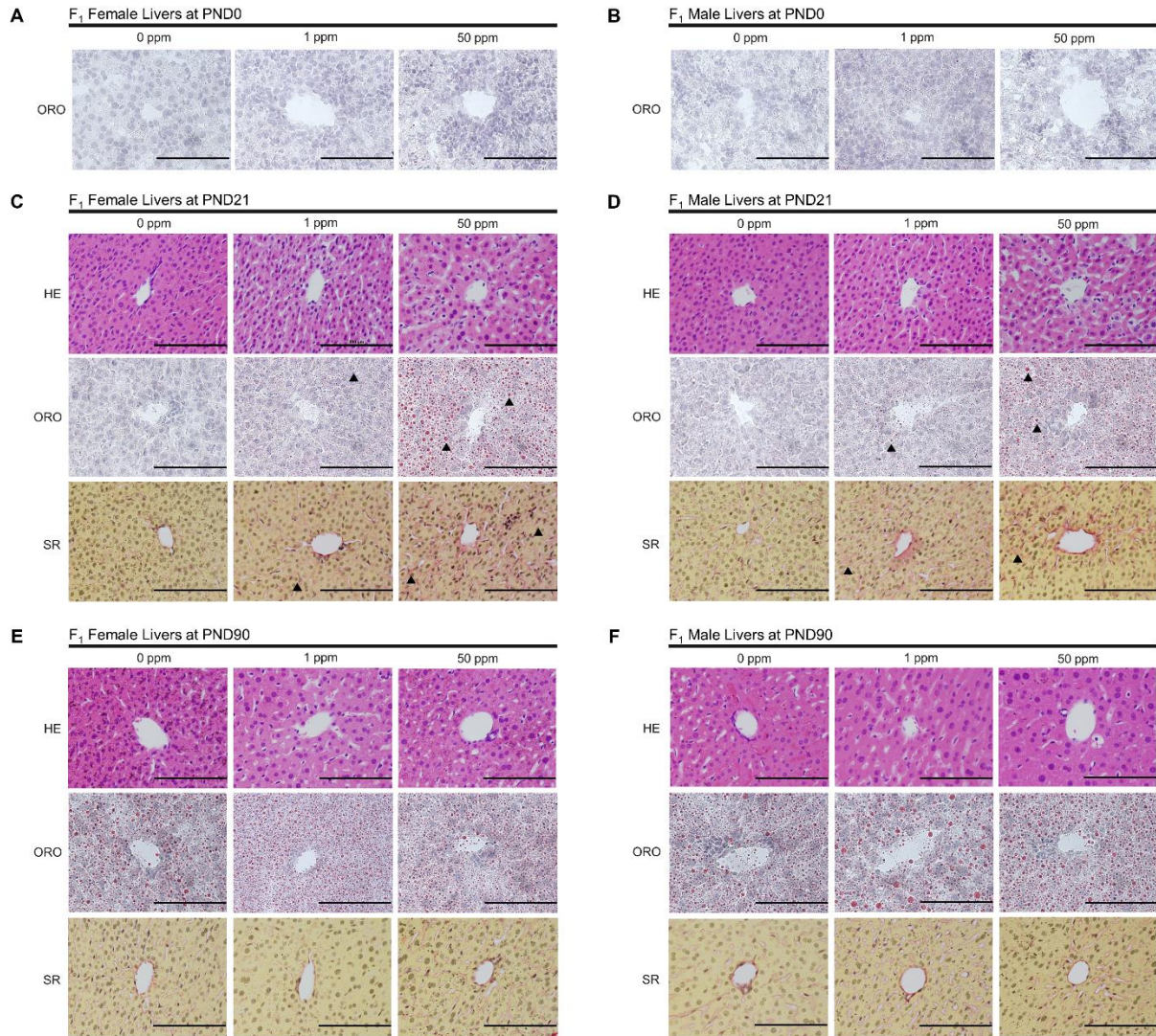


**Figure 2.5.** Effect of developmental  $\text{CdCl}_2$  exposure on NAFLD at PND0, 21, and 90. (A-B) Representative photomicrographs (40x) of PND0 F<sub>1</sub> female and male liver sections stained with ORO. (C-D) Representative photomicrographs (40x) of F<sub>1</sub> female and male liver sections. (E-F) Representative photomicrographs (40x) of PND90 F<sub>1</sub> female and male liver sections. For (C-F): First row: H&E (HE) staining. Second row: Oil Red O (ORO) staining. Third row: Sirius red (SR) staining. All images are centered around a central vein. Scale bars represent 200  $\mu\text{m}$ .

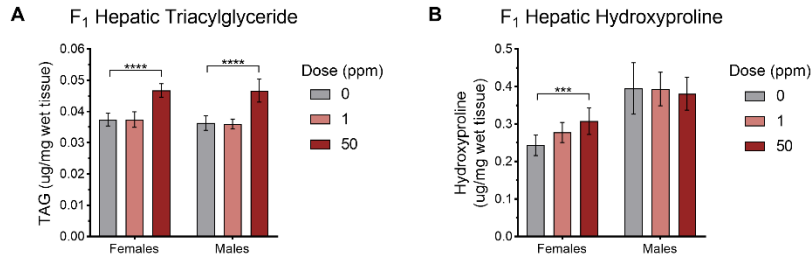


**Figure 2.6.** Effect of developmental CdCl<sub>2</sub> exposure on NAFLD programming at PND21. (A) Quantification of hepatic triacylglycerides. (B) Quantification of hepatic hydroxyproline. All data are presented as means ± S.E. One-way ANOVA with Dunnett’s post-hoc test comparing 1 ppm and 50 ppm CdCl<sub>2</sub>-exposed mice to 0 ppm controls. \*\*\*p<0.001 and \*\*\*\*p<0.0001.

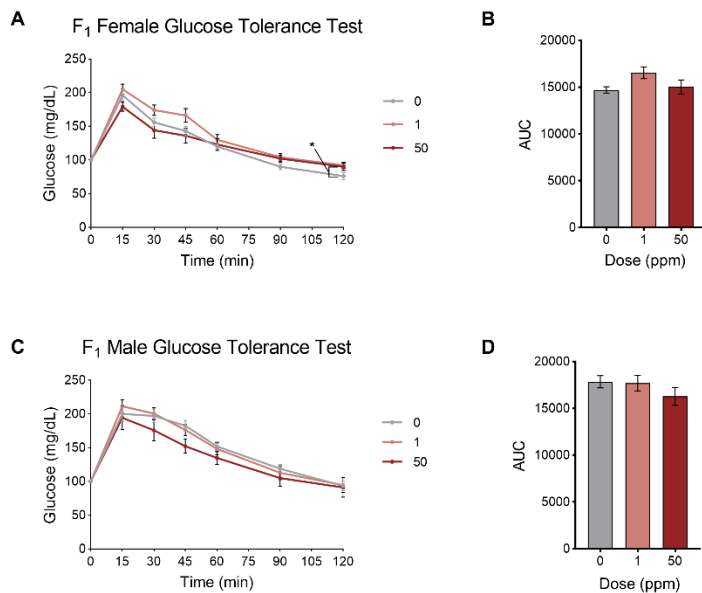


**Figure 2.7.** Effect of developmental CdCl<sub>2</sub> exposure on F<sub>1</sub> response to glucose challenge at PND76. (A, C) Glucose clearance in female and male mice. Repeated measures ANOVA with Dunnett’s post-hoc test comparing 1 ppm and 50 ppm CdCl<sub>2</sub>-exposed mice to 0 ppm controls. (B, D) Glucose AUC for the GTT depicted for each sex. One-way ANOVA with Dunnett’s post-hoc test comparing 1 ppm and 50 ppm CdCl<sub>2</sub>-exposed mice to 0 ppm controls. All data are presented as means ± S.E. \*p<0.05.

Markers of NAFLD are up-regulated at the transcriptional level at PND21

To determine if our observations at the histological and biochemical levels were reflected at the level of gene expression, qRT-PCR was performed on liver tissues. We targeted genes that are canonical markers of steatotic (*Cd36*, *Mgat1*, *Fsp27*, and *Fabp4*), inflammatory (*Il-1β*, *Ccr2*, and *Ccr5*), and fibrotic (*Tgfb-1*, *Snail*, *Colla1*, *Col5a1*, *Col5a2*, *Col6a1*, *Col6a2*, *Vim*, and *Mmp2*)

pathways. At PND0, neither female nor male F<sub>1</sub> mice showed significant overall differences in the expression of these genes between groups (Figure 2.8a-b). However, at PND21, consistent with phenotypic presentation of NAFLD, both sexes in the 50 ppm group showed significant up-regulation of genes indicative of these pathologies (Figure 2.9a-b). At PND90, neither female nor male F<sub>1</sub> mice showed significant overall differences in the expression of these genes between groups (Figure 2.10a-b). These results indicate transcriptional dysregulation of key pathways underlying NAFLD pathogenesis at PND21, consistent with phenotypic presentation at this timepoint.

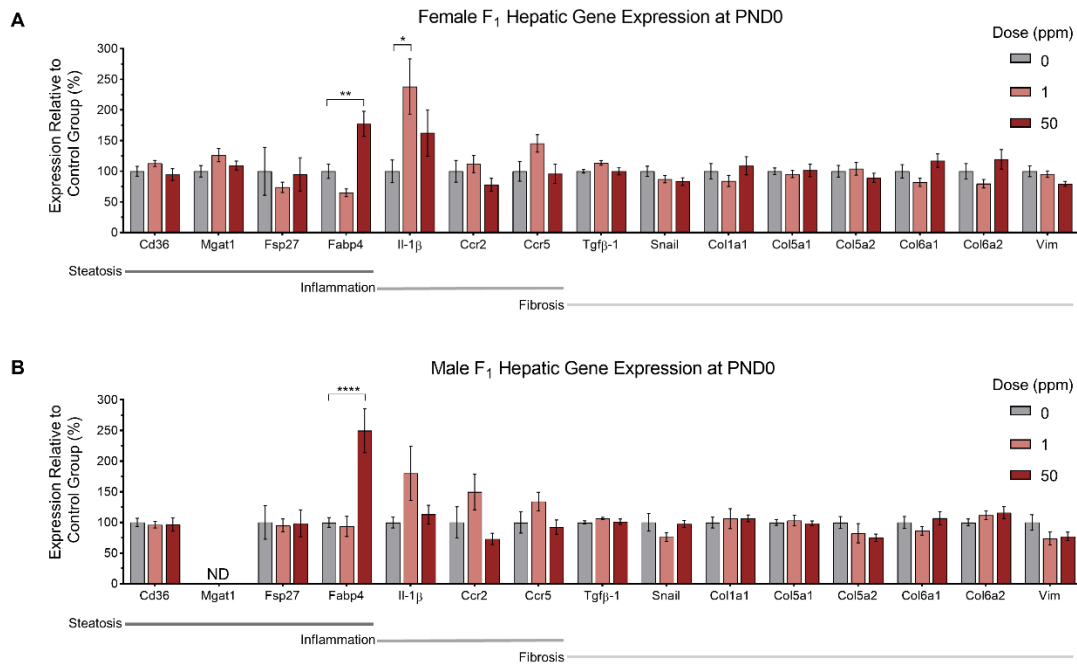


**Figure 2.8.** Effects of CdCl<sub>2</sub> exposure on F<sub>1</sub> hepatic gene expression at PND0. (A-B) Female and male transcript abundance for genes of steatosis, inflammation, and fibrosis pathways. All data are presented as means ± S.E. One-way ANOVA with Dunnett’s post-hoc test comparing 1 ppm and 50 ppm CdCl<sub>2</sub>-exposed mice to 0 ppm controls. ND: not detected. \*p<0.05, \*\*p<0.01, \*\*\*\*p<0.0001.

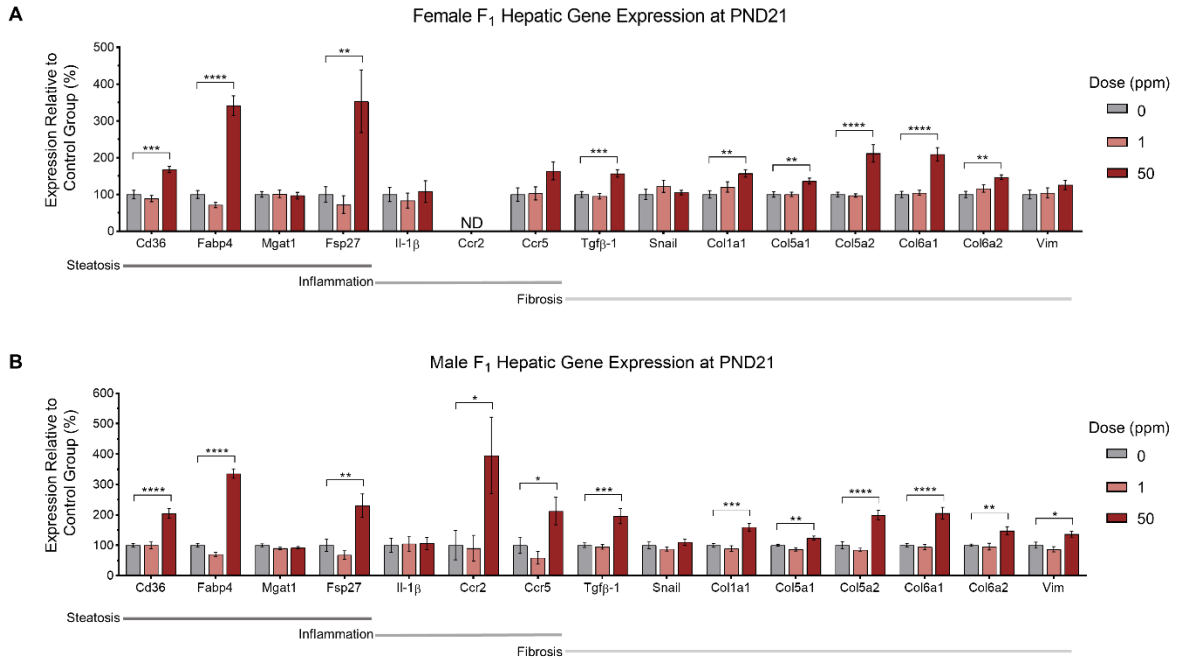


**Figure 2.9.** Effects of Cd exposure on F<sub>1</sub> hepatic gene expression at PND21. (A-B) Female and male transcript abundance for genes of the IGN and steatosis, inflammation, and fibrosis pathways. All data are presented as means  $\pm$  S.E. One-way ANOVA with Dunnett's post-hoc test comparing 1 ppm and 50 ppm CdCl<sub>2</sub>-exposed mice to 0 ppm controls. ND: not detected. \* $p < 0.05$ , \*\* $p < 0.01$ , \*\*\* $p < 0.001$ , \*\*\*\* $p < 0.0001$ .

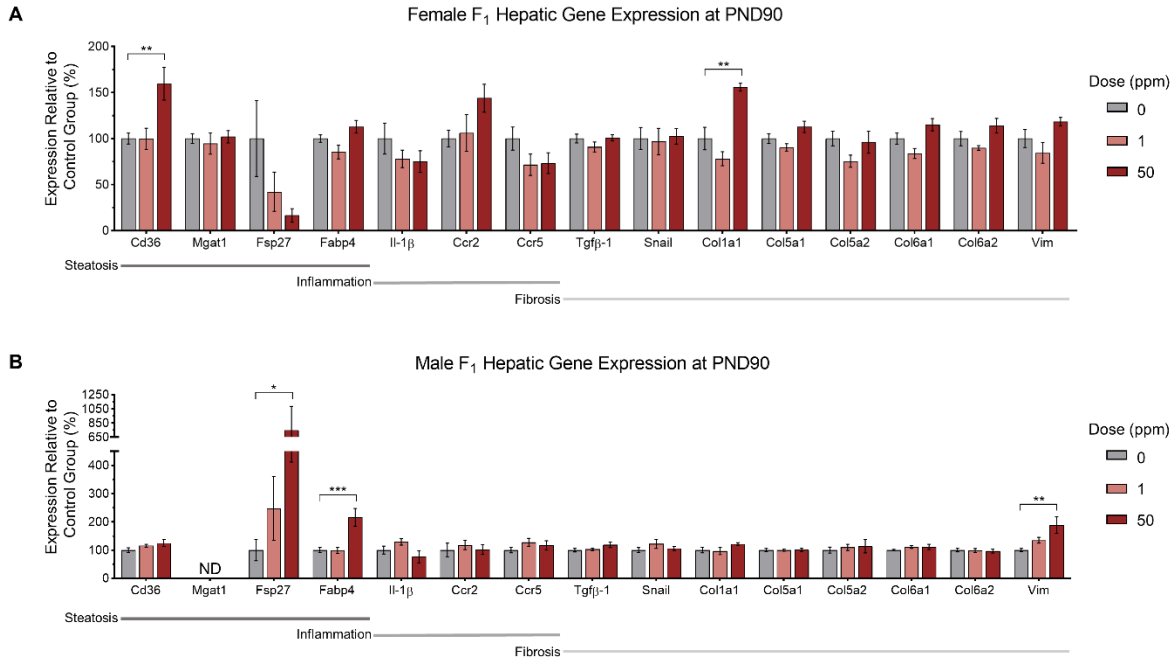


**Figure 2.10.** Effects of CdCl<sub>2</sub> exposure on F<sub>1</sub> hepatic gene expression at PND90. (A-B) Female and male transcript abundance for genes of steatosis, inflammation, and fibrosis pathways. All data are presented as means ± S.E. One-way ANOVA with Dunnett’s post-hoc test comparing 1 ppm and 50 ppm CdCl<sub>2</sub>-exposed mice to 0 ppm controls. ND: not detected. \*p<0.05, \*\*p<0.01, \*\*\*\*p<0.0001.

## Discussion

Cd is naturally present in the soil, but human activities lead to accumulation of it in the environment, presenting a public health concern. Cd is poorly metabolized and excreted<sup>3</sup>. It accumulates in the liver, kidneys, and bone, resulting in negative health effects<sup>17</sup>. The Korean National Environmental Health Survey and Third National Health and Nutrition Examination Survey reveal associations between Cd exposure and liver-related mortality<sup>16,202</sup>. NAFLD is the leading type of chronic liver disease in the US, and observations in humans and model organisms suggest that NAFLD susceptibility can be programmed by the developmental environment. However, the role of Cd exposure in programming NAFLD remains unclear.

To explore the hypothesis that developmental Cd exposure is sufficient to program NAFLD later in life, we exposed hybrid mice to CdCl<sub>2</sub> during development for a period equivalent to human

gestation. 50 ppm CdCl<sub>2</sub> exposure resulted in NAFLD phenotypes in juvenile mice including histological and biochemical evidence of steatosis and fibrosis, and gene expression profiles consistent with diseased liver states. The findings of this study provide evidence that exposure to CdCl<sub>2</sub> during early development is sufficient to program NAFLD.

*Developmental CdCl<sub>2</sub> exposure affects offspring growth and development*

Mice exposed to 50 ppm CdCl<sub>2</sub> through gestation had significantly reduced body masses compared to 0 ppm mice at PND0. This is concordant with human studies that have shown an association between *in utero* Cd exposure, fetal growth restriction, and smaller body size at birth<sup>200,201</sup>.

Mice in the 50 ppm group also showed a significantly lower rate of survival prior to weaning than animals in the 0 ppm group. While the reason for this is unknown, we observed that most deaths occurred around PND14. This timepoint is consistent with the timing at which mice undergo key metabolic changes including a second phase of brown adipose tissue recruitment to enable proper thermoregulation outside the nest<sup>203</sup>. One study showed that increased *Dlk1* expression during this second phase of recruitment led to immature and dysfunctional brown adipose tissue and increased offspring mortality<sup>203</sup>. *Dlk1* is a member of a transcriptionally co-regulated network of genes called the Imprinted Gene Network (IGN) that is controlled by the imprinted gene *Zac1*<sup>111,113</sup>. At PND21, we observed that offspring in the 50 ppm group showed a trend towards decreased brown adipose tissue mass when compared to the 0 ppm group, although the difference was not statistically significant. Our working hypothesis is that developmental CdCl<sub>2</sub> exposure disrupts brown adipose tissue recruitment and function by dysregulating the expression of *Zac1* and the IGN, affecting offspring survival. Further studies are required to test this empirically, including collecting brown adipose tissue at PND14 for molecular and

histological analyses. At PND14, mice undergo a transition to a solid food diet, altering their metabolic state from lipolytic to lipogenic<sup>204</sup>. The same study that associated increased pup mortality at PND14 in mice with improper dosage of the *Dkk1* gene also revealed that the mice exhibited delayed onset of this transition period as measured by adipose tissue<sup>203</sup>. However, in our model of developmental CdCl<sub>2</sub> exposure, there were no significant differences in white adipose tissue weight between groups for either sex. Another possible explanation for loss of viability in these mice is infanticide caused by maternal stress. Stress has been shown to alter maternal behavior in mice, leading to increased pup mortality<sup>205</sup>. Human exposure to Cd during pregnancy has been shown to increase anxiety<sup>206</sup>. However, further studies are required to test the hypothesis that Cd increases maternal stress and leads to increased pup mortality.

#### *Exposure to developmental CdCl<sub>2</sub> programs NAFLD in juvenile mice*

Exposure to Cd in adulthood has been associated with NAFLD<sup>16</sup>. However, increasingly younger individuals are being diagnosed with NAFLD each year. A recent study found an association between epigenetic alterations and liver disease in children, potentially indicating a role for the developmental environment in programming NAFLD<sup>207</sup>. In our study, mice exposed to 50 ppm CdCl<sub>2</sub> during gestation and early postnatal life presented with histological, biochemical, and molecular signatures of NAFLD at PND21, a timepoint corresponding to the onset of adolescence in rodents<sup>208</sup>. These data suggest that early life Cd exposure could be contributing to the increasing rates of juvenile NAFLD in humans.

A recent study, which examined the effects of life-long Cd exposure on high fat diet-induced NAFLD, reported that 5 ppm CdCl<sub>2</sub> exposure exacerbated high fat diet-induced NAFLD but CdCl<sub>2</sub>-exposed mice on a normal diet did not develop the disease<sup>209</sup>. Our 1 ppm CdCl<sub>2</sub> dose is comparable to the levels of Cd typically found in the Earth's crust<sup>2</sup>. We have previously shown

that 50 ppm CdCl<sub>2</sub> in this mouse model leads to blood Cd levels in dams of 5.23 ± 0.99 µg/L (mean ± standard error)<sup>188</sup>. This is similar to the blood Cd levels of ~6 µg/L observed in people in a contaminated area of Japan<sup>210</sup>. The different outcomes between this study and our own are most likely due to differences in CdCl<sub>2</sub> dose. In support of this, mice exposed to 1 ppm CdCl<sub>2</sub> in our own study did not present with NAFLD, indicating that the disease is induced in mice only by exposure to higher levels of Cd.

We identified sex-specific differences in Cd-induced NAFLD phenotypes at PND21. Both females and males presented with steatosis, the first major hallmark of NAFLD, while only females presented with the more advanced stage of fibrosis. This observation is consistent with previous studies reporting sex-specific differences in the metabolic response to developmental Cd exposure, which revealed female mice to be more susceptible to steatosis<sup>192</sup>. This could be explained by Cd having a longer half-life in females, both in mice and humans, and by the increased permeability of the female placenta to Cd<sup>189,211,212</sup>. The significance of this for human NAFLD is unclear since our understanding of sex-specific differences in susceptibility to this disease requires further study<sup>213</sup>.

Neither females nor males showed impaired glucose responses at PND76, indicating CdCl<sub>2</sub> exposure alone is not sufficient to program long-term glucose homeostasis dysregulation in this model, which is indicative of metabolic syndrome in mice. At PND90, there were no differences between the CdCl<sub>2</sub> exposure groups at the histological level. At this timepoint, control mice exhibited considerable accumulation of neutral lipids in hepatocytes, consistent with the propensity of C57Bl/6J mice to develop metabolic deficiencies in adulthood<sup>214</sup>. This result may also be linked to the different gene signatures associated with lipid metabolism and immune response at different liver developmental phases<sup>215</sup>. Genes relevant to steatosis and fibrosis overall

were no longer up-regulated at PND90 in Cd-exposed mice compared to controls. Our results indicate that developmental CdCl<sub>2</sub> exposure is sufficient to program juvenile NAFLD, but that differences are no longer discernible between groups in the absence of continued exposure. We and others have proposed a multiple-hit hypothesis for NAFLD whereby predisposed individuals require another insult to maintain NAFLD phenotypes in later life<sup>216</sup>. Our future work will test whether developmental Cd-induced NAFLD can persist into later life in the presence of a second environmental insult, a model that is potentially more consistent with the life-long exposures experienced by humans<sup>217</sup>.

In summary, our results support the hypothesis that Cd exposure during development is sufficient to program juvenile NAFLD in mice. For pediatric NAFLD in humans, Type 1 NAFLD exhibits steatosis with hepatocyte ballooning and fibrosis without inflammation and Type 2 is characterized by steatosis with inflammation and fibrosis<sup>218</sup>. Like the human juvenile NAFLD pathologies discussed in more detail in **Chapter 1**, the mice in our model exhibited evidence of steatosis and fibrosis, but not inflammation. Work in **Chapter 3** will exploit our model to determine the underlying mechanism that programs NAFLD in response to developmental CdCl<sub>2</sub> exposure.

## **Acknowledgements**

This study was supported in part by the following grants: R01ES031596, K22ES027510, P30ES025128, and T32ES007046. Paraffin-embedded liver sectioning, H&E, and Sirius red staining were performed by the NCSU Histology Laboratory. Cryosectioning was performed by the UNC Histology Research Core Facility. We would like to thank Dr. Scott Belcher and members of his lab for their advice on our cohort model, Dr. Arion Kennedy and members of her lab for

sharing their assay protocols with us, and other members of the Cowley lab and Dr. Jonathan Hall for their assistance with the GTT protocol. We are grateful to the NCSU Toxicology Animal Facility staff for their contributions, which enabled the successful completion of this work.

## **CHAPTER 3**

### **Developmental Cadmium-Induced Non-Alcoholic Fatty Liver Disease is Programmed via Up-Regulation of *Zac1* and the Imprinted Gene Network**

The following chapter has been submitted to a peer-reviewed journal as part of a larger publication.

## Abstract

In humans, exposure to cadmium (Cd) in adulthood is associated with non-alcoholic fatty liver disease (NAFLD), which is a progressive disease characterized by steatosis, inflammation, and fibrosis. NAFLD is predicted to be the leading cause of liver disease in children in the upcoming decade, suggesting a role for the developmental environment in programming susceptibility. In **Chapter 2**, we showed that developmental CdCl<sub>2</sub> exposure is sufficient to program NAFLD in our mouse model. However, the underlying mechanisms remain unclear. We have proposed that imprinted genes are strong candidates for connecting the early life environment and later disease. In support of this, we previously identified roles for the Imprinted Gene Network (IGN) and its regulator *Zac1* in programming NAFLD in response to maternal metabolic dysfunction. Here, we aim to test the hypothesis that developmental Cd-induced NAFLD is mediated by the imprinted gene *Zac1* and the IGN. Using the hybrid mouse model from **Chapter 2**, we show that transcriptomic analyses comparing livers of CdCl<sub>2</sub>-exposed and control mice show up-regulation of *Zac1* and the IGN coincident with disease presentation. Increased hepatic *Zac1* expression is independent of promoter methylation and imprinting statuses. Finally, we show that over-expression of *Zac1* in cultured hepatocytes is sufficient to induce lipid accumulation in a Ppar $\gamma$ -dependent manner, suggesting a direct link between *Zac1* and a key pathway underlying NAFLD pathogenesis. Together with our previous work, our findings establish *Zac1* and the IGN as key regulators of prosteatotic and profibrotic pathways, two of the major pathological hallmarks of NAFLD.

## Introduction

Cadmium (Cd) is toxic heavy metal that is naturally present in the soil at about 0.1-0.5 ppm<sup>3</sup>. However, human industrial processes such as waste incineration, fossil fuel combustion, and metal mining, have led to areas with high Cd levels<sup>7,9,10</sup>. The release of Cd into the environment is a public health concern because it contaminates food and water sources.

In children, adolescents, and adults, exposure to heavy metals has been associated with non-alcoholic fatty liver disease (NAFLD)<sup>9,126,219</sup>. Globally, about 20 % of adolescents are affected by NAFLD<sup>157</sup>. Children and adolescents are at higher risk of developing NAFLD if they are overweight or obese, have insulin resistance, type 2 diabetes, or dyslipidemia, follow a poor diet, do little to no exercise, or carry specific genetic polymorphisms<sup>153</sup>. NAFLD can be diagnosed through urine and blood tests, oral glucose tolerance tests, fibroscans, ultrasounds, and liver biopsies<sup>153</sup>.

NAFLD describes a spectrum of liver defects, including steatosis, inflammation, and fibrosis<sup>154</sup>. The pathogenesis of NAFLD includes the activation of pathways that disrupt lipid metabolism, promote inflammation, and drive fibrogenic transformation. The nuclear receptor peroxisome proliferator-activated receptor (PPAR) $\gamma$  is a major prosteatotic factor that heterodimerizes with retinoid X receptor  $\alpha$  to reprogram transcriptional networks involved in lipid storage and metabolism<sup>162</sup>. While the roles of this and other pathways in NAFLD progression have been extensively studied, the mechanisms through which NAFLD can be programmed by the developmental environment are not well characterized.

Epigenetic mechanisms have been proposed as mediators, but few specific examples of causative epigenetic changes have been described<sup>220,221</sup>. We and others have proposed that perturbation of imprinted genes, defined by their expression from a single parental allele, is a

candidate mechanism for disease programming because of the unique properties and modes of epigenetic regulation of imprinted genes during development. DNA methylation at Imprinting Control Regions (ICRs) is sensitive to environmental perturbation during development, including in response to Cd exposure in humans<sup>117,118,222</sup>. Once established, ICR epigenetic states are maintained throughout life, providing an epigenetic memory of the early life environment<sup>110</sup>. Imprinted genes also play key roles in liver development and energy homeostasis, suggesting that changes to their expression could influence hepatic metabolism<sup>223,224</sup>. In support of this idea, we previously demonstrated a novel role for imprinted genes in our model of NAFLD programmed by maternal metabolic syndrome<sup>136</sup>.

Many imprinted genes are coordinately expressed as part of an Imprinted Gene Network (IGN) controlled by the transcription factor *Zac1* (also called *Plagl1*), itself encoded by an imprinted gene<sup>112</sup>. The IGN, composed of 409 genes, regulates extracellular matrix composition and is implicated in muscle regeneration and adipocyte differentiation<sup>111,113</sup>. Using gene set enrichment analysis, we previously reported that IGN genes are highly predictive of ‘Hepatic Fibrosis’, adding further support for imprinted genes playing a role in programming liver disease<sup>136</sup>. We showed that artificial over-expression of *Zac1* in cultured hepatoma cells activated the IGN and increased procollagen production, a hallmark of fibrosis. This was associated with transcriptional up-regulation of the profibrogenic cytokine *Tgfβ-1* and activation of Tgfβ-1 signaling. Using chromatin immunoprecipitation (ChIP), we demonstrated binding of *Zac1* to the *Tgfβ-1* promoter, forming a direct link between imprinted genes and a major pathway underlying the pathogenesis of NAFLD-related fibrosis.

In **Chapter 2**, we showed that mice exposed to Cd during development have NAFLD as juveniles, presenting with steatosis and fibrosis. An advantage of mouse studies is that they provide

empirical mechanistic evidence for a link between different exposures, including Cd, and NAFLD, which can be difficult to determine in human epidemiological studies. Building on our findings in **Chapter 2**, we tested the hypothesis that developmental CdCl<sub>2</sub>-induced NAFLD is mediated by the imprinted *Zac1* gene in mice. We comprehensively evaluated mice exposed to CdCl<sub>2</sub> during development using molecular approaches. Using cultured mouse hepatocytes, we examined the role of *Zac1* in lipid accumulation via Ppar $\gamma$  signaling.

## **Materials and Methods**

### *Animal model and CdCl<sub>2</sub> exposure from Chapter 2*

Animal work was approved by the North Carolina State University Institutional Animal Care and Use Committee, under protocols 15-013-B and 19-049-B. Experiments were conducted in accordance with the Guiding Principles in the Use of Animals in Toxicology.

Female C57Bl/6J and male CAST/EiJ mice were obtained from Jackson Laboratory at three and four weeks old, respectively, and were allowed an acclimation period of one week before experimental manipulations. Mice were maintained on a 14-hour/10-hour light/dark cycle at 30-70 % humidity, 22°C  $\pm$  4°C and housed in Green Line IVC Sealsafe cage housing systems (Tecniplast) and fed AIN-93G rodent diet (Research Diets, D10012G) ad libitum for the duration of the study. At 4 weeks of age, female mice were provided unrestricted access to filtered drinking water (Millipore RiOs Essential RO water purification system) containing 0, 1, or 50 ppm cadmium chloride (CdCl<sub>2</sub>) (Sigma-Aldrich, 202908). At 9 weeks of age, female mice were mated with unexposed CAST/EiJ males (Figure 2.1a). CdCl<sub>2</sub> exposure ended when offspring reached postnatal day (PND) 10, the developmental equivalent of human birth<sup>195</sup> (Figure 2.1b).

The United States Environmental Protection Agency has determined the maximum contaminant level for Cd in drinking water is 0.005 ppm, which is much less than the water concentrations used in this study<sup>15</sup>. For humans, the Minimal Risk Level (MRL) from oral exposures lasting from 15 to 365 days is 0.5  $\mu\text{g Cd/kg/day}^2$ . Our mice in the 1 ppm and 50 ppm groups were exposed to 28  $\mu\text{g Cd/kg/day}$  and 1501  $\mu\text{g Cd/kg/day}$ , respectively. Though there is a large discrepancy between our doses and the MRL, there are regions of high Cd contamination where humans are exposed to 180 to 600  $\mu\text{g Cd/day}^{196}$ . Our female mice were exposed to about 0.5 to 26  $\mu\text{g Cd/day}$ , indicating that our model is still relevant to human exposures even though it exceeds the established MRL and EPA recommendation. Indeed, we have previously shown that both the 1 ppm and 50 ppm  $\text{CdCl}_2$  exposures lead to maternal blood Cd levels comparable to the circulating blood Cd levels of humans in polluted areas<sup>9,188,197</sup>.

F<sub>1</sub> offspring were euthanized at PND0 to standardize the litters to 6 pups with a male:female ratio of 3:3 whenever possible and tissues were collected and flash frozen. At PND21, a subset of F<sub>1</sub> mice were euthanized after a 6-hour fasting period and tissues were flash frozen and stored at -80°C until processing or prepared for histology as described below. The remaining F<sub>1</sub> mice were weaned at PND21 and given ad libitum access to AIN-93G diet until euthanasia at PND90 after a 6-hour fasting period, at which point tissues were collected and processed as described for PND21. The study was blinded until animals were selected for histological, biochemical, and molecular analyses. For both sexes in all three treatment groups at each timepoint, the 5-8 animals with liver masses closest to the mean for that group, avoiding animals from the same litter, were selected for further analyses.

### Cell culture

AML12 mouse hepatocytes (ATCC, CRL-2254) were cultured with Dulbecco's modified Eagle's medium (DMEM)/F-12 medium (Genesee Scientific, 25-503) containing 10 % fetal bovine serum (FBS) (Genesee Scientific, 25-514) and 100 U/mL penicillin, 100 µg/mL streptomycin (HyClone, SV30010), supplemented with a mixture of 10 µg/mL insulin, 5.5 µg/mL transferrin, 6.7 ng/mL selenium (Gibco, 41400-045), and 40 ng/mL dexamethasone (Sigma, D4902). Cells were maintained in a humidified atmosphere at 5 % CO<sub>2</sub> and 37°C. All cells used for experiments were under twenty passages.

### Transfection

AML12 cells were seeded at 400,000 cells/well in 6-well plates. Cells were starved with serum free medium for 24 hours. Transient expression of *EGFP* (control) or *Zac1* was achieved by transfecting cells with 1 µg of pLenti-CMV-EGFP or pLenti-CMV-Zac1-FLAG using Lipofectamine 3000 according to the manufacturer's instructions (ThermoFisher, L3000015). These constructs have been described previously<sup>136</sup>. For mRNA extraction and qRT-PCR, cells were collected 18 hours after transfection.

### Fatty acid and *Pparγ* inhibitor exposure

AML12 cells were cultured and transfected as described above. At 18 hours post-transfection, cells were exposed to DMEM/F-12 medium containing 50 µg/µL oleic acid-BSA (Sigma-Aldrich, O3008), 100 µg/µL oleic acid-BSA (Sigma-Aldrich, O3008), or comparable levels of BSA (Sigma-Aldrich, A7030) (control). After 24 hours, cells were prepared for histology as described below. For experiments involving the *Pparγ* inhibitor, cells were cultured, transfected, and exposed to fatty acids as described above. At the time of transfection, cells were dosed with 5 or 10 µg/µL of the *Pparγ* inhibitor T0070907 (Selleck Chemicals, S2871) that covalently modifies

its structure to prevent it binding to coactivators and DNA. The cells were then prepared for and processed through histology as described below.

### Histology

AML12 cells were stained with ORO (Sigma, O-0625) after culturing as described above. Briefly, cells were fixed in 10 % formalin (Midland Scientific, MSI N0019) for 5 minutes then dehydrated in 1,2-Propanediol (Sigma, 134368) for 1 minute. Cells were stained with 0.5 % ORO for 10 minutes at 60°C then rinsed with 1,2-Propanediol for 1 minute. The cells were counterstained for 15 seconds with Harris Hematoxylin (Sigma, HHS16) then placed in 0.5 % ammonium water (Ricca Chemical, 633-32) for 1 minute to improve contrast. Within 24 hours, ORO signal was quantified in Photoshop (Adobe). A minimum of three, discrete images were taken at 40X magnification, imported into Photoshop, and lipid color was selected. A fuzziness setting of 50 was applied to the selection color, all pixels with the color range within the image were selected and then pixel area was calculated using the software.

### Nucleic acid isolation

From **Chapter 2**: A portion of the left liver lobe for females and males at PND0, 21, and 90 was homogenized using a microtube homogenizer (Biospec 3110Bx Cell Disrupter 4800, BZ10124883) in Trizol reagent (Invitrogen, 15596026) according to the manufacturer's instructions. Nucleic acids were quantified on a Nanodrop 2000 and RNA integrity was confirmed using a 1.3 % agarose gel.

Additional method: AML12 cells were processed using the NucleoSpin kit (Macherey Nagel, 740955.250) according to the manufacturer's instructions to obtain RNA, which was quantified and validated as described above for liver tissue samples.

### qRT-PCR from Chapter 2

500 ng of total RNA from livers and cells was used to synthesize first strand cDNA according to the manufacturer's protocol (M-MLV RT enzyme, Promega). cDNA was diluted 1/5 or 1/10 for qRT-PCR, which was performed in triplicate on 96-well plates with a QuantStudio 3 system (Thermofisher) using SsoAdvanced Universal SYBR Green Supermix (Bio-Rad, 1725271) with standards in sequential dilution 1/5, 1/10, 1/20, 1/40, and 1/80 and water as a no template control (NTC). The cycling conditions were as follows: 95°C for 30 seconds; 40 cycles of 95°C for 15 seconds, 60°C for 30 seconds. The primer sequences are provided in Supp. Table 3.1. The dissociation curves showed that there were no products in the NTC and that primers amplified a single PCR product. Amplification efficiencies were calculated. Beta actin was used as a reference gene and was not significantly differentially expressed between treatment groups (data not shown). Gene expression was quantified using the  $\Delta\Delta C_t$  method<sup>198</sup>.

### DNA methylation analysis

350 ng of genomic DNA was treated with sodium bisulfite using the Zymo EZ DNA Methylation Kit (Zymo Research, D5006). Bisulfite-converted DNA (bsDNA) was amplified by PCR and products were confirmed on a 1.3 % agarose gel. PCR amplicons were then subjected to pyrosequencing using a Pyromark Q96 MD Pyrosequencer (Qiagen). The primer sequences and conditions are provided in Supp. Table 3.2. Methylation level was determined for each CpG dinucleotide using Pyromark software (Qiagen).

### Allele-specific expression analysis

cDNA was generated as described above and amplified by PCR using gene-specific primers. The hybrid model produced from crossing C57Bl/6J and CAST/EiJ strains produces over 20 million single nucleotide polymorphisms (SNPs) that can be used for target genes in this

analysis. Forward and reverse primers were designed using Pyromark software to include a SNP between the parental strains within the amplified and sequenced region to assign transcripts to the parental alleles. The primer sequences and conditions are provided in Supp. Table 3.2. Products were confirmed on a 1.3 % agarose gel and were subject to pyrosequencing using a Pyromark Q96 MD Pyrosequencer (Qiagen). The percent contribution of each allele to total transcript abundance was determined.

### RNA-sequencing

RNA samples isolated from PND0 and 21 female and male samples as described above were submitted for Illumina RNA library construction and sequencing. RNA integrity, purity, and concentration were assessed using an Agilent 2100 Bioanalyzer with an RNA 6000 Nano Chip (Agilent Technologies, USA). All samples used for RNA-sequencing (RNA-seq) had an RNA integrity number (RIN) > 9.0. cDNA libraries for Illumina sequencing were constructed using the NEBNext Ultra Directional RNA Library Prep Kit (NEB) and NEBNext Multiplex Oligos for Illumina (NEB) using the manufacturer-specified protocol. The samples were sequenced on one lane of an Illumina NovaSeq S4, utilizing a 150x2 bp paired end S4 sequencing reagent kit (Illumina, USA). The software package Real Time Analysis (RTA) was used to generate raw bcl files, which were then de-multiplexed by sample into fastq files for data submission.

An average of ~48.6 million paired-end RNA-seq reads were generated for each replicate. The quality of sequenced data was assessed using fastqc, and 12 poor-quality bases were trimmed from the 5'-end. The remaining reads were aligned to the mouse reference genome (mm38, version 100) downloaded from the Ensembl database using a STAR aligner with a WASP approach. This option allows mapping of one haplotype and supplies the other haplotype variants as VCF files (C57BL\_6NJ version 5 SNPs downloaded from dbSNP142)<sup>225</sup>.

For each replicate, per-gene counts of uniquely mapped reads were calculated using the htseq-count script from the HTSeq python package<sup>226</sup>. The count matrix was imported to R statistical computing environment for further analysis. Initially, genes that have no count in most replicate samples were discarded. The remaining count data were normalized for sequencing depth and distortion, and dispersion was estimated using the DESeq2 Bioconductor package<sup>227</sup>. A linear model was fitted using the treatment levels, and differentially expressed genes were identified after applying multiple testing corrections using the Benjamini-Hochberg procedure<sup>228</sup>. The data discussed in this publication have been deposited in NCBI's Gene Expression Omnibus and are accessible through GEO Series accession number GSE201906.

### Enrichment analysis

To enable comparison, the differentially expressed genes (DEGs) identified from the PND0 and 21 RNA-seq and the IGN and imprinted gene lists<sup>111</sup> were converted to Ensembl ID v104 using the Database Conversions tool (bioDBnet) and the ID history converter (Ensembl) for consistency prior to enrichment analysis (Supp. Table 3.3). After conversion, we retrieved 474/474 female PND0 DEGs, 347/347 male PND0 DEGs, 4600/4602 female PND21 DEGs, 4701/4701 male PND21 DEGs, and 408/409 IGN IDs, including 80 imprinted genes.

To assess enrichment of the IGN and imprinted genes within DEG datasets, only IGN and imprinted gene members expressed in the RNA-seq datasets were considered. The p-values were calculated based on the cumulative distribution function (CDF) of the dataset hypergeometric distribution (Graeber Lab) with  $k$  (number of successes) = number of IGN members within DEGs,  $s$  (sample size) = number of DEGs,  $M$  (number of successes in the population) = number of IGN members measured by RNA-seq, and  $N$  (population size) = total number of genes measured by RNA-seq (Table 3.1). The expected number of successes =  $(s*M)/N$ .

**Table 3.1.** Inputs for hypergeometric calculations of enrichment.

For cutoff p<0.05:	Imprinted Genes				IGN			
	PND0 Females	PND0 Males	PND21 Females	PND21 Males	PND0 Females	PND0 Males	PND21 Females	PND21 Males
k	1	0	30	31	12	5	178	178
M	66	66	66	66	373	373	373	373
N	16572	16572	16572	16572	16572	16572	16572	16572
s	474	347	4600	4701	474	347	4600	4701
Expected Successes	2	1	18	19	11	8	104	106

### Mapping analysis

RNA-seq reads from individual animals at PND21 were pooled based on sex and dose and converted to BAM files to enable them to be uploaded into Integrative Genomics Viewer (IGV) software for read mapping analysis. The SNP track (C57BL\_6NJ version 5 SNPs downloaded from dbSNP142) was converted to a BAM file as well. The IDs for the imprinted genes determined to be enriched between 0 and 50 ppm groups for both sexes were determined as described above. For both females and males, the number of reads aligning to either the maternal or paternal genome at a particular SNP for the enriched imprinted genes were counted for both the 0 and 50 ppm doses to enable gene imprinting status to be determined.

### Statistical analyses

Unless otherwise stated, statistical analyses were performed using a one-way analysis of variance (ANOVA) with Dunnett's post hoc test comparing 0 ppm to 1 ppm and 50 ppm CdCl<sub>2</sub> exposure groups using GraphPad Prism Version 8, or a Student's t-test, two-tailed, comparing 0 ppm and 50 ppm CdCl<sub>2</sub> exposure groups using Excel. Data are presented as the mean ± standard error of the mean. \*p<0.05, \*\*p<0.01, \*\*\*p<0.001, \*\*\*\*p<0.0001.

## Results

### Markers of the IGN are up-regulated at the transcriptional level at PND21

To determine if the IGN was dysregulated in our model of NAFLD, we initially performed qRT-PCR on a subset of IGN genes (*Cd36* (see **Chapter 2**), *Zac1*, *H19*, *Grb10*, *Igf2*, *Cdkn1c*, and *Mmp2*). At PND0, overall, the IGN genes examined were not dysregulated for either sex in response to CdCl<sub>2</sub> exposure (Figure 3.1a-b). However, at PND21, all representative IGN members except for *Mmp2* were up-regulated for both sexes in the 50 ppm group compared to controls (Figure 3.1c-d). At PND90, IGN dysregulation did not persist for females or males, with the exception of *H19*, which remained significantly up-regulated in males (Figure 3.1e-f). The phenotypic presentation of steatosis and fibrosis at PND21 is associated with up-regulation of IGN members suggesting a role for the IGN in CdCl<sub>2</sub>-induced juvenile NAFLD.

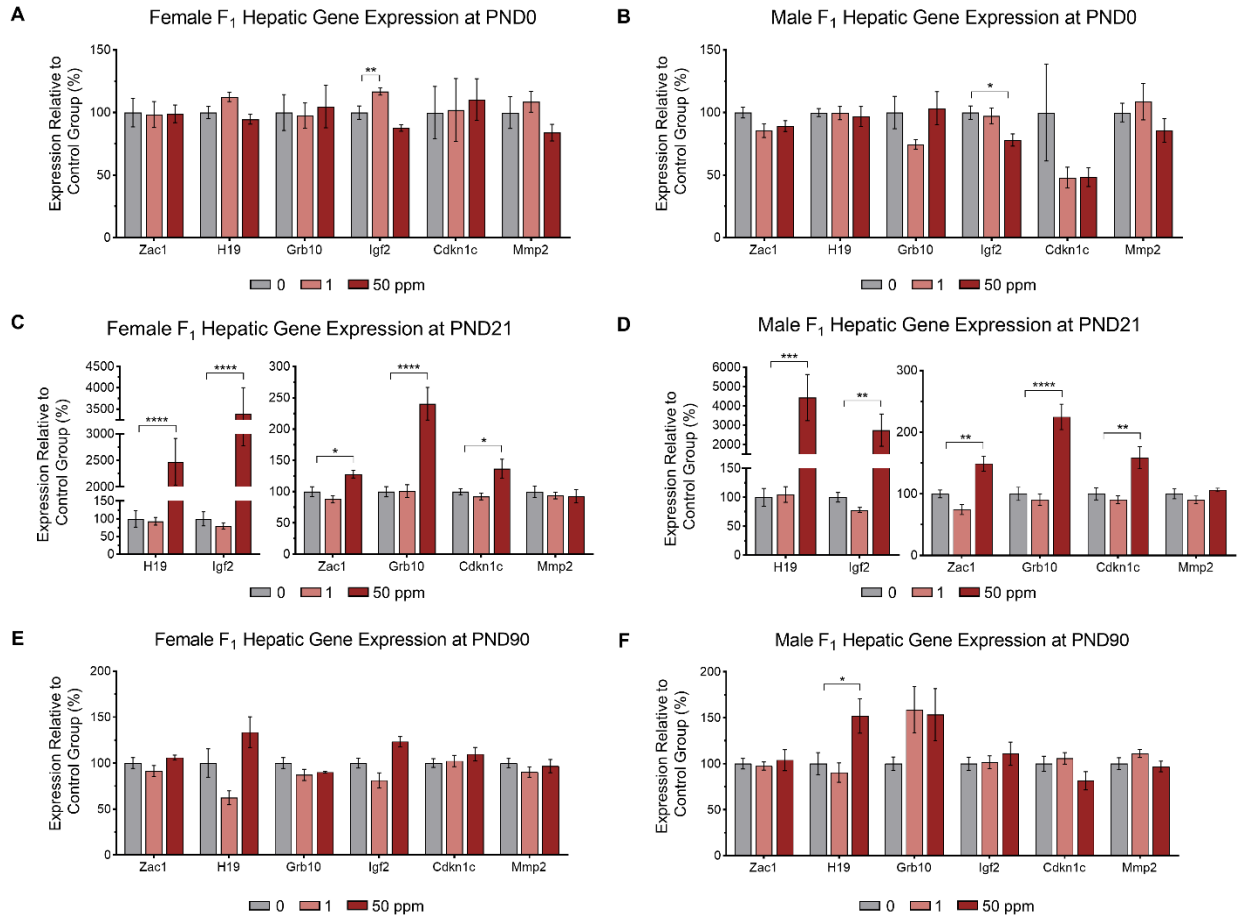


**Figure 3.1.** Effects of CdCl<sub>2</sub> exposure on F<sub>1</sub> hepatic gene expression at PND0, 21, and 90. (A-B) Female and male transcript abundance for genes of the IGN at PND0. (C-D) Female and male transcript abundance for genes of the IGN at PND21. (E-F) Female and male transcript abundance for genes of the IGN at PND90. All data are presented as means ± S.E. One-way ANOVA with Dunnett's post-hoc test comparing 1 ppm and 50 ppm CdCl<sub>2</sub>-exposed mice to 0 ppm controls. \*p<0.05, \*\*p<0.01, \*\*\*p<0.001, \*\*\*\*p<0.0001.

*The IGN is enriched among differentially expressed genes at PND21*

To determine the full extent of IGN genes that are dysregulated in response to developmental CdCl<sub>2</sub> exposure, RNA-seq of F<sub>1</sub> liver was performed on both sexes from the 0 ppm and 50 ppm groups at PND0 and 21. There were 474 and 347 differentially expressed genes (DEGs) (q-value<0.05) between the two groups for F<sub>1</sub> females and males, respectively, at PND0 (Supp. Table 3.3). At PND21, there were 4600 DEGs for F<sub>1</sub> females and 4701 DEGs for F<sub>1</sub> males between the two groups (Supp. Table 3.3). Genes of the IGN were not significantly over-

represented among PND0 DEGs for both F<sub>1</sub> females and males (Figure 3.2a-b) but were significantly over-represented among PND21 DEGs for both sexes (Figure 3.3a-b). At PND21, imprinted genes within the IGN were also significantly over-represented among DEGs for both sexes (Figure 3.3c-d), but not among PND0 DEGs (Figure 3.2c-d)

At PND0, though the IGN was not significantly enriched among DEGs for either sex, most of them were up-regulated by CdCl<sub>2</sub> exposure (Figure 3.2e-f). Most (87 % and 89 % for females and males, respectively) of the differentially expressed IGN genes at PND21 were up-regulated by CdCl<sub>2</sub> exposure (Figure 3.3e-f). Consistent with qRT-PCR data, *Zac1* was up-regulated by CdCl<sub>2</sub> exposure in both sexes in RNA-seq. Altogether, these data show that developmental CdCl<sub>2</sub> exposure is sufficient to up-regulate the IGN at PND21 and provides further support for a role for imprinted genes in the pathogenesis of NAFLD.

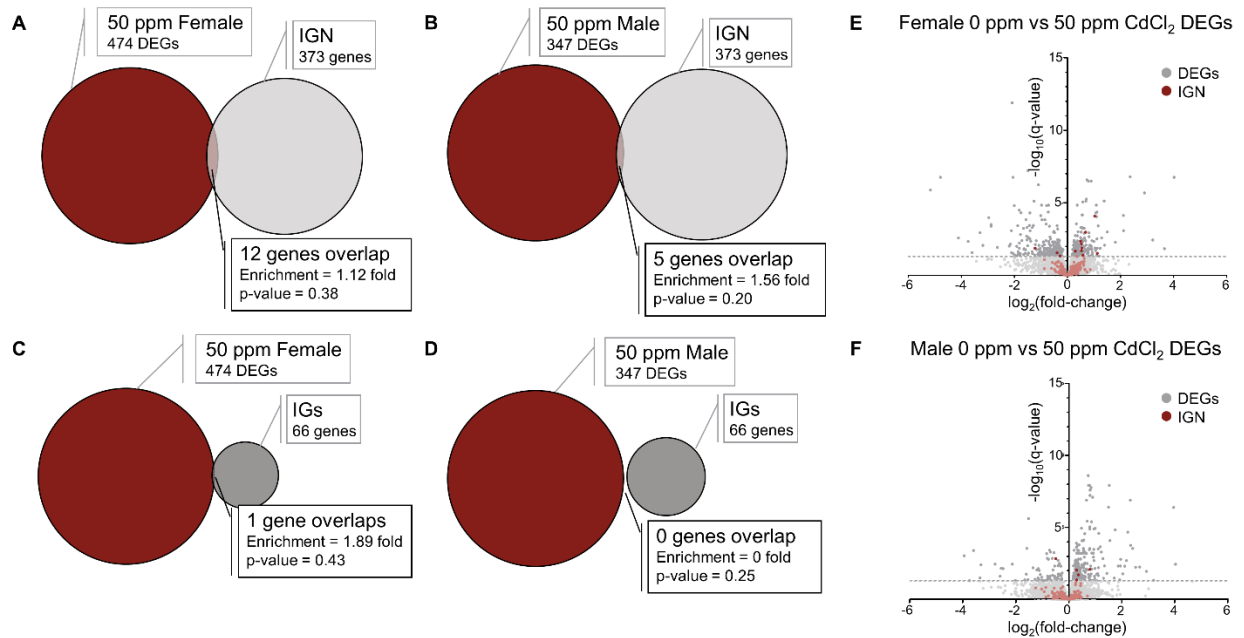


**Figure 3.2.** RNA-sequencing analysis on F<sub>1</sub> livers at PND0. (A-B) Venn diagrams represent the number of DEGs between the 0 ppm and 50 ppm CdCl<sub>2</sub> exposure groups and their intersection with the IGN, for females and males. (C-D) Venn diagrams represent the number of DEGs and their intersection with imprinted genes (IGs), for females and males. (E-F) Volcano plots showing the directionality of gene expression changes between 0 and 50 ppm CdCl<sub>2</sub> exposed female and male. IGN genes are indicated in red. Dashed line indicates q-value = 0.05. For (A-D): Enrichment was determined using a hypergeometric test. Circle sizes are proportional to number of genes.

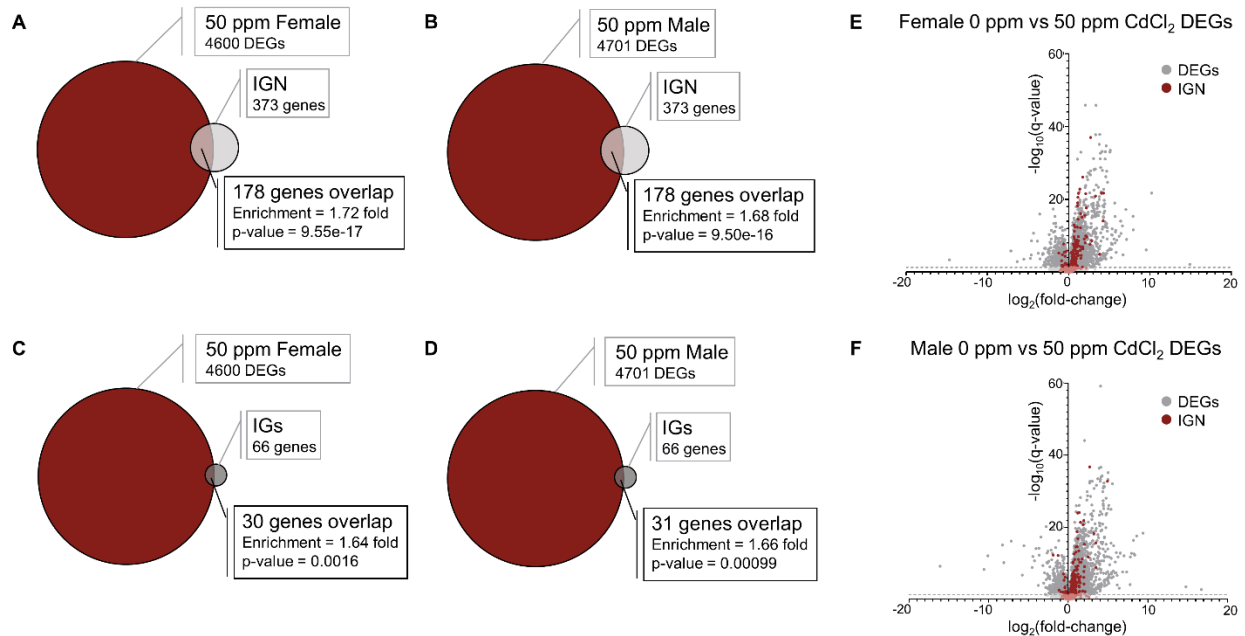


**Figure 3.3.** RNA-sequencing analysis on F<sub>1</sub> livers at PND21. (A-B) Venn diagrams represent the number of DEGs between the 0 ppm and 50 ppm CdCl<sub>2</sub> exposure groups and their intersection with the IGN, for females and males. (C-D) Venn diagrams represent the number of DEGs and their intersection with imprinted genes (IGs), for females and males. (E-F) Volcano plots showing the directionality of gene expression changes between 0 and 50 ppm CdCl<sub>2</sub> exposed female and male. IGN genes are indicated in red. Dashed line indicates q-value = 0.05. For (A-D): Enrichment was determined using a hypergeometric test. Circle sizes are proportional to number of genes.

*Zac1* up-regulation is independent of DNA methylation at its ICR

*Zac1*, the master regulator of the IGN, is a paternally expressed imprinted gene that is silenced on the maternally inherited allele by DNA methylation at its promoter-associated ICR (Figure 3.4a). Because developmental Cd exposure alters the epigenetic state of imprinted genes in humans<sup>118</sup>, we determined whether CdCl<sub>2</sub>-induced *Zac1* up-regulation in our mouse model was due to loss of DNA methylation at the ICR and inappropriate transcription from the maternally inherited allele. For both sexes, control mice showed the expected ~50 % methylation at the ICR, reflecting one methylated and one unmethylated allele (Figure 3.4b). Mice exposed to 50 ppm CdCl<sub>2</sub> showed no significant change in ICR methylation. These data show that *Zac1* up-regulation associated with CdCl<sub>2</sub> exposure is not due to a disruption of ICR DNA methylation.

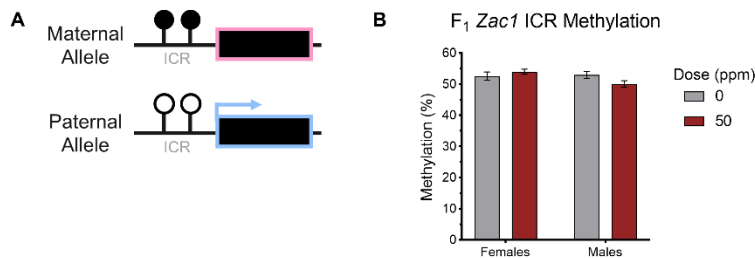


**Figure 3.4.** Determination of F<sub>1</sub> hepatic *Zac1* ICR methylation. (A) Diagram of the imprinted *Zac1* locus. Black boxes represent the *Zac1* gene, closed lollipops represent methylation at the ICR, and the blue arrow represents the transcription of the paternal allele for the gene. (B) *Zac1* ICR methylation levels in male and female 0 and 50 ppm CdCl<sub>2</sub>-exposed mice. Data are presented as means ± S.E. Student's t-test comparing 50 ppm CdCl<sub>2</sub>-exposed mice to 0 ppm controls.

*Zac1* up-regulation is not associated with loss of imprinting

We exploited our hybrid mouse model to measure transcription independently from the maternally and paternally inherited alleles using single nucleotide polymorphisms (SNPs) between the parental genomes. Consistent with no differences in DNA methylation at the *Zac1* ICR, mice from the 50 ppm CdCl<sub>2</sub> group showed no significant difference in allele-specific expression compared to controls (Figure 3.5).

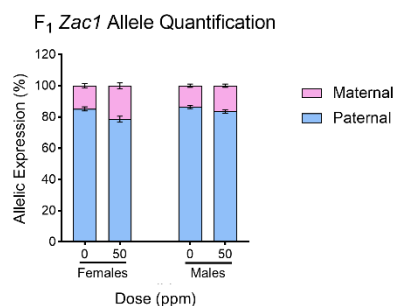


**Figure 3.5.** *Zac1* allele-specific expression in female and male 0 and 50 ppm CdCl<sub>2</sub>-exposed mice. Data are presented as means ± S.E. Student's t-test comparing 50 ppm CdCl<sub>2</sub>-exposed mice to 0 ppm controls.

*Differentially expressed imprinted genes within the IGN did not exhibit loss of imprinting overall*

Taking advantage of our ability to map our RNA-seq data to SNPs within the hybrid mouse genome using IGV software, we determined that both female and male mice from the 50 ppm

CdCl<sub>2</sub> group showed no difference in allele-specific expression of imprinted genes among the DEGs at PND21 when compared to controls overall (Supp. Table 3.4). Together these data show that *Zac1* and IGN up-regulation associated with CdCl<sub>2</sub> exposure is not due to loss of imprinting.

*Zac1 overexpression in cultured mouse hepatocytes is sufficient to promote lipid accumulation*

Our lab has previously shown that *Zac1* drives fibrosis in NAFLD programming<sup>136</sup>. In our model of developmental CdCl<sub>2</sub> exposure, the most striking NAFLD-related phenotype for both females and males is the accumulation of neutral lipids in hepatocytes at PND21. Consistent with this finding, expression of the major prosteatotic factor *Pparγ* is significantly increased in 50 ppm CdCl<sub>2</sub>-exposed mice (Figure 3.6a). A previous study using mouse neuronal cells suggested that *Zac1* regulates *Pparγ*, but whether this signaling pathway is conserved in hepatocytes, and whether *Zac1* plays a role in driving steatosis, have not been determined<sup>229</sup>. To test this, we artificially overexpressed *Zac1* in the AML12 mouse hepatocyte cell line (Figure 3.6b). *Zac1* overexpression was associated with significant up-regulation of *Pparγ* at 18 hours post-transfection compared to control cells over-expressing *EGFP* (Figure 3.6c).

Exposing cells to 50 or 100 μg/μL oleic acid-BSA led to a significant increase in the accumulation of neutral lipids in *Zac1* over-expressing cells compared to controls (Figure 3.7a-b). Together, these data suggest a link between *Zac1*, *Pparγ* expression and lipid accumulation in AML12 cells. To test the dependency of *Zac1*-induced lipid accumulation on *Pparγ* signaling, we treated *Zac1* overexpressing cells with the specific *Pparγ* inhibitor, T0070907, at 5 and 10 μg/μL in the presence of excess oleic acid-BSA. Both doses of the inhibitor significantly attenuated the *Zac1*-driven neutral lipid accumulation (Figure 3.7c-d), suggesting that *Zac1* drives lipid accumulation via the *Pparγ* signaling pathway.

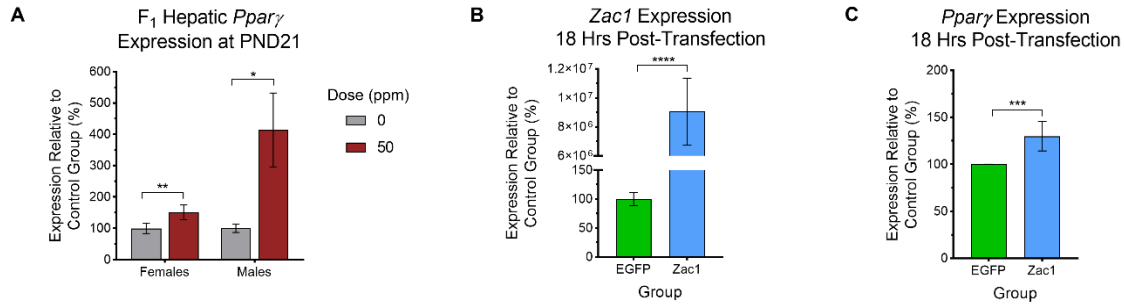


**Figure 3.6.** Association between *Zac1* and *Pparγ* expression. (A) *Pparγ* transcript accumulation in F<sub>1</sub> female and male livers at PND21. (B) *Zac1* transcript accumulation 18 hours after transfection. (C) *Pparγ* transcript accumulation in AML12 cells 18 hours after transfection. All data are presented as means  $\pm$  S.E. Student's t-test comparing 50 ppm CdCl<sub>2</sub> to 0 ppm control group and *Zac1* overexpressing cells to *EGFP* controls. \* $p < 0.05$ , \*\* $p < 0.01$ , \*\*\* $p < 0.001$ , \*\*\*\* $p < 0.0001$ .

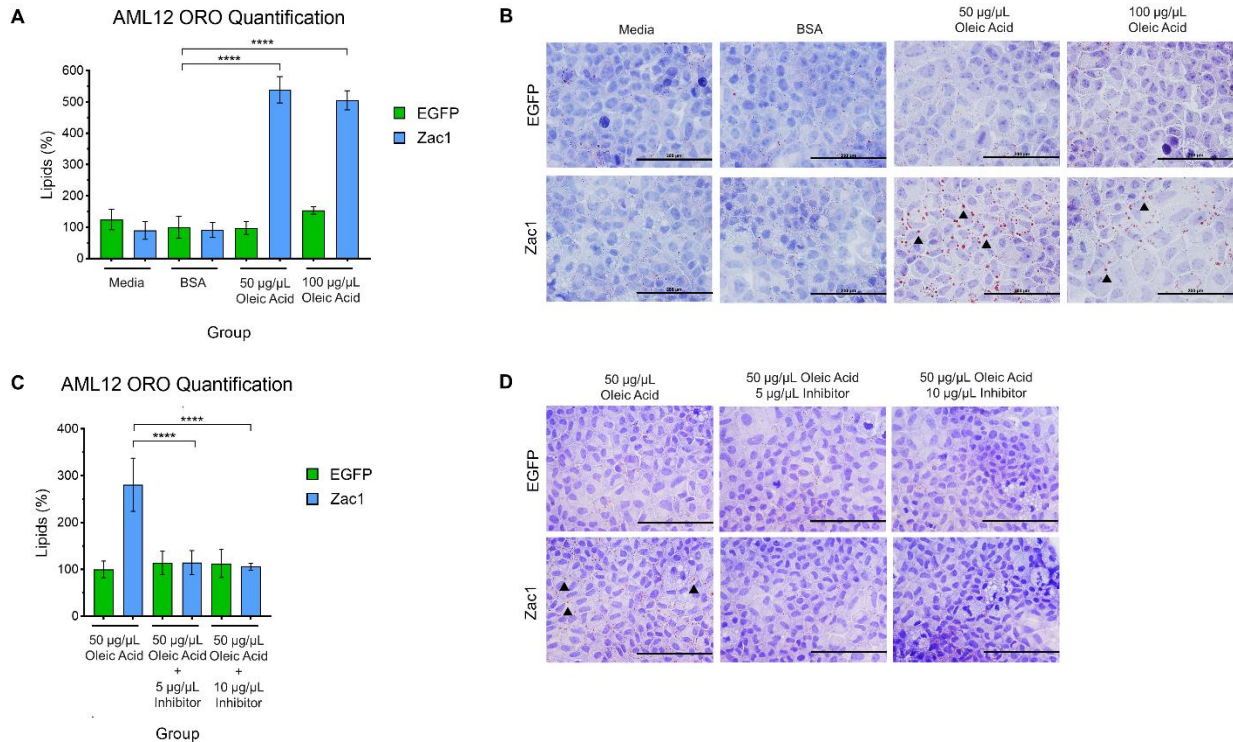


**Figure 3.7.** Role of *Zac1* in lipid accumulation. (A) Quantification of Oil Red O (ORO) staining of AML12 cells exposed to oleic acid-BSA. (B) Representative photomicrographs (40x) of ORO staining from quantification. (C) Quantification of ORO staining of AML12 cells exposed to 50 µg/µL oleic acid with or without 5 or 10 µg/µL T0070907 *Pparγ* inhibitor. (D) Representative photomicrographs (40X) of ORO staining from quantification. For (A, C): Data are presented as means ± S.E. \*\*\*\*p<0.0001. Data represent 3 independent experiments with N=3 replicates/condition. For (A) : One-way ANOVA with Dunnett’s post-hoc test comparing all conditions to *EGFP* overexpressing cells exposed to BSA. For (C) : One-way ANOVA with Dunnett’s post-hoc test comparing all conditions. For (B, D): Arrowheads indicate neutral lipids. Scale bars represent 200 µm. Data represent 3 independent experiments. Histology was quantified using a minimum of 3 discrete images/slide.

## Discussion

The release of the toxic heavy metal Cd into the environment as the result of anthropogenic activities poses a public health concern. Cd is poorly metabolized and excreted from the body, leading to the accumulation of it in the liver, kidneys, and bone and resulting in negative health effects<sup>3,17</sup>. National health surveys in Korea and the United States reveal associations between Cd exposure and liver-related mortality<sup>16,202</sup>. NAFLD is the leading type of chronic liver disease in the US, and observations in humans and model organisms suggest that NAFLD susceptibility can

be programmed by the developmental environment. However, the underlying causes and mechanisms remain unclear. We and others have proposed that imprinted genes are strong candidates for bridging the early developmental environment with later life disease. In support of this, we previously described a role for the imprinted gene *Zac1* in programming NAFLD in response to maternal metabolic syndrome<sup>136</sup>.

To explore the hypothesis that developmental Cd-induced NAFLD is mediated by *Zac1* and IGN signaling, we exposed hybrid mice to CdCl<sub>2</sub> from gestation to PND10 to mimic human gestational exposure. As shown in **Chapter 2**, 50 ppm CdCl<sub>2</sub> exposure resulted in NAFLD phenotypes. In support of our hypothesis, CdCl<sub>2</sub> exposure increased *Zac1* expression and up-regulated the IGN, a well-characterized transcriptional network of imprinted and biallelically-expressed genes. Artificial *Zac1* over-expression *in vitro* promoted lipid accumulation in a Ppar $\gamma$ -dependent manner. The findings of this study provide evidence that developmental Cd-induced NAFLD is mediated through *Zac1* and the IGN.

#### *CdCl<sub>2</sub> up-regulates Zac1 and the IGN*

Our lab previously showed that *Zac1* and the IGN are up-regulated in NAFLD programming after exposure to maternal metabolic syndrome, and that exposure specifically during postnatal development drives the phenotype<sup>136</sup>. Consistent with those findings, developmental exposure to 50 ppm CdCl<sub>2</sub> led to NAFLD-related phenotypes at PND21 (as shown in **Chapter 2**). At the same time, *Zac1* and the IGN are up-regulated in female and male livers, suggesting that these genes form a conserved mechanism that responds to different environmental stressors. Leveraging samples from the Newborn Epigenetics Study (NEST), we previously showed that DNA methylation at ICRs in humans is sensitive to Cd exposure in maternal and newborn cord blood, providing a potential mechanism for imprinted gene dysregulation<sup>118</sup>.

However, *Zac1* up-regulation in our mouse model was independent of methylation changes at its ICR, a finding that is mirrored at additional imprinted loci in other mouse models of developmental CdCl<sub>2</sub> exposure developed by our group<sup>199</sup>.

The differences in the epigenetic response to Cd between mice and humans could be explained by interaction effects from the diverse environmental stressors that humans are exposed to, which can be more carefully controlled in mouse studies. An alternative explanation is that our mouse model examines only the impact of maternal CdCl<sub>2</sub> exposure, whereas in human populations, paternal exposure to environmental insults influences offspring epigenetics. A recent study showed that exposure to Cd can impact the sperm methylome, although the impact this has on imprinted genes in offspring still needs to be determined<sup>230</sup>. Furthermore, the differences could be explained by species-specific variation in ICR sensitivity. Cd-induced *Zac1* up-regulation could occur via alternative epigenetic mechanisms. In embryonic carcinoma cells, the expression of *Zac1* has been shown to be regulated by histone acetylation, which is associated with gene expression<sup>231</sup>. Imprinted genes including *Zac1* are highly expressed in prenatal development; however, they are progressively down-regulated after birth by chromatin remodeling, a process mediated by the  $\alpha$ -thalassemia mental retardation X-linked (Atrx) protein<sup>232–234</sup>. Our future work will test the hypothesis that Cd exposure during this critical time-period disrupts Atrx function and the placement of repressive histone variants using CHIP.

#### *Zac1 regulates Ppar $\gamma$ signaling to drive steatosis*

Fibrosis is dependent upon interactions between hepatocytes and hepatic stellate cells (HSCs)<sup>169,235</sup>. Although we previously showed that hepatocyte-specific overexpression of *Zac1* is sufficient to induce fibrosis, the role of HSCs in this context requires further study<sup>136</sup>. However, hepatocytes are the primary drivers of liver steatosis<sup>236</sup>. It has been shown that NAFLD patients

have increased levels of hepatic *Ppar $\gamma$* , but the specific events triggering this up-regulation during disease progression have not yet been identified<sup>164</sup>. Another study in non-hepatic cell types indicated a link between *Zac1* and the prosteatotic gene *Ppar $\gamma$* <sup>229</sup>. Given our observations *in vivo*, we tested whether *Zac1* could be responsible for Cd-induced hepatic lipid accumulation through this pathway. Overexpressing *Zac1* in the presence of fatty acids in a murine hepatocyte cell line leads to significantly increased lipid accumulation, which can be abrogated by a *Ppar $\gamma$* -specific antagonist.

To summarize, our results support the hypothesis that imprinted genes play a central role in mediating between Cd exposure in development and juvenile NAFLD and, together with our previous findings, identify the imprinted gene *Zac1* as a novel regulator connecting prosteatotic and profibrotic pathways in hepatocytes. Work in **Chapter 4** will exploit this and other models of NAFLD in mice to determine whether *Zac1* and the IGN are part of a conserved hepatic response to environmental stressors.

## **Acknowledgements**

This study was supported in part by the following grants: R01ES031596, K22ES027510, P30ES025128, and T32ES007046. Next generation sequencing was performed by the NCSU Genomic Sciences Laboratory. RNA-sequencing analysis was performed in consultation with Dereje Lima from the Bioinformatics core within the NCSU Center for Human Health and the Environment. We are grateful to our collaborators at NCSU for their valuable advice.

## **CHAPTER 4**

### **Imprinted Gene Network Dysregulation is a Conserved Hepatic Response to Different Environmental Stressors**

The following chapter is the first draft of part of a publication that will be submitted to a peer-reviewed journal.

## Abstract

Non-alcoholic fatty liver disease (NAFLD) is a chronic liver disease characterized by steatosis, inflammation, and fibrosis. It affects 30 % of the adult US population and up to 20 % of children and young adults. NAFLD is predicted to be the leading cause of chronic liver disease in children worldwide in the upcoming decade, suggesting a potential role for the developmental environment in programming susceptibility. In humans, exposure to various environmental stressors such as xenobiotics and diet in adulthood is associated with NAFLD. In **Chapter 2**, we showed that developmental cadmium chloride ( $\text{CdCl}_2$ ) exposure is sufficient to program NAFLD in our mouse model. In **Chapter 3**, we showed that transcriptomic analyses comparing livers of  $\text{CdCl}_2$ -exposed and control mice showed up-regulation of *Zac1* and the Imprinted Gene Network (IGN) coincident with disease presentation. We also showed that over-expression of *Zac1* in cultured hepatocytes was sufficient to induce lipid accumulation in a Ppar $\gamma$ -dependent manner, suggesting a link between *Zac1* and steatosis, which is a key pathway underlying NAFLD pathogenesis. Here we test the hypothesis that up-regulation of *Zac1* and the IGN represent a conserved hepatic response to different environmental stressors and use an *in vitro* model of  $\text{CdCl}_2$  exposure to determine if the response is cell autonomous. Our findings establish *Zac1* and the IGN as a novel mechanism linking different developmental environmental stressors to NAFLD, providing potential therapeutic targets for further investigation.

## Introduction

Non-alcoholic fatty liver disease NAFLD describes a spectrum of liver defects, including steatosis, inflammation, and fibrosis<sup>154</sup>. Exposure to cadmium (Cd), carbon tetrachloride ( $\text{CCl}_4$ ), and 2,3,7,8-tetrachlorodibenzo-p-dioxin (TCDD) in adulthood has been linked to chronic liver

disease, specifically NAFLD<sup>16,219,237,238</sup>. However, toxicant exposure is not the only culprit that can lead to NAFLD, and studies reviewed in detail elsewhere indicate that diet can also play a role in NAFLD development<sup>239,240</sup>.

In support of the developmental origin of health and disease (DoHAD) hypothesis discussed in detail in **Chapter 1**, maternal exposure to endocrine disrupting chemicals, over- or undernutrition, and heavy metals have all been shown to negatively affect offspring health in later life<sup>122–124</sup>. For example, exposure to the endocrine disruptor TCDD during gestation is associated with lower neurodevelopmental, motor, and cognitive scores in children and with neurobehavioral deficits in mice<sup>241–244</sup>. A review of choline deficiency during pregnancy showed that it leads to altered neuron size and decreased electrophysiological responsiveness in mice<sup>245</sup>. Maternal metabolic syndrome has been associated with increased hepatic lipid accumulation in human offspring, and work from our lab and others have shown that it programs NAFLD phenotypes of steatosis and fibrosis in mice<sup>135–138</sup>. CCl<sub>4</sub> exposure during gestation in humans is associated with low birth weight and neural tube and palate defects<sup>246</sup>. Exposure to CCl<sub>4</sub> is a classic model for toxicant-induced liver disease in mice, though it is often combined with exposure to a high fat diet to more accurately recapitulate human NAFLD phenotypes<sup>247</sup>. As discussed previously, prenatal exposure to Cd in humans is associated with harmful effects on fetal development including altered birth weight and cognition<sup>20,21,117</sup>. In studies from our lab and others developmental Cd exposure has been linked to hypertension, metabolic syndrome, and DNA damage, and in **Chapter 2**, we showed that it can program NAFLD in mice<sup>188,192,248</sup>.

Increasingly younger people are being diagnosed with NAFLD each year, suggesting that susceptibility to NAFLD may be programmed by the environment during early life<sup>157</sup>. Research into this area is becoming more critical as pollution increases. Human industrial processes such as

waste incineration, fossil fuel combustion, and metal mining, have led to geographical areas with high Cd levels<sup>7,9,10</sup>. CCl<sub>4</sub> was used to make refrigerants and propellants, and though it is now limited to industrial use, workers can be exposed to it as well as individuals in areas polluted by historic CCl<sub>4</sub> waste<sup>249,250</sup>. Polychlorinated dioxin such as TCDD is mainly used in pesticides and herbicides, so exposure to TCDD usually occurs through occupational means or in areas polluted from industrial accidents<sup>251–253</sup>. The release of toxicants into the environment is a public health concern because they can contaminate food and water sources and lead to negative health outcomes, including NAFLD.

The pathways that promote NAFLD pathogenesis have been well studied; however, the mechanisms through which NAFLD can be induced by the environment are not well characterized. There are currently no FDA approved therapies for NAFLD as targets within the main pathogenesis pathways, including *Pparγ* and *Tgfb-1*, play critical roles in other cellular processes and as such their perturbation results in undesirable side effects, indicating a need to find other pathways critical to NAFLD development that could present novel targets for therapeutic interventions<sup>174</sup>. We previously demonstrated a novel role for imprinted genes in our models of NAFLD programmed by Cd exposure (in **Chapter 3**) and maternal metabolic syndrome<sup>136</sup>. Imprinted genes are expressed from a single parental allele, and many imprinted genes are part of an Imprinted Gene Network (IGN) controlled by the transcription factor encoded by the imprinted gene *Zac1* (also called *Plagl1*)<sup>112,113</sup>. Imprinted genes are known to play key roles in liver development and energy homeostasis, suggesting that changes to their expression could influence hepatic metabolism<sup>223,224</sup>. Supporting this role, we previously reported that IGN genes are highly predictive of ‘Hepatic Fibrosis’, using gene set enrichment analysis<sup>136</sup>.

Building on our findings in **Chapter 3**, we tested the hypothesis that the IGN is a conserved pathway that is up-regulated in the liver in response to different environmental stressors using publicly available RNA-sequencing (RNA-seq) and microarray data. We also used *in vitro* Cd exposure as a model of toxicant exposure to determine whether *Zac1* is up-regulated via a cell-autonomous mechanism in hepatocytes.

## **Materials and Methods**

### Literature search strategy

Searches were performed in PubMed, Web of Science, Google Scholar, and NC State University Libraries. The following terms were used: non-alcoholic fatty liver disease, chronic liver disease, steatosis, fibrosis, mouse, developmental exposure, adult exposure. The bibliographic reference lists of relevant research articles were manually searched for more articles. The literature search was limited to studies performed until February 2022 when this publication was written. In total, six studies were used in the analysis, including data from **Chapter 2** GSE201906 (CdCl<sub>2</sub> [BxC]), data from our collaborator GSE150679 (CdCl<sub>2</sub> [CD-1])<sup>192</sup>, another dataset from our lab GSE183809 (Ct-MetS)<sup>136</sup>, and datasets from other publications GSE81990 (TCDD)<sup>254</sup>, GSE73985 (CCl<sub>4</sub>)<sup>255</sup>, and GSE35961 (MCD)<sup>256</sup> (Supp. Table 4.1). CdCl<sub>2</sub> [BxC], CdCl<sub>2</sub> [CD-1], and Ct-MetS represent developmental exposures and TCDD, CCl<sub>4</sub>, and MCD represent adult exposures.

### Inclusion and exclusion criteria

Mouse model studies with publicly available RNA-seq or microarray data were included in the analysis. Studies were excluded from the analysis if they did not indicate NAFLD

phenotypes of either steatosis or fibrosis, were written in a language other than English, or identified fewer than 25 differentially expressed genes (DEGs), defined by a q-value < 0.05.

#### Data extraction and analysis

From **Chapter 3**: For CdCl<sub>2</sub> [BxC], the quality of sequenced data was assessed using fastqc, and 12 poor-quality bases were trimmed from the 5'-end. The remaining reads were aligned to the mouse reference genome (mm38, version 100) downloaded from the Ensembl database using a STAR aligner with a WASP approach. This option allows mapping of one haplotype and supplies the other haplotype variants as VCF files (C57BL\_6NJ version 5 SNPs downloaded from dbSNP142)<sup>225</sup>. For each replicate, per-gene counts of uniquely mapped reads were calculated using the htseq-count script from the HTSeq python package<sup>226</sup>. The count matrix was imported to R statistical computing environment for further analysis. Initially, genes that have no count in most replicate samples were discarded. The remaining count data were normalized for sequencing depth and distortion, and dispersion was estimated using the DESeq2 Bioconductor package<sup>227</sup>. A linear model was fitted using the treatment levels, and differentially expressed genes were identified after applying multiple testing corrections using the Benjamini-Hochberg procedure<sup>228</sup>.

Additional method: The MCD and CCl<sub>4</sub> microarray datasets were publicly available on GEO and were analyzed with GEO2R. Treatment and control groups were defined on the dropdown menu, and the corresponding groups were selected for each. The results were analyzed on the site and exported to Excel. The TCDD raw RNA-seq dataset was publicly available on GEO and the results were downloaded. For TCDD, Ct-MetS, and CdCl<sub>2</sub> [CD-1], the quality of sequenced data was assessed using fastqc, and 12 poor-quality bases were trimmed from the 5'-end. The remaining reads were aligned to the mouse reference genome (mm38, version 100) downloaded from the Ensembl database using a STAR aligner. For each replicate, per-gene counts

of uniquely mapped reads were calculated using the htseq-count script from the HTSeq python package<sup>226</sup>. The count matrix was imported to R statistical computing environment for further analysis. Genes that had no counts in most replicate samples were discarded, and the remaining count data were normalized for sequencing depth and distortion. Dispersion was estimated using the DESeq2 Bioconductor package<sup>227</sup>. A linear model was fitted using the treatment levels, and differentially expressed genes were identified after applying multiple testing corrections using the Benjamini-Hochberg procedure<sup>228</sup>.

### Enrichment analysis

To enable comparison, the total genes identified from the six studies and the IGN and imprinted gene lists<sup>111</sup> were converted to Ensembl ID v106 using the Database Conversions tool (bioDBnet) and the ID history converter (Ensembl) for consistency prior to enrichment analysis (Supp. Table 4.2). After conversion, we retrieved the following for each dataset: 408/409 IGN IDs including 83 imprinted genes, 4600/4602 female and 4701/4701 male DEGs for CdCl<sub>2</sub> [BxC], 445/446 PND21 and 5777/5789 PND42 DEGs for CdCl<sub>2</sub> [CD-1], 408/408 DEGs for Ct-MetS, 6093/6096 DEGs for TCDD, 6101/6219 DEGs for CCl<sub>4</sub>, and 4800/4805 DEGs for MCD.

To assess enrichment of the IGN and imprinted genes within DEG datasets, only IGN members and imprinted genes expressed in the RNA-seq and microarray datasets were considered. The p-values were calculated based on the cumulative distribution function (CDF) of the dataset hypergeometric distribution (Graeber Lab) with  $k$  (number of successes) = number of IGN members within DEGs,  $s$  (sample size) = number of DEGs,  $M$  (number of successes in the population) = number of IGN members measured by RNA-seq, and  $N$  (population size) = total number of genes measured by RNA-seq (Supp. Table 4.4). The expected number of successes =  $(s*M)/N$ .

### Ingenuity pathway analysis

The IDs of genes found to be significantly differentially expressed were used as input for core analysis using Ingenuity Pathway Analysis (IPA) software (Qiagen). A comparison analysis was performed between all the datasets. The upstream regulators were filtered to only consider the molecule type termed genes, RNAs and proteins.

### Cell culture

From **Chapter 2**: AML12 mouse hepatocytes (ATCC, CRL-2254) were cultured with Dulbecco's modified Eagle's medium (DMEM)/F-12 medium (Genesee Scientific, 25-503). All media contained 10 % fetal bovine serum (FBS) (Genesee Scientific, 25-514) and 100 U/mL penicillin, 100 µg/mL streptomycin (HyClone, SV30010), supplemented with a mixture of 10 µg/mL insulin, 5.5 µg/mL transferrin, 6.7 ng/mL selenium (Gibco, 41400-045), and 40 ng/mL dexamethasone (Sigma, D4902). Cells were maintained in a humidified atmosphere at 5 % CO<sub>2</sub> and 37°C. All cells used for experiments were under twenty passages.

Additional method: HepG2 cells (ATCC, HB-8065) were grown in high-glucose DMEM (Genesee Scientific, 25-501) supplemented as described above and under the conditions described above for AML12 cells.

### CdCl<sub>2</sub> exposure

AML12 and HepG2 cells were seeded at 20,000 cells/well in 96-well plates for viability assays and 600,000 cells/well in 6-well plates for mRNA extraction and qRT-PCR in triplicate. Cells were provided serum free medium for 24 hours then exposed to water (solvent control), media, 0.1, 0.5, 1, and 5 µM CdCl<sub>2</sub> (Sigma-Aldrich, 202908). For viability assays, cells were collected at 6, 24, and 48 hours after exposure. For mRNA extraction and qRT-PCR, cells were serum starved for 24 hours then exposed to water (control), media, 0.1, 0.5, and 1 µM CdCl<sub>2</sub>.

AML12 cells were collected at 24 and 48 hours after exposure. HepG2 cells were collected at 6, 12, 18, and 24 hours after exposure.

These concentrations and timings were based on other cell culture data in primary hepatocytes, AML12 cells, and HepG2 cells<sup>257-260</sup>. The expression of the gene *MT-1* was used as a positive control for Cd exposure based on previous work<sup>261</sup>.

#### Viability assay

AML12 and HepG2 cells were dosed as described above for the Cytotox-Glo viability assay (Promega, G9291) and processed and analyzed on a plate reader (FluoStar Omega, BMG Labtech) according to the manufacturer's instructions.

#### Nucleic acid isolation from **Chapter 2**

AML12 and HepG2 cells were processed using the NucleoSpin kit (Macherey Nagel, 740955.250) according to the manufacturer's instructions to obtain RNA. Nucleic acids were quantified on a Nanodrop 2000 and RNA integrity was confirmed using a 1.3 % agarose gel.

#### qRT-PCR from **Chapter 2**

1 µg of total RNA from cells was used to synthesize first strand cDNA according to the manufacturer's protocol (M-MLV RT enzyme, Promega). cDNA was diluted 1/5 or 1/10 for qRT-PCR, which was performed in triplicate on 96-well plates with a QuantStudio 3 system (ThermoFisher) using SsoAdvanced Universal SYBR Green Supermix (Bio-Rad, 1725271) with standards in sequential dilution 1/5, 1/10, 1/20, 1/40, and 1/80 and water as a no template control (NTC). The cycling conditions were as follows: 95°C for 30 seconds; 40 cycles of 95°C for 15 seconds, 60°C for 30 seconds. The primer sequences are provided in Supp. Table 4.3. The dissociation curves showed that there were no products in the NTC and that primers amplified a single PCR product. Amplification efficiencies were calculated. Beta actin was used as a reference

gene and was not significantly differentially expressed between treatment groups (data not shown). Gene expression was quantified using the  $\Delta\Delta\text{Ct}$  method<sup>198</sup>.

### Statistical analyses

Unless otherwise stated, statistical analyses were performed using a one-way analysis of variance (ANOVA) with Dunnett's post hoc test comparing CdCl<sub>2</sub> conditions to water (solvent control) using GraphPad Prism Version 8. Data are presented as the mean  $\pm$  standard error of the mean. \*p<0.05, \*\*p<0.01, \*\*\*p<0.001, \*\*\*\*p<0.0001.

## **Results**

### Study characteristics

Six mouse studies were used in the analysis and a detailed summary of each is provided in Supp. Table 4.1. Briefly, the CdCl<sub>2</sub> [BxC] study from **Chapter 2** examined C57Bl/6J x Cast/EiJ hybrid F<sub>1</sub> offspring after dams had been exposed to 0, 1, and 50 ppm CdCl<sub>2</sub> in drinking water from five weeks prior to mating until PND10. Markers of steatosis, inflammation, and fibrosis were measured at PND0, 21, and 90. Only the highest dose showed steatosis (males and females) and fibrosis (females only) at PND21. In the analysis for this study, both female and male PND21 RNA-seq data was used comparing the 50 ppm CdCl<sub>2</sub> group to the 0 ppm group.

The CdCl<sub>2</sub> [CD-1] study examined F<sub>1</sub> offspring from the outbred CD-1 strain after dams were exposed to 0 and 500 ppb CdCl<sub>2</sub> in drinking water from five weeks prior to mating until PND10. Markers of steatosis, inflammation, and fibrosis were measured at PND0, 21, 42, 90, and 120. Only steatosis was observed in females at PND42. In the analysis for this study, female PND21 and 42 RNA-seq data were used comparing the 500 ppb CdCl<sub>2</sub> group to the 0 ppb group.

The Ct-MetS study examined PND21 female C57Bl/6J F<sub>1</sub> offspring exposed to maternal metabolic syndrome (MetS) during prenatal development only (MetS-Ct), postnatal development only (Ct-MetS), throughout development (MetS-MetS), or never (Ct-Ct). Markers of steatosis and fibrosis were measured, and only the Ct-MetS group showed evidence of both phenotypes at PND21. Therefore, for the analysis for this study, RNA-seq data comparing the Ct-MetS group to the Ct-Ct group at this timepoint was used.

The TCDD study examined adult C57Bl/6J females orally gavaged with 0.1 mL sesame oil control or 0.01, 0.03, 0.1, 0.3, 1, 3, 10, or 30 mg/kg TCDD every fourth day beginning at PND28 for 92 days. Markers of steatosis, inflammation, and fibrosis were measured, and only the highest dose showed evidence of all three phenotypes of NAFLD. For the analysis for this study, RNA-seq data comparing the control group to the high dose group was used.

The CCl<sub>4</sub> study examined fibrosis in 5-week-old C57Bl/6J males exposed to a 25 % olive oil control or CCl<sub>4</sub> at 0.5 µL/g body weight via intraperitoneal injection twice per week for 8 weeks. Evidence for fibrosis was found, and microarray data comparing both groups was used in the analysis for this study.

The MCD study examined markers of steatosis, inflammation, and fibrosis in C57Bl/6J 8-week-old mice fed a normal chow or methionine- and choline-deficient (MCD) + high fat diet (HFD) with or without 0.1 % metformin for 8 weeks. All three phenotypes were observed in the MCD + HFD group without metformin, so microarray data comparing the MCD + HFD group to the chow control group was used in the analysis for this study.

#### *IGN enrichment among differentially expressed genes after different environmental exposures*

IGN and imprinted genes were examined for enrichment in publicly available RNA-seq and microarray data to determine the full extent of IGN genes that are dysregulated in response to

different environmental exposures during development. Genes of the IGN were significantly over-represented among all developmental exposure DEGs except for PND42 DEGs for CdCl<sub>2</sub> [CD-1] (Figure 4.1a-e). Imprinted genes within the IGN were only significantly over-represented among DEGs for the developmental exposures CdCl<sub>2</sub> [BxC] and Ct-MetS, but not the other developmental exposures (Figure 4.2a-e). Genes of the IGN were significantly over-represented among all adult exposure DEGs, but none of them showed enrichment of the imprinted genes among DEGs (Supp. Table 4.4). These results indicate that the IGN is conserved among DEGs for different environmental exposures occurring during gestation, postnatally, and in adulthood.

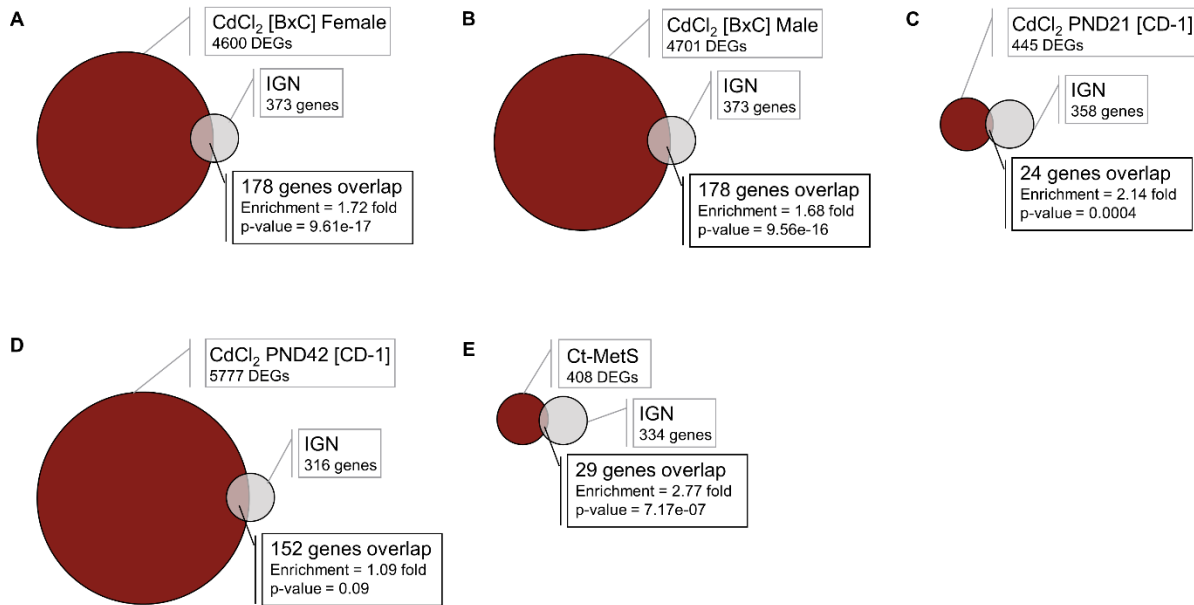


**Figure 4.1.** IGN gene enrichment among different developmental environmental exposure models. (A-B) Venn diagrams represent the number of DEGs between the 0 ppm and 50 ppm CdCl<sub>2</sub> exposure groups and their intersection with the IGN, for females and males. (C-D) Venn diagrams represent the number of DEGs between the 0 ppm and 500 ppb CdCl<sub>2</sub> exposure groups and their intersection with the IGN for PND21 and 42. (E) Venn diagrams represent the number of DEGs between the Ct-Ct and Ct-MetS exposure groups and their intersection with the IGN. Circle sizes are proportional to number of genes.

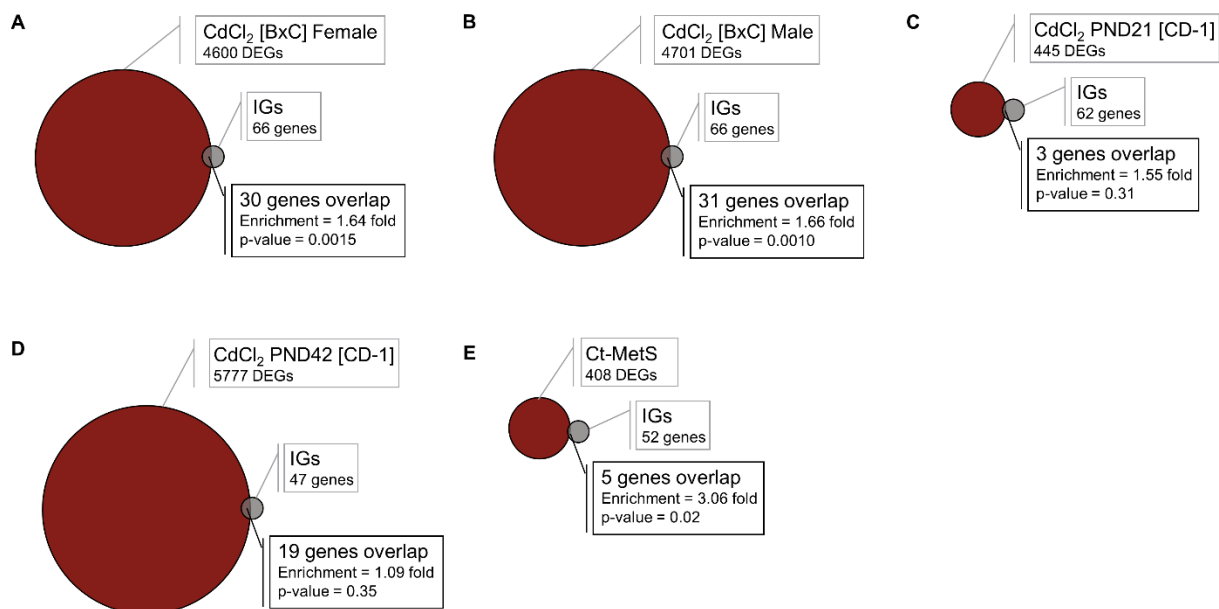


**Figure 4.2.** Imprinted gene enrichment among different developmental environmental exposure models. (A-B) Venn diagrams represent the number of DEGs between the 0 ppm and 50 ppm CdCl<sub>2</sub> exposure groups and their intersection with imprinted genes (IGs), for females and males. (C-D) Venn diagrams represent the number of DEGs between the 0 ppm and 500 ppb CdCl<sub>2</sub> exposure groups and their intersection with IGs for PND21 and 42. (E) Venn diagrams represent the number of DEGs between the Ct-Ct and Ct-MetS exposure groups and their intersection with IGs. Circle sizes are proportional to number of genes.

#### Directionality of IGN dysregulation by environmental exposures

To understand how members of the IGN respond to different environmental exposures, the IGN genes among the DEGs were examined for the various exposures for direction of dysregulation. All of the developmental exposures at PND21 showed overall up-regulation of IGN members within their DEGs (Table 4.1). The adult exposures to CCl<sub>4</sub> and MCD showed a higher proportion of down-regulated IGN members within their DEGs (Table 4.1). For TCDD, a higher proportion of IGN genes within DEGs were up-regulated (Table 4.1). These data show that these developmental exposures and exposure to TCDD in adulthood is sufficient to up-regulate the IGN.

**Table 4.1.** Direction of IGN gene dysregulation in response to different environmental exposures.

<b>Exposure Window</b>	<b>Exposure Model</b>	<b>Up-regulated (%)</b>	<b>Down-regulated (%)</b>
Developmental	CdCl <sub>2</sub> [BxC] Female	87.64044944	12.35955056
Developmental	CdCl <sub>2</sub> [BxC] Male	89.3258427	10.6741573
Developmental	Ct-MetS	86.20689655	13.79310345
Developmental	CdCl <sub>2</sub> [CD-1] PND21	83.33333333	16.66666667
Adult	TCDD	67.41573034	32.58426966
Adult	CCl <sub>4</sub>	11.45374449	88.54625551
Adult	MCD	18.31683168	81.68316832

*IGN member conservation between different exposures*

Since all the studies that were analyzed developed NAFLD phenotypes, shared genes could indicate a core subnetwork within the IGN. The datasets were analyzed to determine if a consistent set of IGN genes was shared between the different environmental exposure models. All exposure models share *Ccdc80*, *Col5a2*, and *Tmsb4x*, which are biallelically expressed genes (Supp. Table 4.5). The developmental models, CdCl<sub>2</sub> [BxC], CdCl<sub>2</sub> [CD-1] at PND21, and Ct-MetS, share these three genes as well as the imprinted gene *H19*, which was up-regulated. Consistent with the overall IGN dysregulation determined previously, *Ccdc80*, *Col5a2*, and *Tmsb4x* were all up-regulated in the developmental exposures and in the TCDD study, but down-regulated in the adult exposure models.

*Hepatic responses to different environmental stressors*

Transcriptome analysis was performed on all the datasets and compared in IPA to determine similarities in hepatic responses to different environmental stressors. Similar responses were observed between the CdCl<sub>2</sub> [BxC], Ct-MetS, CdCl<sub>2</sub> [CD-1] PND21, and TCDD datasets for canonical pathways, upstream regulators, and diseases and functions, with the TCDD and CdCl<sub>2</sub> [BxC] datasets showing more similar z-scores (Figure 4.3a-c). MCD and CCl<sub>4</sub> datasets also exhibited similar trends to each other for canonical pathways, upstream regulators, and diseases

and functions (Figure 4.3a-c). The CdCl<sub>2</sub> [BxC] and TCDD datasets showed positive activation z-scores for hepatic fibrosis signaling pathway, cell movement and leukocyte migration, and interleukin and SMAD3 signaling while the CdCl<sub>2</sub> [CD-1] dataset showed weak positive scores and the MCD and CCl<sub>4</sub> datasets showed an inverse response.

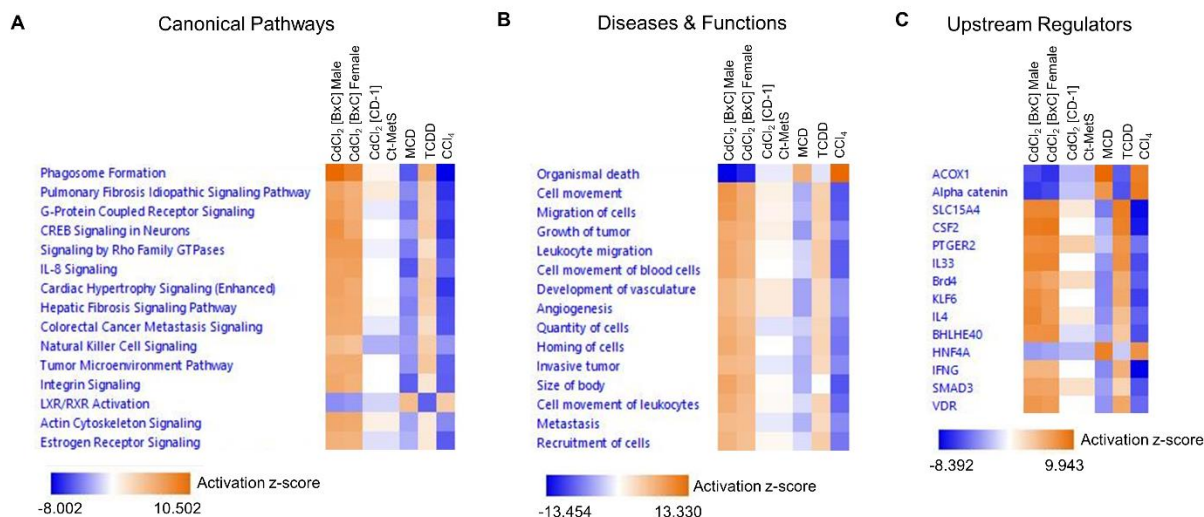


**Figure 4.3.** Hepatic transcriptome changes measured by RNA-sequencing and microarray analysis on different environmental exposure models. (A) Top canonical pathways and their associated activation z-scores. (B) Top diseases and functions and their associated activation z-scores. (C) Top upstream regulators and their associated activation z-scores.

Development of an in vitro model of Cd-induced toxicity: AML12 cells

In response to environmental exposures, the entire organism can be affected and cell signaling from other organs, such as adipose tissue, can alter how the liver responds to the exposure. Our lab has previously shown that *Zac1* dysregulation occurs in hepatocytes<sup>136</sup>, so to test if Cd-induced up-regulation of *Zac1* is cell autonomous, CdCl<sub>2</sub> exposure was modeled in the murine hepatocyte AML12 cell line. AML12 cells were originally isolated from normal mouse liver tissue and exhibit hepatocyte characteristics including peroxisomes and bile canalicular-like structures<sup>262</sup>, making them an ideal potential model.

Cyto-tox glo viability assays were performed on the cells in response to CdCl<sub>2</sub>. For AML12 cells at 6 hours, 0.1, 0.5, 1, and 5 μM CdCl<sub>2</sub> did not significantly decrease viability (Figure 4.4a). At 24 and 48 hours, 0.1, 0.5, and 1 μM CdCl<sub>2</sub> did not result in significantly altered viability (Figure 4.4b-c).

The *Mt-1* gene encodes the protein metallothionein, which is involved in Cd sequestration and handling as described in detail in **Chapter 1**. *Mt-1* was used to verify that the AML12 cells responded to CdCl<sub>2</sub> in a dose-dependent manner (Figure 4.5a-b). Having confirmed this, we tested whether CdCl<sub>2</sub> exposure affected *Zac1* expression. However, after 24 and 48 hours of exposure, *Zac1* could not be robustly detected via qRT-PCR (data not shown). Multiple primer sets were designed to target *Zac1*, but none were able to successfully amplify. This indicates that AML12 cells did not represent a suitable model for assaying the *Zac1* transcript abundance in response to CdCl<sub>2</sub> treatment.

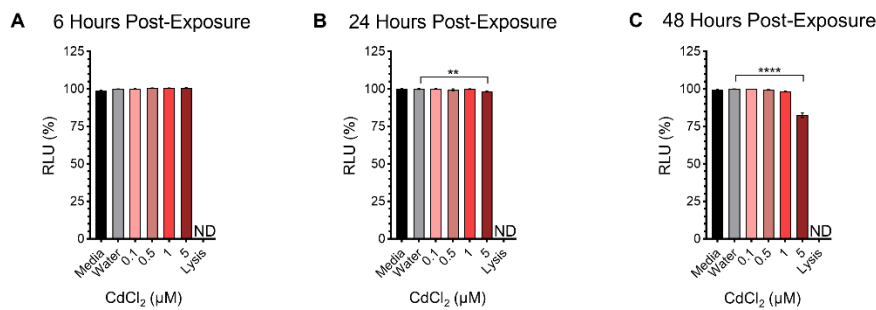


**Figure 4.4.** Viability of AML12 cells after CdCl<sub>2</sub> exposure. (A) Viability after 6 hours exposure. (B) Viability after 24 hours exposure. (C) Viability after 48 hours exposure. All data are presented as means ± S.E. One-way ANOVA with Dunnett's post-hoc test comparing CdCl<sub>2</sub> conditions to water (solvent control). \*\*p<0.01, \*\*\*\*p<0.0001. Data represent 3 independent experiments with N=3 replicates/condition. ND: not detected.

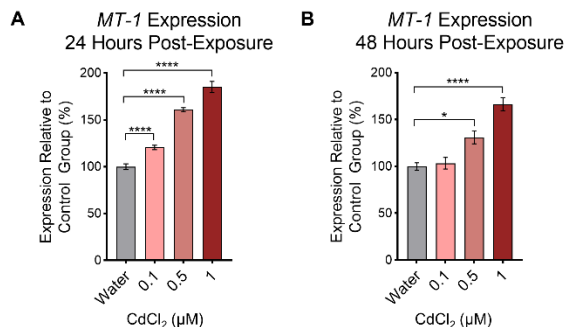


**Figure 4.5.** Effects of CdCl<sub>2</sub> exposure on *Mt-1* gene expression in AML12 cells. (A-B) *Mt-1* transcript accumulation after 24 and 48 hours exposure. All data are presented as means ± S.E. One-way ANOVA with Dunnett's post-hoc test comparing CdCl<sub>2</sub> conditions to water (solvent control). \*p<0.05, \*\*\*\*p<0.0001. Data represent 3 independent experiments with N=3 replicates/condition.

#### Development of an *in vitro* model of Cd-induced toxicity: HepG2 cells

Because of the limitation of the AML12 cell line, HepG2 cells were tested as a model of CdCl<sub>2</sub> exposure *in vitro*. HepG2 cells were derived from human hepatocellular carcinoma<sup>263</sup>. Cytotoxicity assays were performed on the cells in response to CdCl<sub>2</sub>. For HepG2 cells at 6 hours, 0.1, 0.5, 1, and 5 μM CdCl<sub>2</sub> did not significantly decrease viability (Figure 4.6a). As with the AML12 cells, HepG2 cells exposed to 5 μM CdCl<sub>2</sub> at 24 and 48 hours resulted in significantly decreased viability (Figure 4.6b-c).

Again, *Mt-1* expression was tested to verify that the HepG2 cells were responding to CdCl<sub>2</sub> in a dose-dependent manner. At 6, 12, 18, and 24 hours post-treatment, *Mt-1* was significantly up-regulated in 0.5 and 1 μM CdCl<sub>2</sub> (Figure 4.7a-d). These data confirm the validity of the model in testing the response to Cd at the transcriptional level. For HepG2 cells, *Zac1* was not significantly affected by CdCl<sub>2</sub> exposure at 6 hours post-exposure (Figure 4.7e). However, *Zac1* was down-regulated at 12, 18, and 24 hours post-exposure in response to 0.5 and 1 μM CdCl<sub>2</sub> (Figure 4.7f-h). These data indicate that the up-regulation of *Zac1* *in vitro* is not cell autonomous, and the HepG2 cell models of CdCl<sub>2</sub> exposure is not representative of *Zac1* dysregulation *in vivo*.

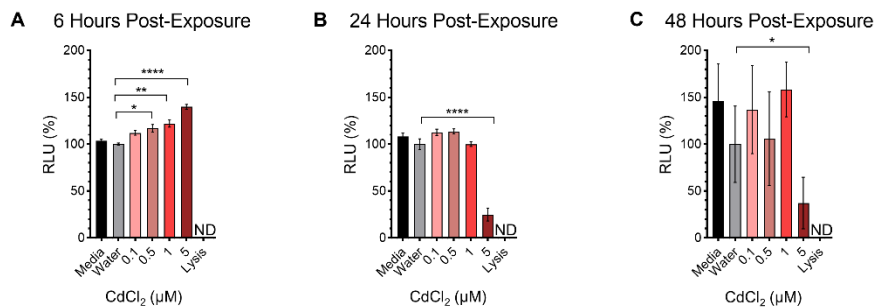


**Figure 4.6.** Viability of HepG2 cells after CdCl<sub>2</sub> exposure. (A) Viability after 6 hours exposure. (B) Viability after 24 hours exposure. (C) Viability after 48 hours exposure. All data are presented as means ± S.E. One-way ANOVA with Dunnett's post-hoc test comparing CdCl<sub>2</sub> conditions to water (solvent control). \*p<0.05, \*\*p<0.01, \*\*\*p<0.0001. Data represent 3 independent experiments with N=3 replicates/condition. ND: not detected.

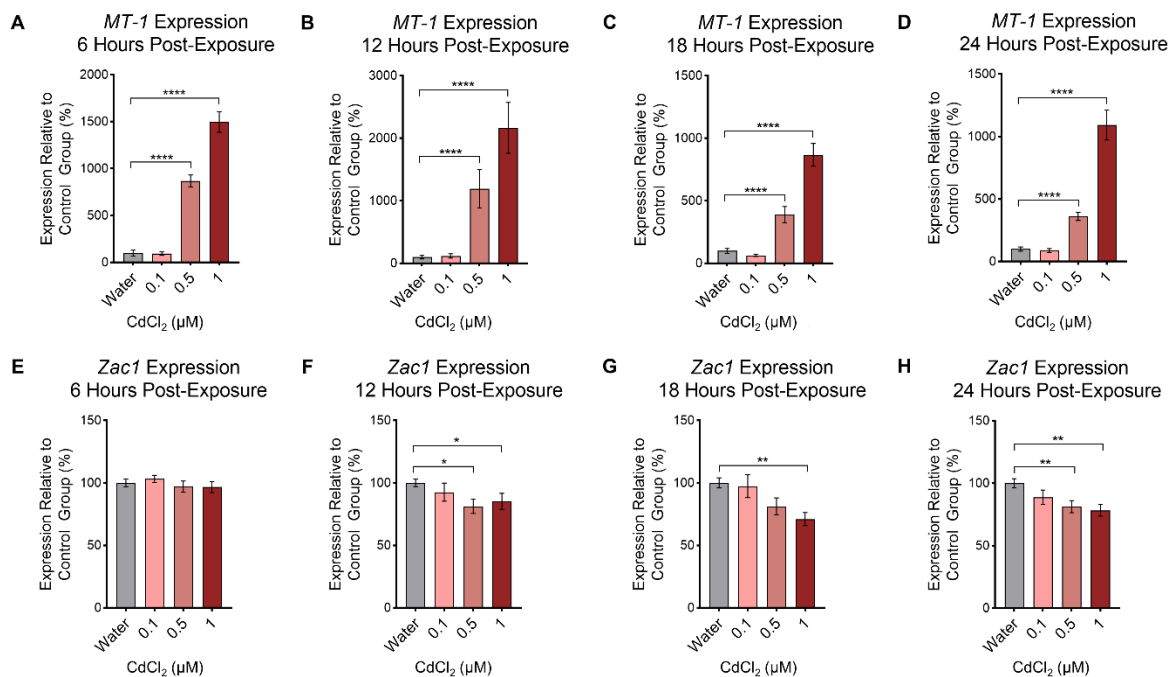


**Figure 4.7.** Effects of CdCl<sub>2</sub> exposure on HepG2 gene expression. (A-D) *MT-1* transcript accumulation after 6, 12, 18, 24 hours exposure. (E-H) *Zac1* transcript accumulation after 6, 12, 18, 24 hours exposure. All data are presented as means ± S.E. One-way ANOVA with Dunnett's post-hoc test comparing CdCl<sub>2</sub> conditions to water (solvent control). \*p<0.05, \*\*p<0.01, \*\*\*p<0.0001. Data represent 3 independent experiments with N=3 replicates/condition.

## Discussion

Human industrial processes have led to areas of increased Cd, CCl<sub>4</sub>, and TCDD, which have negative health impacts<sup>2,7,9,10,250–253</sup>. The release of toxic environmental contaminants into the environment is a public health concern because they can contaminate food and water sources and lead to negative health outcomes, including NAFLD. Each year, increasingly more children and adolescents are being diagnosed with NAFLD, suggesting that susceptibility to it may be programmed by the developmental environment<sup>157</sup>. Evidence suggests that maternal nutrition can also impact the future health of offspring<sup>124</sup>.

The pathways that promote NAFLD pathogenesis have been well studied; however, the mechanisms through which NAFLD can be induced by the environment are not well understood. Our lab has previously demonstrated a novel role for imprinted genes in our models of NAFLD programmed by Cd exposure (in **Chapter 3**) and maternal metabolic syndrome<sup>136</sup>. To further explore the hypothesis that *Zac1* and IGN up-regulation represents a conserved pathway through which different environmental exposures program NAFLD, we analyzed publicly available RNA-seq and microarray data. In support of our hypothesis, the IGN was enriched in all the exposure models; moreover, it was up-regulated in the developmental exposure and adult TCDD models. The findings of this study provide evidence that developmental exposure-induced NAFLD is mediated through the IGN.

### *Transcriptomic trends between the different exposure models*

The CdCl<sub>2</sub> [BxC] and TCDD datasets showed positive activation z-scores for hepatic fibrosis signaling pathway, cell movement and leukocyte migration, and interleukin and SMAD3 signaling, which are all indicative of NAFLD pathologies of steatosis, inflammation, and fibrosis. IL-33 was associated with a positive z-score in these datasets, and injured hepatocytes release IL-

33 to drive HSC activation<sup>264</sup>. Macrophages in the liver promote inflammatory responses by also releasing interleukins<sup>169</sup>. SMAD3 phosphorylation leads to the production of type I and III collagens<sup>165,169</sup>.

*The IGN is a conserved, dysregulated network in response to different exposure models*

The IGN was significantly enriched in all the exposure models; however, it was up-regulated in the developmental models (Ct-MetS, CdCl<sub>2</sub> [BxC], CdCl<sub>2</sub> [CD-1]) and TCDD but down-regulated in the MCD and CCl<sub>4</sub> adult models. The difference in response of the members within the IGN between the adult exposures of TCDD, MCD, and CCl<sub>4</sub> could be caused by the disparities between the dosing timelines. The mice exposed to TCDD were exposed beginning at PND28, which was multiple weeks before the CCl<sub>4</sub> and MCD exposures began, potentially indicating that the IGN is still responsive to prolonged up-regulation at this timepoint.

The IGN was similarly up- or down-regulated in the models where exposure timings and phenotypic outcomes were more closely matched such as between the adult exposures (CCl<sub>4</sub> and MCD) and developmental exposures. Supporting this finding, another study using a diet-induced animal model of NAFLD revealed that the expression of genes are differentially regulated at different timepoints and points in the course of NAFLD progression<sup>265</sup>, indicating that members of the IGN may have temporal or phenotypic regulatory roles in NAFLD development. To overcome some of the discrepancies between these studies, a similar type of analysis could be performed on samples collected at similar timepoints from different environmental exposures dosed similarly such as those from the Toxicant Exposures and Responses by Genomic and Epigenomic Regulators of Transcription (TaRGET) Program<sup>266</sup>.

From the IGN, the biallelically expressed genes, *Ccdc80*, *Col5a2*, and *Tmsb4x* were shared between all the exposure models. These genes, as well as the imprinted gene *H19*, were shared

among the developmental models. *H19* up-regulation has been implicated in NAFLD progression by promoting lipid accumulation and fibrogenesis<sup>267,268</sup>. *Ccdc80*, *Col5a2*, and *Tmsb4x* were up-regulated in the developmental models and TCDD, but down regulated in the adult exposure models. The adult models presented with fibrosis and steatosis outcomes, so this could be the result of a negative feedback signaling mechanism or could indicate a difference in the roles for these genes in NAFLD development temporally. Collagens are known to play a role in fibrotic livers<sup>169</sup>. Thymosin beta-4 is encoded by *Tmsb4x*, and has been implicated in hepatic stellate cell activation<sup>269</sup>. Recent studies have linked *Ccdc80* with altered lipid metabolism in mice<sup>270,271</sup>; however, more research is needed to fully understand the mechanism of *Ccdc80* in the liver in NAFLD pathogenesis. Like thiazolidinedione agonizing *Pparγ* in adipocytes for type 2 diabetes treatment, targeting *Ccdc80* may help alleviate this risk factor for NAFLD<sup>174</sup>, but this requires further interrogation.

#### *Zac1* response to *CdCl<sub>2</sub>* in vitro

Our lab has previously shown that *Zac1* up-regulation occurs in hepatocytes<sup>136</sup>. *CdCl<sub>2</sub>* exposure was modeled in the murine hepatocyte AML12 cell line and the human hepatoma HepG2 cell line to test if Cd induced up-regulation of *Zac1* is cell autonomous. *Zac1* could not be reliably detected in AML12 cells, though *Mt-1* expression was dose-responsive to *CdCl<sub>2</sub>*. Zinc is known to stimulate metallothionein expression, and supplementation with zinc has been shown to mitigate Cd toxicity<sup>33</sup>. AML12 cells are cultured in DMEM-F12 media, which contains zinc. Though *Mt-1* responded to Cd in the AML12 model, the background levels were already high as indicated by a low Ct value compared to HepG2 cells via qRT-PCR (data not shown). The HepG2 cells responded to Cd; however, the dynamics of *Zac1* did not recapitulate what was observed *in vivo*. This could be caused by differences between *in vivo* and *in vitro* models or differences in *Zac1* signaling in

response to Cd between the species. More likely, signaling in the form of circulating microRNAs (discussed in more detail in **Chapter 1**) or other small molecules between the pancreas, adipose tissue, and digestive tract is responsible for the dysregulation of *Zac1* *in vivo*<sup>272</sup>, but this needs to be tested empirically. Future studies in our lab plan to expand on the AML12 cell model by using toxicants that do not interact with metallothionein to determine if *Zac1* up-regulation in response to those exposures is cell autonomous and to further study its mechanism of action. However, in **Chapter 3**, AML12 cells were used to elucidate the mechanism through which *Zac1* programs lipid accumulation via the Ppar $\gamma$  signaling pathway using a *Zac1* overexpression construct. Determining its mechanism in response to CdCl<sub>2</sub> exposure will have to be undertaken *in vivo*.

In summary, our results support the hypothesis that the IGN is a conserved pathway in the liver that is dysregulated in response to different environmental stressors. Whether the conserved genes between the exposure models that were identified here can be exploited as therapeutic targets to alleviate NAFLD outcomes requires further study.

## **Acknowledgements**

This study was supported in part by the following grants: R01ES031596, K22ES027510, P30ES025128, and T32ES007046. RNA-sequencing was performed in consultation with Dereje Lima from the Bioinformatics core within the NCSU Center for Human Health and the Environment.

## CHAPTER 5

### Conclusions & Future Directions

The toxic heavy metal cadmium (Cd) is a top ten chemical of public health concern according to the World Health Organization. Exposure to it during gestation and adulthood have been shown to lead to various negative health outcomes discussed previously in this dissertation. Overall, the research described here sought to understand 1) if developmental exposure to CdCl<sub>2</sub> could program non-alcoholic fatty liver disease (NAFLD), 2) if imprinted genes, including *Zac1* and other members of the Imprinted Gene Network (IGN), are dysregulated in response to developmental CdCl<sub>2</sub> exposure and contribute to NAFLD pathologies, 3) if the IGN is a conserved network that is dysregulated in response to different environmental stressors. We modified a mouse exposure paradigm used previously in our lab and used this to test the effects of two doses of CdCl<sub>2</sub>: 1 ppm that represents an environmentally relevant low-dose and 50 ppm, which produces maternal circulating blood levels similar to those observed in humans in areas with high Cd pollution<sup>9,10,210</sup>. Utilizing our mouse model in combination with cell culture models, we were able to interrogate possible mechanisms through which developmental CdCl<sub>2</sub> exposure acts to program NAFLD.

As discussed throughout this dissertation, increasing evidence from human and animal studies shows that maternal exposures to environmental stressors, including to the toxic heavy metal Cd, are associated with negative health outcomes in offspring, supporting the theory of developmental origins of health and disease. Therefore, to contribute to this body of knowledge, we tested the hypothesis that maternal CdCl<sub>2</sub> exposure is sufficient to program NAFLD in offspring in **Chapter 2**. Using histological, biochemical, and molecular techniques, we showed that offspring exposed to 50 ppm CdCl<sub>2</sub> developed steatosis (females and males) and fibrosis

(females) at postnatal day (PND) 21, a time point that corresponds to the onset of adolescence in rodents and offers many comparisons to human juvenile NAFLD<sup>208</sup>. The sex-specific differences in Cd-induced NAFLD observed in our study are consistent with another recent study, which revealed female mice to be more susceptible to Cd-induced steatosis; however, that study did not identify evidence of fibrosis<sup>192</sup>. Our study is, therefore, the first to demonstrate that developmental CdCl<sub>2</sub> exposure is sufficient to program phenotypes associated with advanced NAFLD. Future studies can utilize our model to test potential therapeutic interventions for both steatosis and fibrosis, two major pathologies underlying NAFLD.

In **Chapter 3**, we tested the hypothesis that developmental CdCl<sub>2</sub>-induced NAFLD is programmed by dysregulation of the Imprinted Gene Network (IGN) and its master regulator, the imprinted gene *Zac1*. Exploiting our mouse model of developmental CdCl<sub>2</sub>-induced NAFLD at PND21 from **Chapter 2**, we showed that 50 ppm exposure increased *Zac1* expression and up-regulated the IGN in the liver at the same time. Though evidence from our lab suggests that hepatocytes are the primary hepatic cell types in which *Zac1* and IGN respond to environmental stress<sup>136</sup>, our RNA-sequencing (RNA-seq) analysis was performed on bulk tissue. Future studies can take advantage of cell sorting and single cell RNA sequencing to confirm for the first time that hepatocytes are responsible for the majority of prosteatotic Ppar $\gamma$  and profibrotic Tgf $\beta$ -1 signaling after Cd exposure.

Results from a previous study from our lab analyzing samples from the Newborn Epigenetics Study (NEST) showed that DNA methylation at imprinting control regions (ICRs) in humans is sensitive to Cd exposure in maternal and newborn cord blood<sup>118</sup>. This provided a potential mechanism for imprinted gene dysregulation in our model; however, *Zac1* up-regulation in mice was independent of methylation changes at its ICR, consistent with results observed at

additional imprinted loci in other mouse models of developmental CdCl<sub>2</sub> exposure developed by our group<sup>199</sup>, indicating another mechanism is responsible.

A study in non-hepatic cell types indicated a link between *Zac1* and the prosteatotic gene *Pparγ*<sup>229</sup>. Given our observations of steatosis in both sexes *in vivo*, we tested whether *Zac1* could be responsible for Cd-induced hepatic lipid accumulation through this pathway. We artificially overexpressed *Zac1* in a murine hepatocyte cell line, promoting lipid accumulation in a *Pparγ*-dependent manner, which could be abrogated by the addition of a *Pparγ*-specific antagonist. Our results draw a direct mechanistic link between *Zac1* and hepatic lipid accumulation for the first time and reveal that imprinted genes play a central role in mediating between Cd exposure in development and juvenile NAFLD. Using chromatin immunoprecipitation (ChIP), future work will exploit this overexpression model to show that *Zac1* directly controls *Pparγ* expression by binding to its promoter region in hepatocytes.

Outside of the liver, appropriate *Pparγ* signaling is critical for proper pancreas and adipose tissue functions. It is unclear if the relationship between *Zac1* and *Pparγ* that we identified in the liver is conserved in these tissues. In rodent models, it has been shown that up-regulation of *Pparγ* in the pancreas inhibits β-cell proliferation and compromises pancreas insulin secretion<sup>273,274</sup>. If altered *Zac1* signaling dysregulates proper *Pparγ* dosage in this tissue, diabetes may result. In adipose tissue, *Pparγ* induces adipocyte differentiation<sup>275</sup>. Up-regulation of *Pparγ* has been shown to increase adipose tissue fat storage, which helps to alleviate insulin insensitivity<sup>276</sup>. *Zac1* may have a role in regulating *Pparγ* signaling in this tissue and may lead to increased adiposity and weight gain if up-regulated. Our lab previously showed a direct link between *Zac1* signaling and the profibrogenic cytokine Tgfβ-1 in the liver<sup>136</sup>. Appropriate Tgfβ-1 signaling is also critical to lung function, and improper up-regulation of *Tgfβ-1* in the lungs has been shown to lead to

pulmonary fibrosis<sup>277</sup>. If *Zac1* regulates *Tgfb-1* in lung cells in a similar manner as the liver, it may be a potential therapeutic target in that organ as well.

Building on our findings from **Chapter 3** and another study from our lab that previously demonstrated a novel role for imprinted genes in developmental models of NAFLD<sup>136</sup>, in **Chapter 4**, we tested the hypothesis that the IGN is a conserved pathway that is up-regulated in the liver in response to different environmental stressors using publicly available RNA-seq and microarray data. We also used *in vitro* CdCl<sub>2</sub> exposure as a model of toxicant exposure to determine whether *Zac1* is up-regulated via a cell-autonomous mechanism in hepatocytes. Our results revealed that the IGN is significantly enriched in all the exposure models, but it was overall up-regulated in response to developmental CdCl<sub>2</sub>, maternal metabolic syndrome, and early adulthood 2,3,7,8-tetrachlorodibenzo-p-dioxin (TCDD) exposure. We also showed that the up-regulation of *Zac1* in response to CdCl<sub>2</sub> exposure is not cell autonomous, and AML12 and HepG2 cells exposed directly to CdCl<sub>2</sub> do not reproduce the *Zac1* dysregulation observed *in vivo*. As discussed in **Chapter 1**, juvenile NAFLD affects about one in five children globally<sup>157</sup>, and different developmental exposures have been shown to negatively impact offspring health later in life. To our knowledge, this is the first time the IGN has been shown to be dysregulated in response to different environmental stressors, implicating the IGN as a mechanism through which developmental exposures act to program NAFLD and providing novel potential therapeutic targets for further studies.

Future studies are needed to continue elucidating the mechanism through which developmental CdCl<sub>2</sub> exposure acts to dysregulate imprinted genes to program juvenile NAFLD. As shown in **Chapter 3**, *Zac1* was up-regulated in response to CdCl<sub>2</sub> exposure independent of changes to its ICR methylation or imprinting status at PND21. Therefore, Cd-induced *Zac1* up-

regulation could occur via alternative epigenetic mechanisms. For example, imprinted genes, including *Zac1*, are highly expressed in prenatal development. They are progressively down-regulated within a few days of birth by chromatin remodeling, a process mediated by the  $\alpha$ -thalassemia mental retardation X-linked (Atrx) protein<sup>232-234</sup>. The Atrx remodeling complex adds the H3.3 histone variant and the repressive histone mark H3K9me3 to down-regulate these genes<sup>233,234</sup>. One mechanism we propose is that Cd exposure during early postnatal development disrupts normal imprinted gene down-regulation by the Atrx complex, leading to developmentally inappropriate high levels of imprinted gene expression. Future studies will test the hypothesis that Cd exposure during this critical time-period disrupts Atrx function and the placement of repressive histone variants using ChIP.

Studies described here have provided associative evidence linking *Zac1* and IGN dysregulation and NAFLD outcomes but have not shown that *Zac1* dysregulation is necessary or sufficient to program juvenile NAFLD in response to CdCl<sub>2</sub> exposure. To address this, future studies in our lab will utilize a novel conditional *Zac1* knockout mouse model that allows for deletion of *Zac1* in the presence of Cre recombinase in an exposure regime similar to that described in **Chapter 2**. Because data from our lab suggest that *Zac1* dysregulation occurs predominantly in hepatocytes<sup>136</sup>, future work will delete the gene in a hepatocyte-specific manner using albumin (Alb)-Cre<sup>278</sup>. We propose that *Zac1* deletion in hepatocytes will result in partial or full abrogation of Cd-induced steatosis and fibrosis, revealing that it is necessary for Cd-induced NAFLD. To further demonstrate the role of *Zac1* signaling and critical windows of susceptibility in programming juvenile NAFLD in the absence of environmental perturbation, future work will overexpress *Zac1 in vivo* using an adeno-associated virus (AAV) 8 delivery system or transfection<sup>136,279</sup>. We propose that *Zac1* overexpressing mice will show statistically significant

evidence of NAFLD via histological, molecular, and biochemical analysis when compared to control mice, revealing that *Zac1* up-regulation is sufficient to program NAFLD. Together, our future work will test the hypothesis that *Zac1* signaling is necessary and sufficient for developmental Cd-induced NAFLD in mice.

The IGN contains other potential regulators of NAFLD such as the one encoding the long non-coding RNA (lncRNA) *H19*, which could potentially act to control other members within the network to program NAFLD<sup>113</sup>. *Zac1* has been shown to regulate the expression of *H19* by binding to its enhancer<sup>113</sup>. As shown in **Chapter 3**, *H19* is highly up-regulated in the livers of female and male mice developmentally exposed to 50 ppm CdCl<sub>2</sub> at PND21, the same timepoint when *Zac1* is up-regulated and NAFLD is observed. Other studies have also shown that *H19* up-regulation is linked to steatosis and fibrosis outcomes in adult mice<sup>267,268</sup>, indicating a potential role for the lncRNA *H19* in NAFLD programming. Future work will aim to further build on our understanding of IGN signaling presented in this dissertation by examining the epistatic interactions between IGN members. To determine if *Zac1* up-regulation can program juvenile NAFLD in response to developmental CdCl<sub>2</sub> exposure independent of *H19*, we intend to utilize a genetic *H19* hepatocyte-specific knockout mouse model in an exposure regime similar to our paradigm described in **Chapter 2**. We propose that *Zac1* programs NAFLD partially through *H19*. Therefore, we expect *H19* knockout mice exposed to 50 ppm CdCl<sub>2</sub> will show statistically significant evidence of NAFLD when compared to littermates exposed to 0 ppm CdCl<sub>2</sub>. However, we expect the phenotypes to be less severe as those described in the model within this dissertation. Future work could also utilize the *H19* knockout mouse model by overexpressing *Zac1* in vivo using AAV8 to confirm our results in the absence of CdCl<sub>2</sub> exposure. This work will test the hypothesis that *Zac1* signaling independent of *H19* is sufficient for developmental Cd-induced NAFLD in mice and will

further elucidate individual contributions of different IGN members to the programming of NAFLD.

To date, our *in vitro* studies investigating the role of *Zac1* signaling in lipid accumulation via *Ppary* and collagen deposition via *Tgfb-1* have used small molecule inhibitors and ChIP, respectively, to associate *Zac1* expression and measurable biochemical and molecular outcomes. However, to definitively show that *Zac1* signaling controls these outcomes, future work will use the CRISPR/Cas9 system to mutate the *Zac1* binding sites in the promoter regions for both *Ppary* and *Tgfb-1* and expose those mutated cell lines to the *Zac1* overexpression construct from **Chapter 3**<sup>280</sup>. We propose that mutating these sites will inhibit *Zac1* binding at these promoter regions, which will be confirmed with ChIP. Ultimately, we predict that the mutated cells will show significantly decreased accumulation of lipids and collagens compared to the mutated cells overexpressing the EGFP control construct and the non-mutated cells, indicating that these phenotypes depend on *Zac1* signaling. Future studies will test the hypothesis that *Zac1* binding at these promoter regions is necessary to lead to lipid and collagen accumulation *in vitro*.

Our results from our mouse model in **Chapter 2** indicate that after PND21, phenotypic differences are no longer discernible between groups in the absence of continued CdCl<sub>2</sub> exposure. We and others have proposed a multiple-hit hypothesis for NAFLD, whereby developmental exposures prime an individual for susceptibility to another environmental insult later in life to lead to negative health outcomes<sup>209,216</sup>. Future work will test whether developmental Cd-induced NAFLD can persist into later life in the presence of a second environmental insult, such as high fat diet, continued Cd exposure, or exposure to one or multiple other contaminants— models that are potentially more consistent with the life-long exposures experienced by humans.

In children, adolescents, and adults, exposure to heavy metals and endocrine disruptors have been associated with NAFLD<sup>16,126,127,219</sup>. However, human studies are difficult to control and eliminate all potential confounding variables, especially adult models where even minimal alcohol intake can affect liver health outcomes. Mice are a useful tool for exposure studies because their environment is easy to control. They are also a useful model of human biology and disease because about 80 % of their genes have a human ortholog, 90 % of their genome has synteny with the human genome, and mice have similar physiological processes to humans<sup>181,182</sup>. An advantage of mouse studies is that they provide empirical mechanistic evidence for a link between different exposures, including Cd, and NAFLD, and we showed in **Chapter 1** that Cd exposure alone is sufficient to program NAFLD in mice and provided evidence that this was via *Zac1* and IGN signaling. To provide translational evidence that *Zac1* and IGN signaling is relevant to human NAFLD, future studies can capitalize on biological repositories such as the Non-Alcoholic Steatohepatitis Clinical Research Network established by the National Institute of Diabetes and Digestive and Kidney Diseases. Analysis of preserved samples could reveal *ZAC1* and IGN gene dysregulation in response to different exposures in humans with NAFLD. Cultured cells from fresh human biopsies could provide a model to study the conservation of IGN signaling and function in humans, which has not yet been determined.

In summary, utilizing the mouse as a model allowed us to investigate the potential mechanism connecting developmental Cd exposure and liver disease, which would not have been feasible in human studies. The work described in this dissertation builds on current knowledge in the fields of toxicology and epigenetics by identifying imprinted genes as novel mediators between exposure to environmental stressors, such as Cd, and later life disease, including juvenile non-alcoholic fatty liver disease. Further research is needed to fully elucidate the mechanism through

which Cd exposure dysregulates imprinted genes to program NAFLD. However, the studies discussed here highlight the importance of imprinted genes in programming NAFLD and reveal the need to consider them as potential therapeutic targets for disease mitigation in the future.

## REFERENCES

1. Nies DH. Mini-review: Microbial heavy-metal resistance. *Appl Microbiol Biotechnol.* 1999;51(6):730-750.
2. Agency for Toxic Substances and Disease Registry (ATSDR). Toxicological profile for cadmium. *US Dep Heal Hum Serv Public Heal Serv.* Published online 2012.
3. Sigel RKO, Skilandat M, Sigel A, Operschall BP, Sigel H. *Cadmium: From Toxicity to Essentiality.* Springer London; 2013. doi:10.1007/978-94-007-5179-8\_8/FIGURES/000817
4. Peralta-Videa JR, Lopez ML, Narayan M, Saupe G, Gardea-Torresdey J. The biochemistry of environmental heavy metal uptake by plants: Implications for the food chain. *Int J Biochem Cell Biol.* 2009;41(8-9):1665-1677. doi:10.1016/J.BIOCEL.2009.03.005
5. Babich H SG. *Effects of Cadmium on the Biota: Influence of Environmental Factors.* (D P, ed.). Academic Press; 1978.
6. Nriagu J. A global assessment of natural sources of atmospheric trace metals. *Nature.* 1989;338(6210):47-49.
7. WHO. Exposure to Cadmium: A Major Public Health Concern. Published online 2010.
8. Järup L, Åkesson A. Current status of cadmium as an environmental health problem. *Toxicol Appl Pharmacol.* 2009;238(3):201-208. doi:10.1016/J.TAAP.2009.04.020
9. King KE, Darrah TH, Money E, et al. Geographic clustering of elevated blood heavy metal levels in pregnant women Environmental health. *BMC Public Health.* 2015;15(1):1-12. doi:10.1186/S12889-015-2379-9/TABLES/5
10. Nishijo M, Nakagawa H, Suwazono Y, Nogawa K, Kido T. Causes of death in patients

- with Itai-itai disease suffering from severe chronic cadmium poisoning: a nested case-control analysis of a follow-up study in Japan. *BMJ Open*. 2017;7(7):e015694.  
doi:10.1136/BMJOPEN-2016-015694
11. Trevors JT, Stratton GW, Gadd GM. Cadmium transport, resistance, and toxicity in bacteria, algae, and fungi. *Can J Microbiol*. 1986;32(6):447-464. doi:10.1139/M86-085
  12. Orell A, Remonsellez F, Arancibia R, Jerez CA. Molecular Characterization of Copper and Cadmium Resistance Determinants in the Biomining Thermoacidophilic Archaeon *Sulfolobus metallicus*. *Archaea*. 2013;2013:289236. doi:10.1155/2013/289236
  13. Qi X, Xu X, Zhong C, Jiang T, Wei W, Song X. Removal of Cadmium and Lead from Contaminated Soils Using Sophorolipids from Fermentation Culture of *Starmerella bombicola* CGMCC 1576 Fermentation. *Int J Environ Res Public Health*. 2018;15(11):2334. doi:10.3390/IJERPH15112334
  14. Satarug S, Baker JR, Urbenjapol S, et al. A global perspective on cadmium pollution and toxicity in non-occupationally exposed population. *Toxicol Lett*. 2003;137(1-2):65-83. doi:10.1016/S0378-4274(02)00381-8
  15. Agency for Toxic Substances and Disease Registry (ATSDR). Cadmium Toxicity Case Studies in Environmental Medicine (CSEM). Accessed July 29, 2022.  
<https://www.atsdr.cdc.gov/csem/cadmium/Safety-Standards.html>
  16. Hyder O, Chung M, Cosgrove D, et al. Cadmium Exposure and Liver Disease among US Adults. *J Gastrointest Surg*. 2013;17(7):1265-1273. doi:10.1007/s11605-013-2210-9
  17. Satarug S, Garrett SH, Sens MA, Sens DA. Cadmium, Environmental Exposure, and Health Outcomes. *Environ Health Perspect*. 2010;118(2):182. doi:10.1289/EHP.0901234
  18. Rahimzadeh MR, Rahimzadeh MR, Kazemi S, Moghadamnia AA. Cadmium toxicity and

- treatment: An update. *Casp J Intern Med*. 2017;8(3):135. doi:10.22088/CJIM.8.3.135
19. Wallia A, Allen NB, Badon S, El Muayed M. Association between urinary cadmium levels and prediabetes in the NHANES 2005-2010 population. *Int J Hyg Environ Health*. 2014;217(8):854-860. doi:10.1016/J.IJHEH.2014.06.005
  20. Al-Saleh I, Shinwari N, Mashhour A, Rabah A. Birth outcome measures and maternal exposure to heavy metals (lead, cadmium and mercury) in Saudi Arabian population. *Int J Hyg Environ Health*. 2014;217(2-3):205-218. doi:10.1016/J.IJHEH.2013.04.009
  21. Tian LL, Zhao YC, Wang XC, et al. Effects of gestational cadmium exposure on pregnancy outcome and development in the offspring at age 4.5 years. *Biol Trace Elem Res*. 2009;132(1-3):51-59. doi:10.1007/S12011-009-8391-0/TABLES/6
  22. Waalkes MP. Cadmium carcinogenesis. *Mutat Res*. 2003;533(1-2):107-120. doi:10.1016/J.MRFMMM.2003.07.011
  23. Kjellström T, Nordberg GF. A kinetic model of cadmium metabolism in the human being. *Environ Res*. 1978;16(1-3):248-269. doi:10.1016/0013-9351(78)90160-3
  24. Satarug S, Baker JR, Reilly PEB, Moore MR, Williams DJ. Cadmium levels in the lung, liver, kidney cortex, and urine samples from Australians without occupational exposure to metals. *Arch Environ Health*. 2002;57(1):69-77. doi:10.1080/00039890209602919
  25. Akesson A, Berglund M, Schütz A, Bjellerup P, Bremme K, Vahter M. Cadmium Exposure in Pregnancy and Lactation in Relation to Iron Status. *Am J Public Health*. 2011;92(2):284-287. doi:10.2105/AJPH.92.2.284
  26. Waalkes MP, Goering PL. Perspective Metallothionein and Other Cadmium-Binding Proteins: Recent Developments. 1990;3(4):281-288. Accessed May 30, 2022. <https://pubs.acs.org/sharingguidelines>

27. Jacobo-Estrada T, Santoyo-Sánchez M, Thévenod F, Barbier O. Molecular Sciences Cadmium Handling, Toxicity and Molecular Targets Involved during Pregnancy: Lessons from Experimental Models. *Int J Mol Sci.* 2017;18(7):1590. doi:10.3390/ijms18071590
28. Clarkson TW. MOLECULAR AND IONIC MIMICRY OF TOXIC METALS. *Annu Rev Pharmacol Toxicol.* 1993;32:545-571. Accessed May 30, 2022. www.annualreviews.org
29. Wetterhahn Jennette by K. The role of metals in carcinogenesis: biochemistry and metabolism. *Environ Health Perspect.* 1981;40:233-252. doi:10.1289/EHP.8140233
30. Thévenod F, Fels J, Lee WK, Zarbock R. Channels, transporters and receptors for cadmium and cadmium complexes in eukaryotic cells: myths and facts. *BioMetals.* 2019;32(3):469-489. doi:10.1007/S10534-019-00176-6
31. Gunshin H, Mackenzie B, Berger U V., et al. Cloning and characterization of a mammalian proton-coupled metal-ion transporter. *Nat* 1997 3886641. 1997;388(6641):482-488. doi:10.1038/41343
32. Margoshes M, Valiee BL. A Cadmium Protein from Equine Kidney Cortex. *J Am Chem Soc.* 1957;79(17):4813-4814. doi:10.1021/JA01574A064/ASSET/JA01574A064.FP.PNG\_V03
33. McCarty MF. Zinc and multi-mineral supplementation should mitigate the pathogenic impact of cadmium exposure. *Med Hypotheses.* 2012;79(5):642-648. doi:10.1016/J.MEHY.2012.07.043
34. Thirumoorthy N, Shyam Sunder A, Manisenthil Kumar KT, Senthil kumar M, Ganesh GNK, Chatterjee M. A review of metallothionein isoforms and their role in pathophysiology. *World J Surg Oncol.* 2011;9(54). doi:10.1186/1477-7819-9-54
35. Thévenod F. Cadmium and cellular signaling cascades: to be or not to be? *Toxicol Appl*

- Pharmacol.* 2009;238(3):221-239. doi:10.1016/J.TAAP.2009.01.013
36. Johnson MD, Kenney N, Stoica A, et al. Cadmium mimics the in vivo effects of estrogen in the uterus and mammary gland. *Nat Med.* 2003;9(8):1081-1084. doi:10.1038/NM902
  37. Ye J, Wang S, Barger M, Castranova V SX. Activation of androgen response element by cadmium: a potential mechanism for a carcinogenic effect of cadmium in the prostate. *J Environ Pathol Toxicol Oncol.* 2000;19(3):275-280.
  38. Byrne C, Divekar SD, Storchan GB, Parodi DA, Martin MB. Cadmium--a metalloestrogen? *Toxicol Appl Pharmacol.* 2009;238(3):266-271. doi:10.1016/J.TAAP.2009.03.025
  39. Brama M, Politi L, Santini P, Migliaccio S, Scandurra R. Cadmium-induced apoptosis and necrosis in human osteoblasts: role of caspases and mitogen-activated protein kinases pathways. *J Endocrinol Invest.* 2012;35(2):198-208. doi:10.3275/7801
  40. Cooke MS, Evans MD, Dizdaroglu M, Lunec J. Oxidative DNA damage: mechanisms, mutation, and disease. *FASEB J.* 2003;17(10):1195-1214. doi:10.1096/FJ.02-0752REV
  41. Hwan Jin Y, Clark AB, C Slebos RJ, et al. *Cadmium Is a Mutagen That Acts by Inhibiting Mismatch Repair.* Vol 34.; 2003. <http://www.nature.com/naturegenetics>
  42. Li S, Wang Y, Wang H, et al. MicroRNAs as participants in cytotoxicity of CdTe quantum dots in NIH/3T3 cells. *Biomaterials.* 2011;32(15):3807-3814. doi:10.1016/J.BIOMATERIALS.2011.01.074
  43. Waddington CH. The Epigenotype. *Int J Epidemiol.* 2012;41(1):10-13. doi:10.1093/IJE/DYR184
  44. Deans C, Maggert KA. What Do You Mean, "Epigenetic"? *Genetics.* 2015;199(4):887-896. doi:10.1534/GENETICS.114.173492

45. Allis C, Jenuwein T. The molecular hallmarks of epigenetic control. *Nat Rev Genet.* 2016;17(8):487-500. doi:10.1038/nrg.2016.59
46. Wu, C; Morris J. Genes, genetics, and epigenetics: A correspondence - ProQuest. *Science* (80- ). 2001;293(5532):1103-1105. Accessed May 31, 2022.  
<https://www.proquest.com/docview/213573595?accountid=12725&parentSessionId=g1QVwUeSHk0YCT3AzbNsFuP%2F8%2FqF%2BoNxxp1eVt4DHF%3D&pq-origsite=summon>
47. Fitz-James MH, Cavalli G. Molecular mechanisms of transgenerational epigenetic inheritance. *Nat Rev Genet.* 2022;23(6):325-341. doi:10.1038/s41576-021-00438-5
48. Guil S, Esteller M. RNA–RNA interactions in gene regulation: the coding and noncoding players. *Trends Biochem Sci.* 2015;40(5):248-256. doi:10.1016/J.TIBS.2015.03.001
49. Watson J. *Molecular Biology of the Gene.* (Benjamin W, ed.); 1965.
50. Bure I V., Nemtsova M V., Kuznetsova EB. Histone Modifications and Non-Coding RNAs: Mutual Epigenetic Regulation and Role in Pathogenesis. *Int J Mol Sci.* 2022;23(10):5801. doi:10.3390/IJMS23105801
51. Cech TR, Steitz JA. The Noncoding RNA Revolution—Trashing Old Rules to Forge New Ones. *Cell.* 2014;157(1):77-94. doi:10.1016/J.CELL.2014.03.008
52. Wei JW, Huang K, Yang C, Kang CS. Non-coding RNAs as regulators in epigenetics (Review). *Oncol Rep.* 2017;37(1):3-9. doi:10.3892/OR.2016.5236/HTML
53. Park J, Ahn H, Shin MG, Kim HK, Chang S. tRNA-Derived Small RNAs: Novel Epigenetic Regulators. *Cancers (Basel).* 2020;12(10):2773. doi:10.3390/cancers12102773
54. Morris K V, -L Chan SW, Jacobsen SE, Looney DJ. Small Interfering RNA-Induced Transcriptional Gene Silencing in Human Cells. *New Ser.* 2004;305(5688):1289-1292.

55. Yuan J hang, Yang F, Chen B feng, et al. The histone deacetylase 4/SP1/microRNA-200a regulatory network contributes to aberrant histone acetylation in hepatocellular carcinoma. *Hepatology*. 2011;54(6):2025-2035. doi:10.1002/HEP.24606
56. Wu L, Zhou H, Zhang Q, et al. DNA methylation mediated by a microRNA pathway. *Mol Cell*. 2010;38(3):465-475. doi:10.1016/J.MOLCEL.2010.03.008
57. Fabbri M, Garzon R, Cimmino A, et al. MicroRNA-29 family reverts aberrant methylation in lung cancer by targeting DNA methyltransferases 3A and 3B. *Proc Natl Acad Sci U S A*. 2007;104(40):15805-15810. doi:10.1073/PNAS.0707628104
58. Khraiwesh B, Arif MA, Seumel GI, et al. Transcriptional Control of Gene Expression by MicroRNAs. *Cell*. 2010;140(1):111-122.  
doi:10.1016/J.CELL.2009.12.023/ATTACHMENT/BA25DDFE-2E03-4F70-A3F1-086B3B92DDBB/MMC1.XLS
59. Hanson A, Piras IS, Wilhelmsen D, et al. Chemokine ligand 20 (CCL20) expression increases with NAFLD stage and hepatic stellate cell activation and is regulated by miR-590-5p. *Cytokine*. 2019;123. doi:10.1016/J.CYTO.2019.154789
60. Ogawa T, Enomoto M, Fujii H, et al. MicroRNA-221/222 upregulation indicates the activation of stellate cells and the progression of liver fibrosis. *Gut*. 2012;61(11):1600-1609. doi:10.1136/GUTJNL-2011-300717
61. Zhang Z, Zha Y, Hu W, et al. The autoregulatory feedback loop of microRNA-21/programmed cell death protein 4/activation protein-1 (MiR-21/PDCD4/AP-1) as a driving force for hepatic fibrosis development. *J Biol Chem*. 2013;288(52):37082-37093. doi:10.1074/JBC.M113.517953
62. Huang XA, Yin H, Sweeney S, Raha D, Snyder M, Lin H. A major epigenetic

- programming mechanism guided by piRNAs. *Dev Cell*. 2013;24(5):502-516.  
doi:10.1016/J.DEVCEL.2013.01.023
63. Kuramochi-Miyagawa S, Watanabe T, Gotoh K, et al. DNA methylation of retrotransposon genes is regulated by Piwi family members MILI and MIWI2 in murine fetal testes. *Genes Dev*. 2008;22(7):908-917. doi:10.1101/GAD.1640708
64. Yin H, Lin H. An epigenetic activation role of Piwi and a Piwi-associated piRNA in *Drosophila melanogaster*. *Nature*. 2007;450(7167):304-308. doi:10.1038/NATURE06263
65. Chen Q, Yan M, Cao Z, et al. Sperm tsRNAs contribute to intergenerational inheritance of an acquired metabolic disorder. *Science*. 2016;351(6271):397-400.  
doi:10.1126/SCIENCE.AAD7977
66. Yu Y, Zhang Y, Chen X, Chen Y. Plant Noncoding RNAs: Hidden Players in Development and Stress Responses. *Annu Rev Cell Dev Biol*. 2019;35:407-431.  
doi:10.1146/ANNUREV-CELLBIO-100818-125218
67. Kretz M, Saprashvili Z, Chu C, et al. Control of somatic tissue differentiation by the long non-coding RNA TINCR. *Nat 2012 4937431*. 2012;493(7431):231-235.  
doi:10.1038/nature11661
68. Monnier P, Martinet C, Pontis J, Stancheva I, Ait-Si-Ali S, Dandolo L. H19 lncRNA controls gene expression of the Imprinted Gene Network by recruiting MBD1. *PNAS*. 2013;110(51):20693-20698.  
doi:10.1073/PNAS.1310201110/SUPPL\_FILE/PNAS.201310201SI.PDF
69. Li L, Liu B, Wapinski OL, et al. Targeted disruption of Hotair leads to homeotic transformation and gene derepression. *Cell Rep*. 2013;5(1):3-12.  
doi:10.1016/J.CELREP.2013.09.003

70. Clemson CM, McNeil JA, Willard HF, Lawrence JB. XIST RNA paints the inactive X chromosome at interphase: evidence for a novel RNA involved in nuclear/chromosome structure. *J Cell Biol.* 1996;132(3):259-275. doi:10.1083/JCB.132.3.259
71. Loda A, Heard E. Xist RNA in action: Past, present, and future. *PLoS Genet.* 2019;15(9). doi:10.1371/JOURNAL.PGEN.1008333
72. Bhan A, Soleimani M, Mandal SS. Long noncoding RNA and cancer: A new paradigm. *Cancer Res.* 2017;77(15):3965-3981. doi:10.1158/0008-5472.CAN-16-2634/660907/P/LONG-NONCODING-RNA-AND-CANCER-A-NEW
73. Dempsey JL, Cui JY. Long Non-Coding RNAs: A Novel Paradigm for Toxicology. *Toxicol Sci.* 2017;155(1):3-21. doi:10.1093/TOXSCI/KFW203
74. Kornberg RD. Chromatin Structure: A Repeating Unit of Histones and DNA. *Science (80-)*. 1974;184(4139):868-871.
75. Kornberg RD, Lorch Y. Twenty-five years of the nucleosome, fundamental particle of the eukaryote chromosome. *Cell.* 1999;98(3):285-294. doi:10.1016/S0092-8674(00)81958-3
76. Widom J, Klug A. Structure of the 3008 Chromatin Filament: X-Ray Diffraction from Oriented Samples. *Cell.* 1965;43:207-213.
77. Phillips DM, Johns EW. A fractionation of the histones of group F2a from calf thymus. *Biochem J.* 1965;94(1):127-130. doi:10.1042/BJ0940127
78. Gardner KE, David Allis C, Strahl BD. OPERating ON chromatin, a colorful language where context matters. *J Mol Biol.* 2012;409(1):36-46. doi:10.1016/j.jmb.2011.01.040
79. Feinberg AP. The Key Role of Epigenetics in Human Disease Prevention and Mitigation. *N Engl J Med.* 2018;378(14):1323-1334. doi:10.1056/NEJMRA1402513
80. Brownell JE, Zhou J, Ranalli T, et al. Tetrahymena Histone Acetyltransferase A: A

- Homolog to Yeast Gcn5p Linking Histone Acetylation to Gene Activation. *Cell*. 1996;84(6):843-851. doi:10.1016/S0092-8674(00)81063-6
81. Taunton J, Hassig CA, Schreiber SL. A mammalian histone deacetylase related to the yeast transcriptional regulator Rpd3p. *Science* (80- ). 1996;272(5260):408-411. doi:10.1126/SCIENCE.272.5260.408
  82. Tschiersch B, Hofmann A, Krauss V, Dorn R, Korge G, Reuter G. The protein encoded by the *Drosophila* position-effect variegation suppressor gene *Su(var)3-9* combines domains of antagonistic regulators of homeotic gene complexes. *EMBO J*. 1994;13(16):3822-3831. doi:10.1002/J.1460-2075.1994.TB06693.X
  83. Tsukada YI, Fang J, Erdjument-Bromage H, et al. Histone demethylation by a family of JmjC domain-containing proteins. *Nature*. 2005;439(7078):811-816. doi:10.1038/nature04433
  84. Strahl BD, David Allis C. The language of covalent histone modifications. *Nature*. 2000;403:41-45. www.nature.com
  85. Bowers EC, Mccullough SD. Linking the Epigenome with Exposure Effects and Susceptibility: The Epigenetic Seed and Soil Model. *Toxicol Sci*. 2017;155(2):302-314. doi:10.1093/toxsci/kfw215
  86. Thomson JP, Skene PJ, Selfridge J, et al. CpG islands influence chromatin structure via the CpG-binding protein Cfp1. *Nature*. 2010;464:1082-1086. doi:10.1038/nature08924
  87. Domcke S, Flore Bardet A, Ginno PA, Hartl D, Burger L, Schübeler D. Competition between DNA methylation and transcription factors determines binding of NRF1. *Nature*. 2015;528:575-579. doi:10.1038/nature16462
  88. Blackledge NP, Zhou JC, Tolstorukov MY, Farcas AM, Park PJ, Klose RJ. CpG Islands

- Recruit a Histone H3 Lysine 36 Demethylase. *Mol Cell*. 2010;38(2):179-190.  
doi:10.1016/J.MOLCEL.2010.04.009
89. Li E, Zhang Y, Allis D, Caparros ML, Jenuwein T, Reinberg D. DNA Methylation in Mammals. *Cold Spring Harb Perspect Biol*. 2014;6(5). doi:10.1101/cshperspect.a019133
90. Bird A, Taggart M, Frommer M, Miller OJ, Macleod D. A fraction of the mouse genome that is derived from islands of nonmethylated, CpG-rich DNA. *Cell*. 1985;40(1):91-99.  
doi:10.1016/0092-8674(85)90312-5
91. Jung M, Pfeifer GP. CpG Islands. *Brenner's Encycl Genet*. 2013;2:205-207.  
doi:10.1016/B978-0-12-374984-0.00349-1
92. Bestor TH, Ingram VM. Two DNA methyltransferases from murine erythroleukemia cells: purification, sequence specificity, and mode of interaction with DNA. *Proc Natl Acad Sci U S A*. 1983;80(18). doi:10.1073/PNAS.80.18.5559
93. Okano M, Bell DW, Haber DA, Li E. DNA methyltransferases Dnmt3a and Dnmt3b are essential for de novo methylation and mammalian development. *Cell*. 1999;99(3):247-257. doi:10.1016/S0092-8674(00)81656-6
94. Bhutani N, Burns DM, Blau HM. DNA demethylation dynamics. *Cell*. 2011;146(6):866-872. doi:10.1016/J.CELL.2011.08.042
95. Tahiliani M, Koh KP, Shen Y, et al. Conversion of 5-methylcytosine to 5-hydroxymethylcytosine in mammalian DNA by MLL partner TET1. *Science (80- )*. 2009;324(5929):930-935. doi:10.1126/SCIENCE.1170116
96. He YF, Li BZ, Li Z, et al. Tet-mediated formation of 5-carboxylcytosine and its excision by TDG in mammalian DNA. *Science (80- )*. 2011;333(6047):1303-1307.  
doi:10.1126/SCIENCE.1210944

97. Ito S, Shen L, Dai Q, et al. Tet proteins can convert 5-methylcytosine to 5-formylcytosine and 5-carboxylcytosine. *Science* (80- ). 2011;333(6047):1300-1303.  
doi:10.1126/SCIENCE.1210597
98. Maiti A, Drohat AC. Thymine DNA glycosylase can rapidly excise 5-formylcytosine and 5-carboxylcytosine: potential implications for active demethylation of CpG sites. *J Biol Chem*. 2011;286(41):35334-35338. doi:10.1074/JBC.C111.284620
99. Smith ZD, Chan MM, Mikkelsen TS, et al. A unique regulatory phase of DNA methylation in the early mammalian embryo. *Nature*. 2012;484:339-344.  
doi:10.1038/nature10960
100. Smallwood SA, Tomizawa SI, Krueger F, et al. Dynamic CpG island methylation landscape in oocytes and preimplantation embryos. *Nat Genet*. 2011;43(8):811-814.  
doi:10.1038/ng.864
101. Seisenberger S, Andrews S, Krueger F, et al. The Dynamics of Genome-wide DNA Methylation Reprogramming in Mouse Primordial Germ Cells. *Mol Cell*. 2012;48(6):849-862. doi:10.1016/J.MOLCEL.2012.11.001
102. Popp C, Dean W, Feng S, et al. Genome-wide erasure of DNA methylation in mouse primordial germ cells is affected by AID deficiency. *Nature*. 2010;463:1101-1105.  
doi:10.1038/nature08829
103. Chess A. Random and Non-Random Monoallelic Expression. *Neuropsychopharmacology*. 2013;38(1):55-61. doi:10.1038/NPP.2012.85
104. Ferguson-Smith AC. Genomic imprinting: the emergence of an epigenetic paradigm. *Nat Rev Genet*. 2011;12(8):565-575. doi:10.1038/NRG3032
105. Plasschaert RN, Bartolomei MS. Genomic imprinting in development, growth, behavior

- and stem cells. *Development*. 2014;141(9):1805-1813. doi:10.1242/DEV.101428
106. Hata K, Okano M, Lei H, Li E. Dnmt3L cooperates with the Dnmt3 family of de novo DNA methyltransferases to establish maternal imprints in mice. *Development*. 2002;129(8):1983-1993. doi:10.1242/DEV.129.8.1983
  107. Jirtle RL. Imprinted gene database. GeneImprint. Published 2012.  
<https://www.geneimprint.com/site/genes-by-species>
  108. Bartolomei MS, Ferguson-Smith AC. Mammalian genomic imprinting. *Cold Spring Harb Perspect Biol*. 2011;3(7):1-17. doi:10.1101/CSHPERSPECT.A002592
  109. Ferguson-Smith AC, Bourc'his D. The discovery and importance of genomic imprinting. *Elife*. 2018;7. doi:10.7554/ELIFE.42368
  110. Tucci V, Isles AR, Kelsey G, et al. Genomic Imprinting and Physiological Processes in Mammals. *Cell*. 2019;176(5):952-965. doi:10.1016/J.CELL.2019.01.043
  111. Al Adhami H, Evano B, Le Digarcher A, et al. A systems-level approach to parental genomic imprinting: the imprinted gene network includes extracellular matrix genes and regulates cell cycle exit and differentiation. *Genome Res*. 2015;25(3):353-367.  
doi:10.1101/GR.175919.114
  112. Varrault A, Dantec C, Le Digarcher A, et al. Identification of Plagl1/Zac1 binding sites and target genes establishes its role in the regulation of extracellular matrix genes and the imprinted gene network. *Nucleic Acids Res*. 2017;45(18):10466-10480.  
doi:10.1093/NAR/GKX672
  113. Varrault A, Gueydan C, Delalbre A, et al. Zac1 regulates an imprinted gene network critically involved in the control of embryonic growth. *Dev Cell*. 2006;11(5):711-722.  
doi:10.1016/J.DEVCEL.2006.09.003

114. Nicholls RD, Knepper JL. Genome organization, function, and imprinting in Prader-Willi and Angelman syndromes. *Annu Rev Genomics Hum Genet.* 2001;2:153-175.  
doi:10.1146/ANNUREV.GENOM.2.1.153
115. Soejima H, Higashimoto K. Epigenetic and genetic alterations of the imprinting disorder Beckwith–Wiedemann syndrome and related disorders. *J Hum Genet.* 2013;58(7):402-409. doi:10.1038/jhg.2013.51
116. Susiarjo M, Sasson I, Mesaros C, Bartolomei MS. Bisphenol a exposure disrupts genomic imprinting in the mouse. *PLoS Genet.* 2013;9(4). doi:10.1371/JOURNAL.PGEN.1003401
117. Vidal AC, Semenova V, Darrah T, et al. Maternal cadmium, iron and zinc levels, DNA methylation and birth weight. *BMC Pharmacol Toxicol.* 2015;16:20. doi:10.1186/S40360-015-0020-2
118. Cowley M, Skaar DA, Jima DD, et al. Effects of Cadmium Exposure on DNA Methylation at Imprinting Control Regions and Genome-Wide in Mothers and Newborn Children. *Environ Health Perspect.* 2018;126(3):037003. doi:10.1289/EHP2085
119. Barker DJP. The origins of the developmental origins theory. *J Intern Med.* 2007;261(5):412-417. doi:10.1111/J.1365-2796.2007.01809.X
120. Wadhwa PD, Buss C, Entringer S, Swanson JM. Developmental origins of health and disease: brief history of the approach and current focus on epigenetic mechanisms. *Semin Reprod Med.* 2009;27(5):358-368. doi:10.1055/S-0029-1237424
121. Haugen AC, Schug TT, Collman G, Heindel JJ. Evolution of DOHaD: the impact of environmental health sciences. *J Dev Orig Health Dis.* 2015;6(2):55-64.  
doi:10.1017/S2040174414000580
122. Young JL, Cai L. Implications for prenatal cadmium exposure and adverse health

- outcomes in adulthood. *Toxicol Appl Pharmacol.* 2020;403.  
doi:10.1016/J.TAAP.2020.115161
123. Janesick A, Blumberg B. Endocrine Disrupting Chemicals and the Developmental Programming of Adipogenesis and Obesity HHS Public Access. *Birth Defects Res Part C Embryo Today.* 2011;93(1):34-50. doi:10.1002/bdrc.20197
124. Lee HS. Impact of Maternal Diet on the Epigenome during In Utero Life and the Developmental Programming of Diseases in Childhood and Adulthood. *Nutrients.* 2017;7:9492–507. doi:10.3390/nu7115467
125. Soullane S, Willems P, Lee GE, Auger N. Early life programming of nonalcoholic fatty liver disease in children. *Early Hum Dev.* 2022;168.  
doi:10.1016/J.EARLHUMDEV.2022.105578
126. Stratakis N, Golden-Mason L, Margetaki K, et al. In Utero Exposure to Mercury Is Associated With Increased Susceptibility to Liver Injury and Inflammation in Childhood. *Hepatology.* 2021;74(3):1546-1559. doi:10.1002/HEP.31809
127. Verstraete SG, Wojcicki JM, Perito ER, Rosenthal P. Bisphenol a increases risk for presumed non-alcoholic fatty liver disease in Hispanic adolescents in NHANES 2003-2010. *Environ Heal.* 2018;17(1). doi:10.1186/S12940-018-0356-3
128. La Merrill MA, Vandenberg LN, Smith MT, et al. Consensus on the key characteristics of endocrine-disrupting chemicals as a basis for hazard identification. *Nat Rev Endocrinol* 2019 161. 2019;16(1):45-57. doi:10.1038/s41574-019-0273-8
129. Giulivo M, Lopez de Alda M, Capri E, Barceló D. Human exposure to endocrine disrupting compounds: Their role in reproductive systems, metabolic syndrome and breast cancer. A review. *Environ Res.* 2016;151:251-264. doi:10.1016/J.ENVRES.2016.07.011

130. Sifakis S, Androutsopoulos VP, Tsatsakis AM, Spandidos DA. Human exposure to endocrine disrupting chemicals: effects on the male and female reproductive systems. *Environ Toxicol Pharmacol.* 2017;51:56-70. doi:10.1016/J.ETAP.2017.02.024
131. Heindel JJ, Skalla LA, Joubert BR, Dilworth CH, Gray KA. Review of developmental origins of health and disease publications in environmental epidemiology. *Reprod Toxicol.* 2017;68:34-48. doi:10.1016/J.REPROTOX.2016.11.011
132. Treviño LS, Katz TA. Endocrine Disruptors and Developmental Origins of Nonalcoholic Fatty Liver Disease. *Endocrinology.* 2018;159(1):20-31. doi:10.1210/EN.2017-00887
133. (USDA) USD of A. USDA Dietary Guidelines 2020-2025. *US Dep Heal Hum Serv Public Heal Serv.* Published online 2020.
134. Gernand AD, Schulze KJ, Stewart CP, West KP, Christian P. Micronutrient deficiencies in pregnancy worldwide: health effects and prevention HHS Public Access. *Nat Rev Endocrinol.* 2016;12(5):274-289. doi:10.1038/nrendo.2016.37
135. Mouralidarane A, Soeda J, Visconti-Pugmire C, et al. Maternal obesity programs offspring nonalcoholic fatty liver disease by innate immune dysfunction in mice. *Hepatology.* 2013;58(1):128-138. doi:10.1002/HEP.26248
136. Baptissart M, Bradish CM, Brie, et al. Zac1 and the Imprinted Gene Network program juvenile NAFLD in response to maternal metabolic syndrome. *Hepatology.* 2022;00:1-15. doi:10.1002/hep.32363
137. Modi N, Murgasova D, Ruager-Martin R, et al. The influence of maternal body mass index on infant adiposity and hepatic lipid content. *Pediatr Res.* 2011;70(3):287-291. doi:10.1203/PDR.0B013E318225F9B1
138. Brumbaugh DE, Tearse P, Cree-Green M, et al. Intrahepatic fat is increased in the

- neonatal offspring of obese women with gestational diabetes. *J Pediatr*. 2013;162(5):930-936. doi:10.1016/J.JPEDS.2012.11.017
139. Sekkarie A, Welsh JA, Northstone K, Stein AD, Ramakrishnan U, Vos MB. Associations of maternal diet and nutritional status with offspring hepatic steatosis in the Avon longitudinal study of parents and children. *BMC Nutr*. 2021;7(1). doi:10.1186/S40795-021-00433-3
140. Shih YH, Islam T, Kumar Hore S, et al. Associations between prenatal arsenic exposure with adverse pregnancy outcome and child mortality HHS Public Access Author manuscript. *Env Res*. 2017;158:456-461. doi:10.1016/j.envres.2017.07.004
141. Andrews KW, Savitz DA, Hertz-Picciotto I. Prenatal lead exposure in relation to gestational age and birth weight: a review of epidemiologic studies. *Am J Ind Med*. 1994;26(1):13-32. doi:10.1002/AJIM.4700260103
142. Heng YY, Asad I, Coleman B, et al. Heavy metals and neurodevelopment of children in low and middle-income countries: A systematic review. Lehmann DM, ed. *PLoS One*. 2022;17(3):e0265536. doi:10.1371/JOURNAL.PONE.0265536
143. Karagas MR, Choi AL, Oken E, et al. Evidence on the human health effects of low-level methylmercury exposure. *Environ Health Perspect*. 2012;120(6):799-806. doi:10.1289/EHP.1104494
144. Chen R, Xu Y, Xu C, et al. Associations between mercury exposure and the risk of nonalcoholic fatty liver disease (NAFLD) in US adolescents. *Environ Sci Pollut Res Int*. 2019;26(30):31384-31391. doi:10.1007/S11356-019-06224-5
145. Trefts E, Gannon M, Wasserman DH. The liver. *Curr Biol*. 2017;27(21):R1147-51. doi:10.1016/J.CUB.2017.09.019

146. Ober EA, Lemaigre FP. Development of the liver: Insights into organ and tissue morphogenesis. *J Hepatol.* 2018;68(5):1049-1062. doi:10.1016/J.JHEP.2018.01.005
147. Abdel-Misih SRZ, Bloomston M, Bismuth H. Liver Anatomy. Published online 2010. doi:10.1016/j.suc.2010.04.017
148. Pineiro-Carrero V, Pifheiro E. Liver. *Pediatrics.* 2004;113:1097-1106.
149. Wake K. "Sternzellen" in the liver: Perisinusoidal cells with special reference to storage of vitamin A. *Am J Anat.* 1971;132(4):429-461. doi:10.1002/AJA.1001320404
150. Kruepunga N, Hakvoort TBM, Hikspoors JPJM, Köhler SE, Lamers WH. Anatomy of rodent and human livers: What are the differences? *Biochim Biophys Acta.* 2019;1865(5):869-878. doi:10.1016/J.BBADIS.2018.05.019
151. Gu X, Manautou JE. Molecular mechanisms underlying chemical liver injury. *Expert Rev Mol Med.* 2012;14. doi:10.1017/S1462399411002110
152. Moran J, Ghishan F, Halter S, Greene H. Steatohepatitis in obese children: a cause of chronic liver dysfunction. *Am J Gastroenterol.* 1983;78(6):374-377.
153. (CLDF) CLDF. Non-Alcoholic Fatty Liver Disease (NAFLD): A Guide. Published online 2019.
154. Bertot LC, Adams LA. The Natural Course of Non-Alcoholic Fatty Liver Disease. *Int J Mol Sci.* 2016;17(5):774. doi:10.3390/IJMS17050774
155. Temple JL, Cordero P, Li J, Nguyen V, Oben JA. A Guide to Non-Alcoholic Fatty Liver Disease in Childhood and Adolescence. *Int J Mol Sci.* 2016;17(6). doi:10.3390/IJMS17060947
156. Younossi ZM, Blissett D, Blissett R, et al. The economic and clinical burden of nonalcoholic fatty liver disease in the United States and Europe. *Hepatology.*

- 2016;64(5):1577-1586. doi:10.1002/HEP.28785
157. Paik JM, Kabbara K, Eberly KE, Younossi Y, Henry L, Younossi ZM. Global burden of NAFLD and chronic liver disease among adolescents and young adults. *Hepatology*. 2022;75(5):1204-1217. doi:10.1002/HEP.32228
158. Anderson EL, Howe LD, Jones HE, Higgins JPT, Lawlor DA, Fraser A. The Prevalence of Non-Alcoholic Fatty Liver Disease in Children and Adolescents: A Systematic Review and Meta-Analysis. *PLoS One*. 2015;10(10). doi:10.1371/JOURNAL.PONE.0140908
159. Le MH, Devaki P, Ha NB, et al. Prevalence of non-alcoholic fatty liver disease and risk factors for advanced fibrosis and mortality in the United States. *PLoS One*. 2017;12(3):1577–86. doi:10.1371/JOURNAL.PONE.0173499
160. Estes C, Razavi H, Loomba R, Younossi Z, Sanyal AJ. Modeling the epidemic of nonalcoholic fatty liver disease demonstrates an exponential increase in burden of disease. *Hepatology*. 2018;67(1):123-133. doi:10.1002/HEP.29466
161. Loomba R, Friedman SL, Shulman GI. Mechanisms and disease consequences of nonalcoholic fatty liver disease. *Cell*. 2021;184(10):2537-2564. doi:10.1016/J.CELL.2021.04.015
162. Morán-Salvador E, López-Parra M, García-Alonso V, et al. Role for PPAR $\gamma$  in obesity-induced hepatic steatosis as determined by hepatocyte- and macrophage-specific conditional knockouts. *FASEB J*. 2011;25(8):2538-2550. doi:10.1096/FJ.10-173716
163. Yu S, Matsusue K, Kashireddy P, et al. Adipocyte-specific gene expression and adipogenic steatosis in the mouse liver due to peroxisome proliferator-activated receptor gamma1 (PPARgamma1) overexpression. *J Biol Chem*. 2003;278(1):498-505. doi:10.1074/JBC.M210062200

164. Skat-Rørdam J, Højland Ipsen D, Lykkesfeldt J, Tveden-Nyborg P. A role of peroxisome proliferator-activated receptor  $\gamma$  in non-alcoholic fatty liver disease. *Basic Clin Pharmacol Toxicol*. 2019;124(5):528-537. doi:10.1111/BCPT.13190
165. Friedman SL, Neuschwander-Tetri BA, Rinella M, Sanyal AJ. Mechanisms of NAFLD development and therapeutic strategies. *Nat Med*. 2018;24(7):908-922. doi:10.1038/S41591-018-0104-9
166. Lomonaco R, Ortiz-Lopez C, Orsak B, et al. Effect of adipose tissue insulin resistance on metabolic parameters and liver histology in obese patients with nonalcoholic fatty liver disease. *Hepatology*. 2012;55(5):1389-1397. doi:10.1002/HEP.25539
167. Koyama Y, Brenner DA. Liver inflammation and fibrosis. *J Clin Invest*. 2017;127(1):55-64.
168. Ibrahim SH, Hirsova P, Gores GJ. Non-alcoholic steatohepatitis pathogenesis: sublethal hepatocyte injury as a driver of liver inflammation. *Gut*. 2018;67(5):963-972. doi:10.1136/GUTJNL-2017-315691
169. Tsuchida T, Friedman SL. Mechanisms of hepatic stellate cell activation. *Nat Rev Gastroenterol Hepatol* 2017 147. 2017;14(7):397-411. doi:10.1038/nrgastro.2017.38
170. An P, Wei LL, Zhao S, et al. Hepatocyte mitochondria-derived danger signals directly activate hepatic stellate cells and drive progression of liver fibrosis. *Nat Commun*. 2020;11(1). doi:10.1038/S41467-020-16092-0
171. Zhu C, Kim KJ, Wang X, et al. Hepatocyte Notch activation induces liver fibrosis in nonalcoholic steatohepatitis. *Sci Transl Med*. 2018;10(468). doi:10.1126/SCITRANSLMED.AAT0344
172. Hellerbrand C, Stefanovic B, Giordano F, Burchardt ER, Brenner DA. The role of

- TGFbeta1 in initiating hepatic stellate cell activation in vivo. *J Hepatol.* 1999;30(1):77-87.  
doi:10.1016/S0168-8278(99)80010-5
173. Ma K, Saha PK, Chan L, Moore DD. Farnesoid X receptor is essential for normal glucose homeostasis. *J Clin Invest.* 2006;116(4):1102-1109. doi:10.1172/JCI25604
174. Wong VWS, Singal AK. Emerging medical therapies for non-alcoholic fatty liver disease and for alcoholic hepatitis. *Transl Gastroenterol Hepatol.* 2019;4(53).  
doi:10.21037/TGH.2019.06.06
175. Staels B, Rubenstrunk A, Noel B, et al. Hepatoprotective effects of the dual peroxisome proliferator-activated receptor alpha/delta agonist, GFT505, in rodent models of nonalcoholic fatty liver disease/nonalcoholic steatohepatitis. *Hepatology.* 2013;58(6):1941-1952. doi:10.1002/HEP.26461
176. Cariou B, Hanf R, Lambert-Porcheron S, et al. Dual peroxisome proliferator-activated receptor  $\alpha/\delta$  agonist GFT505 improves hepatic and peripheral insulin sensitivity in abdominally obese subjects. *Diabetes Care.* 2013;36(10):2923-2930. doi:10.2337/DC12-2012
177. Krenkel O, Puengel T, Govaere O, et al. Therapeutic inhibition of inflammatory monocyte recruitment reduces steatohepatitis and liver fibrosis. *Hepatology.* 2018;67(4):1270-1283. doi:10.1002/HEP.29544
178. Olefsky JM. Treatment of insulin resistance with peroxisome proliferator-activated receptor gamma agonists. *J Clin Invest.* 2000;106(4):467-472. doi:10.1172/JCI10843
179. Bedoucha M, Atzpodien E, Boelsterli UA. Diabetic KKAy mice exhibit increased hepatic PPARgamma1 gene expression and develop hepatic steatosis upon chronic treatment with antidiabetic thiazolidinediones. *J Hepatol.* 2001;35(1):17-23. doi:10.1016/S0168-

8278(01)00066-6

180. *Scientific Frontiers in Developmental Toxicology and Risk Assessment*. National Academies Press; 2000. doi:10.17226/9871
181. Fox JG, Barthold S, Davisson M, Newcomer CE, Quimby FW SA, ed. *The Mouse in Biomedical Research*. Elsevier Science & Technology; 2006.
182. Waterston RH, Lindblad-Toh K, Birney E, et al. Initial sequencing and comparative analysis of the mouse genome. *Nature*. 2002;420(6915):520-562.  
doi:10.1038/nature01262
183. Boxenbaum H. Interspecies variation in liver weight, hepatic blood flow, and antipyrine intrinsic clearance: Extrapolation of data to benzodiazepines and phenytoin. *J Pharmacokinet Biopharm*. 1980;8(2):165-176. doi:10.1007/BF01065191
184. Perlman RL. Mouse models of human disease An evolutionary perspective. *Evol Med Public Heal*. Published online 2016:170-176. doi:10.1093/emph/eow014
185. Cox B, Kotlyar M, Evangelou AI, et al. Comparative systems biology of human and mouse as a tool to guide the modeling of human placental pathology. *Mol Syst Biol*. 2009;5(279). doi:10.1038/MSB.2009.37
186. Soncin F, Khater M, To C, et al. Comparative analysis of mouse and human placentae across gestation reveals species-specific regulators of placental development. *Development*. 2018;145(dev156273). doi:10.1242/dev.156273
187. Gundacker C, Hengstschläger M. The role of the placenta in fetal exposure to heavy metals. *Wien Med Wochenschrift*. 2012;162(9):201-206. doi:10.1007/s10354-012-0074-3
188. Hudson KM, Belcher SM, Cowley M. Maternal cadmium exposure in the mouse leads to increased heart weight at birth and programs susceptibility to hypertension in adulthood.

- Sci Rep.* 2019;9(1):13553. doi:10.1038/S41598-019-49807-5
189. Taguchi T, Suzuki S. Influence of sex and age on the biological half-life of cadmium in mice. *J Toxicol Environ Health.* 1981;7(2):239-249. doi:10.1080/15287398109529975
190. Foster JR, Lund G, Sapelnikova S, Tyrrell DL, Kneteman NM. Chimeric rodents with humanized liver: bridging the preclinical/clinical trial gap in ADME/toxicity studies. *Xenobiotica.* 2014;44(2):109-122. doi:10.3109/00498254.2013.867553
191. Go YM, Sutliff RL, Chandler JD, et al. Low-Dose Cadmium Causes Metabolic and Genetic Dysregulation Associated With Fatty Liver Disease in Mice. *Toxicol Sci.* 2015;147(2):524-534. doi:10.1093/TOXSCI/KFV149
192. Jackson TW, Ryherd GL, Scheibly CM, Sasser AL, Guillette TC, Belcher SM. Gestational Cd Exposure in the CD-1 Mouse Induces Sex-Specific Hepatic Insulin Insensitivity, Obesity, and Metabolic Syndrome in Adult Female Offspring. *Toxicol Sci.* 2020;178(2):264-280. doi:10.1093/TOXSCI/KFAA154
193. Ciesielski T, Weuve J, Bellinger DC, Schwartz J, Lanphear B, Wright RO. Cadmium exposure and neurodevelopmental outcomes in U.S. children. *Environ Health Perspect.* 2012;120(5):758-763. doi:10.1289/EHP.1104152
194. Swaddiwudhipong W, Mahasakpan P, Jeekeeree W, et al. Renal and blood pressure effects from environmental cadmium exposure in Thai children. *Environ Res.* 2015;136:82-87. doi:10.1016/J.ENVRES.2014.10.017
195. Semple BD, Blomgren K, Gimlin K, Ferriero DM, Noble-Haeusslein LJ. Brain development in rodents and humans: Identifying benchmarks of maturation and vulnerability to injury across species. *Prog Neurobiol.* 2013;106-107:1-16. doi:10.1016/J.PNEUROBIO.2013.04.001

196. WHO. Environmental Health Criteria 134 Cadmium. Published online 1992.
197. Nishijo M, Nambunmee K, Suvagandha D, Swaddiwudhipong W, Ruangyuttikarn W, Nishino Y. Gender-Specific Impact of Cadmium Exposure on Bone Metabolism in Older People Living in a Cadmium-Polluted Area in Thailand. *Int J Environ Res Public Health*. 2017;14(4):1-11. doi:10.3390/IJERPH14040401
198. Livak KJ, Schmittgen TD. Analysis of Relative Gene Expression Data Using Real-Time Quantitative PCR and the  $2^{-\Delta\Delta CT}$  Method. *Methods*. 2001;25(4):402-408. doi:10.1006/METH.2001.1262
199. Simmers MD, Hudson KM, Baptissart M CM. Epigenetic control of the imprinted growth regulator *Cdkn1c* in cadmium-induced placental dysfunction. :In press.
200. Huang S, Kuang J, Zhou F, et al. The association between prenatal cadmium exposure and birth weight: A systematic review and meta-analysis of available evidence. *Environ Pollut*. 2019;251:699-707. doi:10.1016/J.ENVPOL.2019.05.039
201. Wang H, Liu L, Hu YF, et al. Maternal serum cadmium level during pregnancy and its association with small for gestational age infants: a population-based birth cohort study. *Sci Reports* 2016 61. 2016;3(6):22631. doi:10.1038/srep22631
202. Kim DW, Ock J, Moon KW, Park CH. Association between pb, cd, and hg exposure and liver injury among Korean adults. *Int J Environ Res Public Health*. 2021;18(13):6783. doi:10.3390/IJERPH18136783/S1
203. Charalambous M, Ferron SR, Da Rocha ST, et al. Imprinted gene dosage is critical for the transition to independent life. *Cell Metab*. 2012;15(2):209-221. doi:10.1016/J.CMET.2012.01.006
204. Rugh R. *The Mouse; Its Reproduction and Development*. Burgess Pub. Co.; 1968.

205. Leidinger CS, Thöne-Reineke C, Baumgart N, Baumgart J. Environmental enrichment prevents pup mortality in laboratory mice. *Lab Anim.* 2019;53(1):53-62.  
doi:10.1177/0023677218777536
206. Levin-Schwartz Y, Cowell W, Leon Hsu HH, et al. Metal mixtures are associated with increased anxiety during pregnancy. *Environ Res.* 2022;204.  
doi:10.1016/J.ENVRES.2021.112276
207. Moylan CA, Mavis AM, Jima D, et al. Alterations in DNA methylation associate with fatty liver and metabolic abnormalities in a multi-ethnic cohort of pre-teenage children. *Epigenetics.* Published online 2022:1-16. doi:10.1080/15592294.2022.2039850
208. Laviola G, Macrì S, Morley-Fletcher S, Adriani W. Risk-taking behavior in adolescent mice: psychobiological determinants and early epigenetic influence. *Neurosci Biobehav Rev.* 2003;27(1-2):19-31. doi:10.1016/S0149-7634(03)00006-X
209. Young JL, Cave MC, Xu Q, et al. Whole life exposure to low dose cadmium alters diet-induced NAFLD. *Toxicol Appl Pharmacol.* 2022;436:115855.  
doi:10.1016/J.TAAP.2021.115855
210. Sasaki T, Horiguchi H, Arakawa A, et al. Hospital-based screening to detect patients with cadmium nephropathy in cadmium-polluted areas in Japan. *Environ Health Prev Med.* 2019;24(1). doi:10.1186/S12199-019-0762-3
211. Suwazono Y, Kido T, Nakagawa H, et al. Biological half-life of cadmium in the urine of inhabitants after cessation of cadmium exposure. *Biomarkers.* 2009;14(2):77-81.  
doi:10.1080/13547500902730698
212. Jackson TW, Baars O, Belcher SM. Gestational Cd Exposure in the CD-1 Mouse Sex-Specifically Disrupts Essential Metal Ion Homeostasis. *Toxicol Sci.* Published online

February 25, 2022. doi:10.1093/TOXSCI/KFAC027

213. Lonardo A, Nascimbeni F, Ballestri S, et al. Sex Differences in Nonalcoholic Fatty Liver Disease: State of the Art and Identification of Research Gaps. *Hepatology*. 2019;70(4):1457-1469. doi:10.1002/HEP.30626
214. Stahl EC, Delgado ER, Alencastro F, et al. Inflammation and Ectopic Fat Deposition in the Aging Murine Liver Is Influenced by CCR2. *Am J Pathol*. 2020;190(2):372-387. doi:10.1016/J.AJPATH.2019.10.016
215. Gong T, Zhang C, Ni X, et al. A time-resolved multi-omic atlas of the developing mouse liver. *Genome Res*. 2020;30(2):263-275. doi:10.1101/GR.253328.119/-/DC1
216. Buzzetti E, Pinzani M, Tsochatzis EA. The multiple-hit pathogenesis of non-alcoholic fatty liver disease (NAFLD). *Metabolism*. 2016;65(8):1038-1048. doi:10.1016/J.METABOL.2015.12.012
217. Wild CP. Complementing the genome with an “exposome”: the outstanding challenge of environmental exposure measurement in molecular epidemiology. *Cancer Epidemiol Biomarkers Prev*. 2005;14(8):1847-1850. doi:10.1158/1055-9965.EPI-05-0456
218. Schwimmer JB, Behling C, Newbury R, et al. Histopathology of pediatric nonalcoholic fatty liver disease. *Hepatology*. 2005;42(3):641-649. doi:10.1002/HEP.20842
219. Wahlang B, Beier JI, Clair HB, et al. Toxicant-associated Steatohepatitis. *Toxicol Pathol*. 2013;41(2):343–60. doi:10.1177/0192623312468517
220. Gallego-Durán R, Romero-Gómez M. Epigenetic mechanisms in non-alcoholic fatty liver disease: An emerging field. *World J Hepatol*. 2015;7(24):2497-2502. doi:10.4254/WJH.V7.I24.2497
221. Sookoian S, Gianotti TF, Burgueño AL, Pirola CJ. Fetal metabolic programming and

- epigenetic modifications: a systems biology approach. *Pediatr Res.* 2013;73(4 Pt 2):531-542. doi:10.1038/PR.2013.2
222. House JS, Hall J, Park SS, et al. Cadmium exposure and MEG3 methylation differences between Whites and African Americans in the NEST Cohort. *Environ epigenetics.* 2019;5(3):dvz014. doi:10.1093/EEP/DVZ014
223. Pope C, Mishra S, Russell J, Zhou Q, Zhong XB. diseases Targeting H19, an Imprinted Long Non-Coding RNA, in Hepatic Functions and Liver Diseases. *Diseases.* 2017;5(1):11. doi:10.3390/diseases5010011
224. Smith FM, Garfield AS, Ward A. Regulation of growth and metabolism by imprinted genes. *Cytogenet Genome Res.* 2006;113(1-4):279-291. doi:10.1159/000090843
225. Van De Geijn B, Mcvicker G, Gilad Y, Pritchard JK. WASP: allele-specific software for robust molecular quantitative trait locus discovery. *Nat Methods.* 2015;12(11):1061-1063. doi:10.1038/NMETH.3582
226. Anders S, Pyl PT, Huber W. HTSeq--a Python framework to work with high-throughput sequencing data. *Bioinformatics.* 2015;31(2):166-169. doi:10.1093/BIOINFORMATICS/BTU638
227. Love MI, Huber W, Anders S. Moderated estimation of fold change and dispersion for RNA-seq data with DESeq2. *Genome Biol.* 2014;15(12):1-21. doi:10.1186/S13059-014-0550-8/FIGURES/9
228. Benjamini Y, Hochberg Y. Controlling the False Discovery Rate: A Practical and Powerful Approach to Multiple Testing. *J R Stat Soc Ser B.* 1995;57(1):289-300. doi:10.1111/J.2517-6161.1995.TB02031.X
229. Barz T, Hoffmann A, Panhuysen M, Spengler D. Peroxisome Proliferator-Activated

- Receptor ; Is a Zac Target Gene Mediating Zac Antiproliferation. *Cancer Res.* 2006;66(24):11975-11982. doi:10.1158/0008-5472.CAN-06-1529
230. Saintilnord WN, Tenlep SYN, Preston JD, et al. Chronic Exposure to Cadmium Induces Differential Methylation in Mice Spermatozoa. *Toxicol Sci.* 2021;180(2):262–76. doi:10.1093/toxsci/kfab002
231. Shu G, Tang Y, Zhou Y, Wang C, Song JG. Zac1 is a histone acetylation-regulated NF- $\kappa$ B suppressor that mediates histone deacetylase inhibitor-induced apoptosis. *Cell Death Differ.* 2011;18(12):1825-1835. doi:10.1038/CDD.2011.51
232. Lui JC, Finkielstain GP, Barnes KM, Baron J. An imprinted gene network that controls mammalian somatic growth is down-regulated during postnatal growth deceleration in multiple organs. *Am J Physiol Regul Integr Comp Physiol.* 2008;295(1):R189-96. doi:10.1152/AJPREGU.00182.2008
233. Kernohan KD, Jiang Y, Tremblay DC, et al. ATRX partners with cohesin and MeCP2 and contributes to developmental silencing of imprinted genes in the brain. *Dev Cell.* 2010;18(2):191-202. doi:10.1016/J.DEVCEL.2009.12.017
234. Voon HPJ, Hughes JR, Rode C, et al. ATRX Plays a Key Role in Maintaining Silencing at Interstitial Heterochromatic Loci and Imprinted Genes. *Cell Rep.* 2015;11(3):405-418. doi:10.1016/J.CELREP.2015.03.036
235. Zeisberg M, Yang C, Martino M, et al. Fibroblasts derive from hepatocytes in liver fibrosis via epithelial to mesenchymal transition. *J Biol Chem.* 2007;282(32):23337-23347. doi:10.1074/JBC.M700194200
236. Sovaila S, Purcarea A, Gheonea D, Ionescu S, Ciurea T. Cellular Interactions in the Human Fatty Liver. *J Med Life.* 2019;12(4):338-340. doi:10.25122/JML-2019-1010

237. Zober A, Ott MG, Messerer P. Morbidity follow up study of BASF employees exposed to 2,3,7, 8-tetrachlorodibenzo-p-dioxin (TCDD) after a 1953 chemical reactor incident. *Occup Environ Med.* 1994;51(7):479-486. doi:10.1136/OEM.51.7.479
238. Neuberger M, Rappe C, Bergek S, et al. Persistent health effects of dioxin contamination in herbicide production. *Environ Res.* 1999;81(3):206-214. doi:10.1006/ENRS.1999.3983
239. Berná G, Romero-Gomez M. The role of nutrition in non-alcoholic fatty liver disease: Pathophysiology and management. *Liver Int.* 2020;40(S1):102-108. doi:10.1111/LIV.14360
240. Perdomo CM, Frühbeck G, Escalada J. Impact of Nutritional Changes on Nonalcoholic Fatty Liver Disease. *Nutrients.* 2019;11(3):677. doi:10.3390/nu11030677
241. Vreugdenhil HJI, Lanting CI, Mulder PGH, Boersma ER, Weisglas-Kuperus N. Effects of prenatal PCB and dioxin background exposure on cognitive and motor abilities in Dutch children at school age. *J Pediatr.* 2002;140(1):48-56. doi:10.1067/MPD.2002.119625
242. Nakajima S, Saijo Y, Kato S, et al. Effects of prenatal exposure to polychlorinated biphenyls and dioxins on mental and motor development in Japanese children at 6 months of age. *Environ Health Perspect.* 2006;114(5):773-778. doi:10.1289/EHP.8614
243. Gileadi TE, Swamy AK, Hore Z, et al. Effects of Low-Dose Gestational TCDD Exposure on Behavior and on Hippocampal Neuron Morphology and Gene Expression in Mice. *Environ Health Perspect.* 2021;129(5). doi:10.1289/EHP7352
244. Sha R, Chen Y, Wang Y, et al. Gestational and lactational exposure to 2,3,7,8-tetrachlorodibenzo-p-dioxin in mice: Neurobehavioral effects on female offspring. *Sci Total Environ.* 2021;752. doi:10.1016/J.SCITOTENV.2020.141784
245. McCann JC, Hudes M, Ames BN. An overview of evidence for a causal relationship

- between dietary availability of choline during development and cognitive function in offspring. *Neurosci Biobehav Rev.* 2006;30(5):696-712.  
doi:10.1016/J.NEUBIOREV.2005.12.003
246. Bove FJ, Fulcomer MC, Klotz JB, Esmart J, Dufficy EM, Savrin JE. Public drinking water contamination and birth outcomes. *Am J Epidemiol.* 1995;141(9):850-862.  
doi:10.1093/OXFORDJOURNALS.AJE.A117521
247. Zhong F, Zhou X, Xu J, Gao L. Rodent Models of Nonalcoholic Fatty Liver Disease. *Digestion.* 2020;101:522-535. doi:10.1159/000501851
248. Zhu J, Huang Z, Yang F, et al. Cadmium disturbs epigenetic modification and induces DNA damage in mouse preimplantation embryos. *Ecotoxicol Environ Saf.* 2021;219.  
doi:10.1016/J.ECOENV.2021.112306
249. Agency for Toxic Substances and Disease Registry (ATSDR). Toxicological Profile for Carbon Tetrachloride. *US Dep Heal Hum Serv Public Heal Serv.* Published online 2005.
250. Office of Drinking Water. Carbon Tetrachloride Health Advisory. *US Environ Prot Agency.* Published online 1987.
251. Agency for Toxic Substances and Disease Registry (ATSDR). TOXICOLOGICAL PROFILE FOR CHLORINATED DIBENZO-p-DIOXINS. *US Dep Heal Hum Serv Public Heal Serv.* Published online 1998.
252. Sweeney MH, Mocarelli P. Human health effects after exposure to 2,3,7,8-TCDD. *Arch Environ Health.* 2000;17(4):303-316. doi:10.1080/026520300283379
253. Kimbrough RD, Carter CD, Liddle JA, Cline RE. Epidemiology and Pathology of a Tetrachlorodibenzodioxin Poisoning Episode. *Food Addit Contam.* 1977;32(2):77-86.  
doi:10.1080/00039896.1977.10667259

254. Nault R, Fader KA, Ammendolia DA, et al. Dose-Dependent Metabolic Reprogramming and Differential Gene Expression in TCDD-Elicited Hepatic Fibrosis. *Toxicol Sci.* 2016;154(2):253–66. doi:10.1093/toxsci/kfw163
255. Li J, Wang Y, Ma M, et al. Autocrine CTHRC1 activates hepatic stellate cells and promotes liver fibrosis by activating TGF- $\beta$  signaling. *EBioMedicine.* 2019;40:43-55. doi:10.1016/J.EBIOM.2019.01.009
256. Kita Y, Takamura T, Misu H, et al. Metformin Prevents and Reverses Inflammation in a Non-Diabetic Mouse Model of Nonalcoholic Steatohepatitis. *PLoS One.* 2012;7(9). doi:10.1371/journal.pone.0043056
257. Zhou XL, Wan XM, Fu XX, Xie CG. Puerarin prevents cadmium-induced hepatic cell damage by suppressing apoptosis and restoring autophagic flux. *Biomed Pharmacother.* 2019;115. doi:10.1016/J.BIOPHA.2019.108929
258. Wang J, Hao M, Liu C, Liu R. Cadmium induced apoptosis in mouse primary hepatocytes: the role of oxidative stress-mediated ERK pathway activation and the involvement of histone H3 phosphorylation †. *R Soc Chem.* 2015;5. doi:10.1039/c5ra03210e
259. Bruscalupi G, Massimi M, Devirgiliis LC, Leoni S. Multiple parameters are involved in the effects of cadmium on prenatal hepatocytes. *Toxicol Vitro.* 2009;23(7):1311-1318. doi:10.1016/J.TIV.2009.07.018
260. Miranda RR, Gorshkov V, Korzeniowska B, Kempf SJ, Neto FF, Kjeldsen F. Co-exposure to silver nanoparticles and cadmium induce metabolic adaptation in HepG2 cells. *Nanotoxicology.* 2018;12(7):781-795. doi:10.1080/17435390.2018.1489987
261. Sabolić I, Breljak D, Škarica M, Herak-Kramberger CM. Role of metallothionein in

- cadmium traffic and toxicity in kidneys and other mammalian organs. *Biometals*. 2010;23(5):897-926. doi:10.1007/S10534-010-9351-Z
262. ATCC. AML12 (CRL-2254). Published 2022. <https://www.atcc.org/products/crl-2254#detailed-product-information>
263. ATCC. Hep G2 (HB-8065). Published online 2022. <https://www.atcc.org/products/hb-8065>
264. Mchedlidze T, Waldner M, Zopf S, et al. Interleukin-33-dependent innate lymphoid cells mediate hepatic fibrosis. *Immunity*. 2013;39(2):357-371. doi:10.1016/J.IMMUNI.2013.07.018
265. Cazanave S, Podtelezchnikov A, Jensen K, et al. The Transcriptomic Signature Of Disease Development And Progression Of Nonalcoholic Fatty Liver Disease. *Sci Rep*. 2017;7(1). doi:10.1038/S41598-017-17370-6
266. Wang T, Pehrsson EC, Purushotham D, et al. The NIEHS TaRGET II Consortium and environmental epigenomics. *Nat Biotechnol*. 2018;36(3):225-227. doi:10.1038/NBT.4099
267. Wang H, Cao Y, Shu L, et al. Long non-coding RNA (lncRNA) H19 induces hepatic steatosis through activating MLXIPL and mTORC1 networks in hepatocytes. *J Cell Mol Med*. 2020;24(2):1399-1412. doi:10.1111/JCMM.14818
268. Zhu J, Luo Z, Pan Y, et al. H19/miR-148a/USP4 axis facilitates liver fibrosis by enhancing TGF- $\beta$  signaling in both hepatic stellate cells and hepatocytes. *J Cell Physiol*. 2019;234(6):9698-9710. doi:10.1002/JCP.27656
269. Kim J, Hyun J, Wang S, et al. Thymosin beta-4 regulates activation of hepatic stellate cells via hedgehog signaling. *Sci Rep*. 2017;7(1). doi:10.1038/S41598-017-03782-X
270. Li W, Kuang Z, Zheng M, He G, Liu Y. Multi-omics integrative analysis to access role of

- coiled-coil domain-containing 80 in lipid metabolism. *Biochem Biophys Res Commun.* 2020;526(3):813-819. doi:10.1016/J.BBRC.2020.03.121
271. Grill JI, Neumann J, Herbst A, et al. Loss of DRO1/CCDC80 results in obesity and promotes adipocyte differentiation. *Mol Cell Endocrinol.* 2017;439:286-296. doi:10.1016/J.MCE.2016.09.014
272. Zhang X, Ji X, Wang Q, Li JZ. New insight into inter-organ crosstalk contributing to the pathogenesis of non-alcoholic fatty liver disease (NAFLD). *Protein Cell.* 2018;9(2):164-177. doi:10.1007/S13238-017-0436-0
273. Rosen ED, Kulkarni RN, Sarraf P, et al. Targeted elimination of peroxisome proliferator-activated receptor gamma in beta cells leads to abnormalities in islet mass without compromising glucose homeostasis. *Mol Cell Biol.* 2003;23(20):7222-7229. doi:10.1128/MCB.23.20.7222-7229.2003
274. Ravnskjaer K, Boergesen M, Rubi B, et al. Peroxisome proliferator-activated receptor alpha (PPARalpha) potentiates, whereas PPARgamma attenuates, glucose-stimulated insulin secretion in pancreatic beta-cells. *Endocrinology.* 2005;146(8):3266-3276. doi:10.1210/EN.2004-1430
275. Chawla A, Schwarz EJ, Dimaculangan DD, Lazar MA. Peroxisome proliferator-activated receptor (PPAR) gamma: adipose-predominant expression and induction early in adipocyte differentiation. *Endocrinology.* 1994;135(2):798-800. doi:10.1210/ENDO.135.2.8033830
276. Tontonoz P, Spiegelman BM. Fat and beyond: the diverse biology of PPARgamma. *Annu Rev Biochem.* 2008;77:289-312. doi:10.1146/ANNUREV.BIOCHEM.77.061307.091829
277. Khalil N, Greenberg AH. *The Role of TGF- $\beta$  in Pulmonary Fibrosis.* (Bock G, Marsh J,

- eds.). John Wiley & Sons, Ltd; 2007. doi:10.1002/9780470514061.CH13
278. Gandhi CR, Chaillet JR, Nalesnik MA, et al. Liver-specific deletion of augmenter of liver regeneration accelerates development of steatohepatitis and hepatocellular carcinoma in mice. *Gastroenterology*. 2015;148(2):379-391. doi:10.1053/J.GASTRO.2014.10.008
279. Fernandes GW, Bocco BMLC, Fonseca TL, et al. The Foxo1-Inducible Transcriptional Repressor Zfp125 Causes Hepatic Steatosis and Hypercholesterolemia. *Cell Rep*. 2018;22(2):523-534. doi:10.1016/J.CELREP.2017.12.053
280. Kim YW, Kim AR. Deletion of transcription factor binding motifs using the CRISPR/spCas9 system in the  $\beta$ -globin LCR. *Biosci Rep*. 2017;37(4). doi:10.1042/BSR20170976

## APPENDICES

## Appendix A

### Chapter 2 Supplemental Data

**Supp. Table 2.1.** Primer sequences used for qRT-PCR.

Target	Fwd (5'-3')	Rev (5'-3')
Tgf $\beta$ -1	AAGTTGGCATGGTAGCCCTT	GCCCTGGATACCAACTATTGC
Il-1 $\beta$	CCTGTTCTTTGAAGTTGACG	CCTGAAGCTCTTGTTGATGTGC
Mgat1	CTGGTTCTGTTTCCCGTTGT	TGGGTCAAGGCCATCTTAAC
Cd36	GGAGCCATCTTTGAGCCTTCA	GAACCAAAGTGAAGGATGGATCT
Vim	CGAGCAGCAGAACAAAATCC	GGCAATTTCTCCTGCAAGGATTCC
Fabp4	TCTCCAGTGAAAACCTTCGAT	TTACGCTGATGATCATGTTG
Fsp27	GGAGACAGAAGAATACTTCC	GCGAGTATGTGTCATAGAGG
Ccr2	TTTGCAACTGCCTCTTTCCT	CTTCTGTCCCTGCTTCATCC
Ccr5	ATGGATTTTCAAGGGTCAGTTCC	CTGAGCCGCAATTTGTTTCAC
Snail	CGGAAGATCTTCAACTGC	GGTATCTCTTCACATCCG
Col1a1	CCATCAAGGTCTACTGCAACATGG	GCTGTTCTTGCAAGTATAGG
Col5a1	CCGAATCACATGACCTAGCCA	ACCTATCCTGAGAGCTGAAGGGT
Col5a2	GGAAGTCAAGTAGGACTCATGC	CCTTCAAGACCTTTGTGTCC
Col6a1	CCCCTGACAAAACAGGAATAGG	GCATCTCAGCGTTCCCTTTAA
Col6a2	GAACCCAAAGCCCCTTACCTACT	GGGCAAGGTATAGGTAGGATGGA
ActB	GGCTGTATTCCCCTCCATCG	CCAGTTGGTAACAATGCCATGT

**Supp. Table 2.2.** F<sub>1</sub> proportional organ data at PND0, 21, and 90.

This table is provided as an additional document that is downloadable on the repository page for this ETD.

## Appendix B

### Chapter 3 Supplemental Data

**Supp. Table 3.1.** Primer sequences used for qRT-PCR.

Target	Fwd (5'-3')	Rev (5'-3')
Zac1	CCATTCAAGTGCTCGAAGG	CACTGGTGAATCTTCTGTGG
H19	CTTGTCGTAGAAGCCGTCTGTTC	GTAGCACCATTCTTTTCATCTTGAGG
Grb10	AGGATCATCAAGCAACAAGGTCTC	ATTACTCTGGCTGTCACGAAGGA
Mmp2	CGTAAAGTATGGGAACGCTGATGG	CCTCGGTGGTACAGCTGTTGTAGG
Igf2	TACGGCCCCGGAGAGACT	GGTTGGCACGGCTTGAAG
Cdkn1c	AACGTCTGAGATGAGTTAGTTTAGAGG	AAGCCCAGAGTTCTTCCATCGT
ActB	GGCTGTATTCCCCTCCATCG	CCAGTTGGTAACAATGCCATGT

**Supp. Table 3.2.** Primer sequences used for pyrosequencing.

Target	BS-Modified Fwd (5'-3')	BS-Modified Rev (5'-3')	BS-Modified Seq (5'-3')
Zac1	GGTTAGGGTAGGTAAGTAGTGA	ACACCCAAATTCAAATTTATCACCTC	GGTAGGTAAGTAGTGATAAT
Zac1-AQ	ATGCTTCTACACCCGAAAGATG	GGAGGCATGGGATCAACCTTTA	AACTCATTGCGCCTT

**Supp. Table 3.3.** RNA-sequencing DEG information and enrichment data for PND0 and 21. This table is provided as an additional document that is downloadable on the repository page for this ETD.

**Supp. Table 3.4.** Determination of allele-specific expression of imprinted genes among DEGs for females and males at PND21.

This table is provided as an additional document that is downloadable on the repository page for this ETD.

## Appendix C

### Chapter 4 Supplemental Data

**Supp. Table 4.1.** Details for the studies used in the analysis.

This table is provided as an additional document that is downloadable on the repository page for this ETD.

**Supp. Table 4.2.** Ensembl gene IDs for RNA-sequencing and microarray datasets.

This table is provided as an additional document that is downloadable on the repository page for this ETD.

**Supp. Table 4.3.** Primer sequences used for qRT-PCR.

	Target	Fwd (5'-3')	Rev (5'-3')
<b>Mouse</b>	Zac1	CCATTCAAGTGCTCGAAGG	CACTGGTGAATCTTCTGTGG
<b>Primers</b>	ActB	GGCTGTATCCCCTCCATCG	CCAGTTGGTAACAATGCCATGT
	MT1	AACTGTCCTGCTCCAC	GCCCTGGGCACATTTGG

	Target	Fwd (5'-3')	Rev (5'-3')
<b>Human</b>	Zac1	CAAGTGTGTGCAGCCTGACTGT	GAACGTCTTCTCACAGTGAGCAC
<b>Primers</b>	Gapdh	GCACCGTCAAGGCTGAGAAC	TGGTGAAGACGCCAGTGGA
	MT1	TCCTGCAAGTGCAAAGAGTG	AAAGTTGTCCTGGCATCAG

**Supp. Table 4.4.** RNA-sequencing and microarray analysis from various adult environmental exposures.

This table is provided as an additional document that is downloadable on the repository page for this ETD.

**Supp. Table 4.5.** Exposure model comparisons for shared IGN genes.

This table is provided as an additional document that is downloadable on the repository page for this ETD.